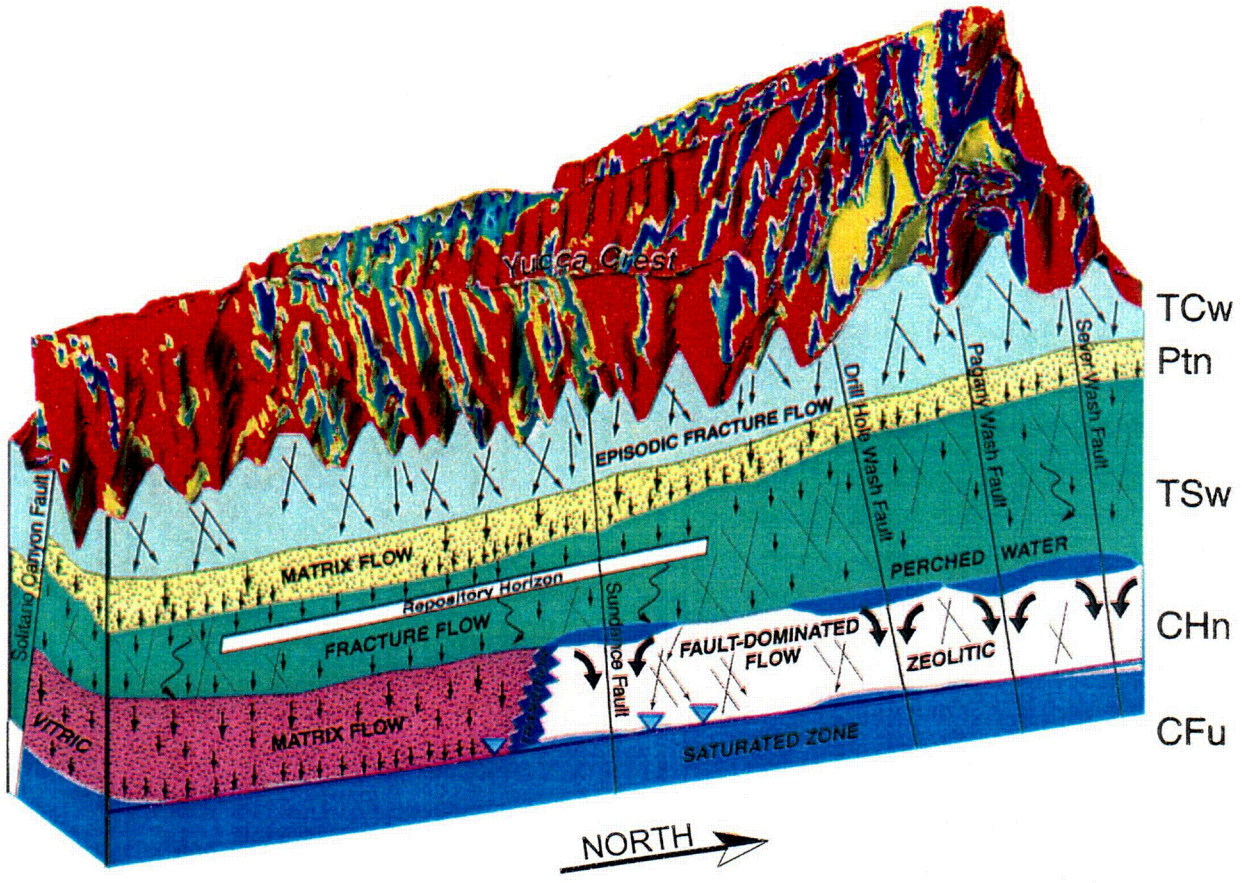

Source: CRWMS M&O (2000m, Figure 1)

NOTE: Schematic cross section is west of the Ghost Dance fault. The color patterns at the top of the diagram represent shallow infiltration flux. Red is the lowest flux; blue is the highest flux; green, yellow, and beige are intermediate fluxes in descending order.

Figure 8.9-1. Schematic Diagram of Conceptual Model of Liquid Water Flow through the Unsaturated Zone at Yucca Mountain

INTENTIONALLY LEFT BLANK

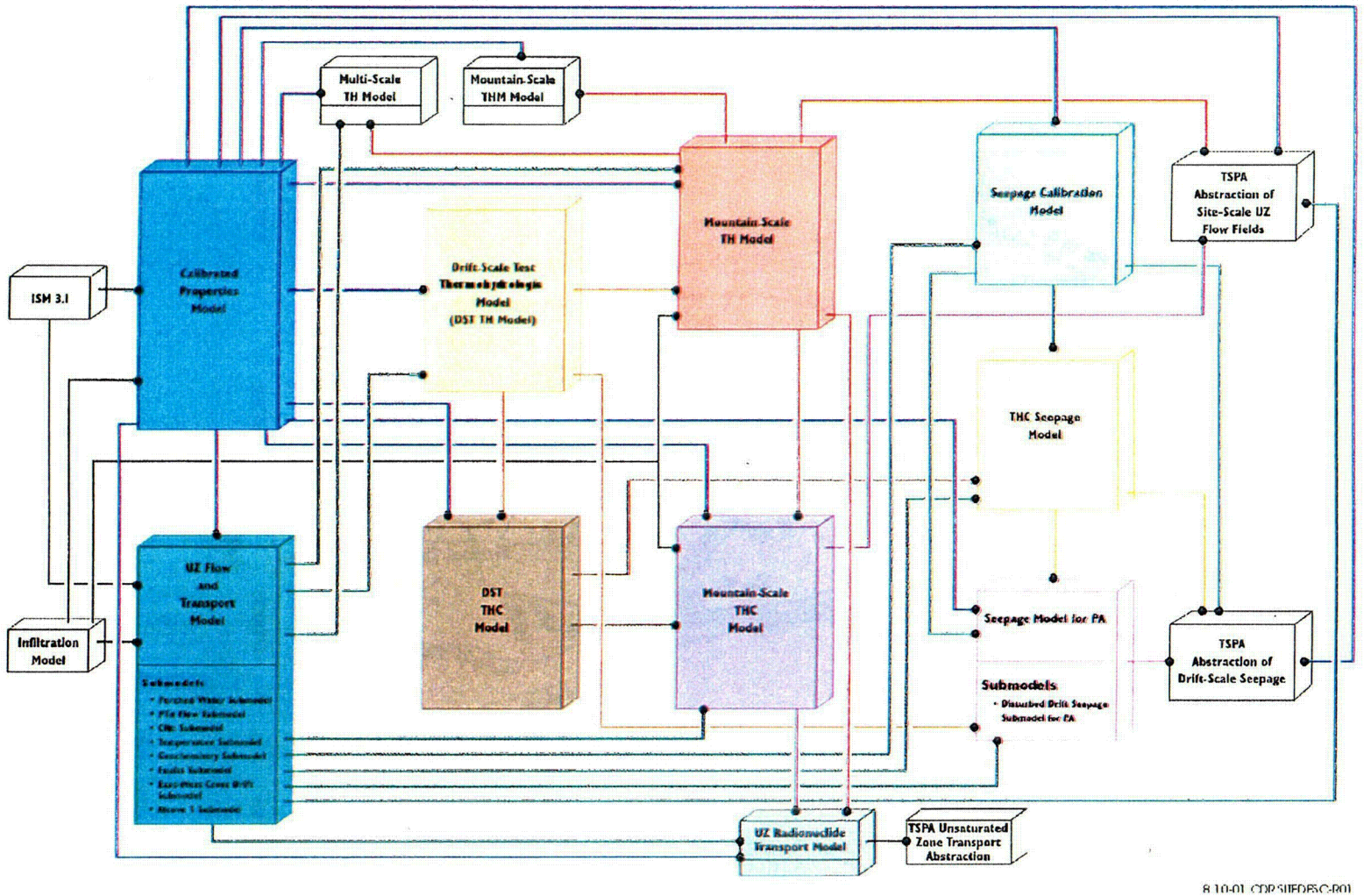

NOTES: ISM = integrated site model; TH = thermohydrologic; THM = thermohydrologic-mechanical; DST = Drift Scale Test; TSPA = total system performance assessment; UZ = unsaturated zone; THC = thermohydrologic-chemical; PA = performance assessment

Figure 8.10-1. Schematic Diagram of the Relationships among the Various Process Models and Performance Assessment Abstractions for the Unsaturated Zone at Yucca Mountain

C079

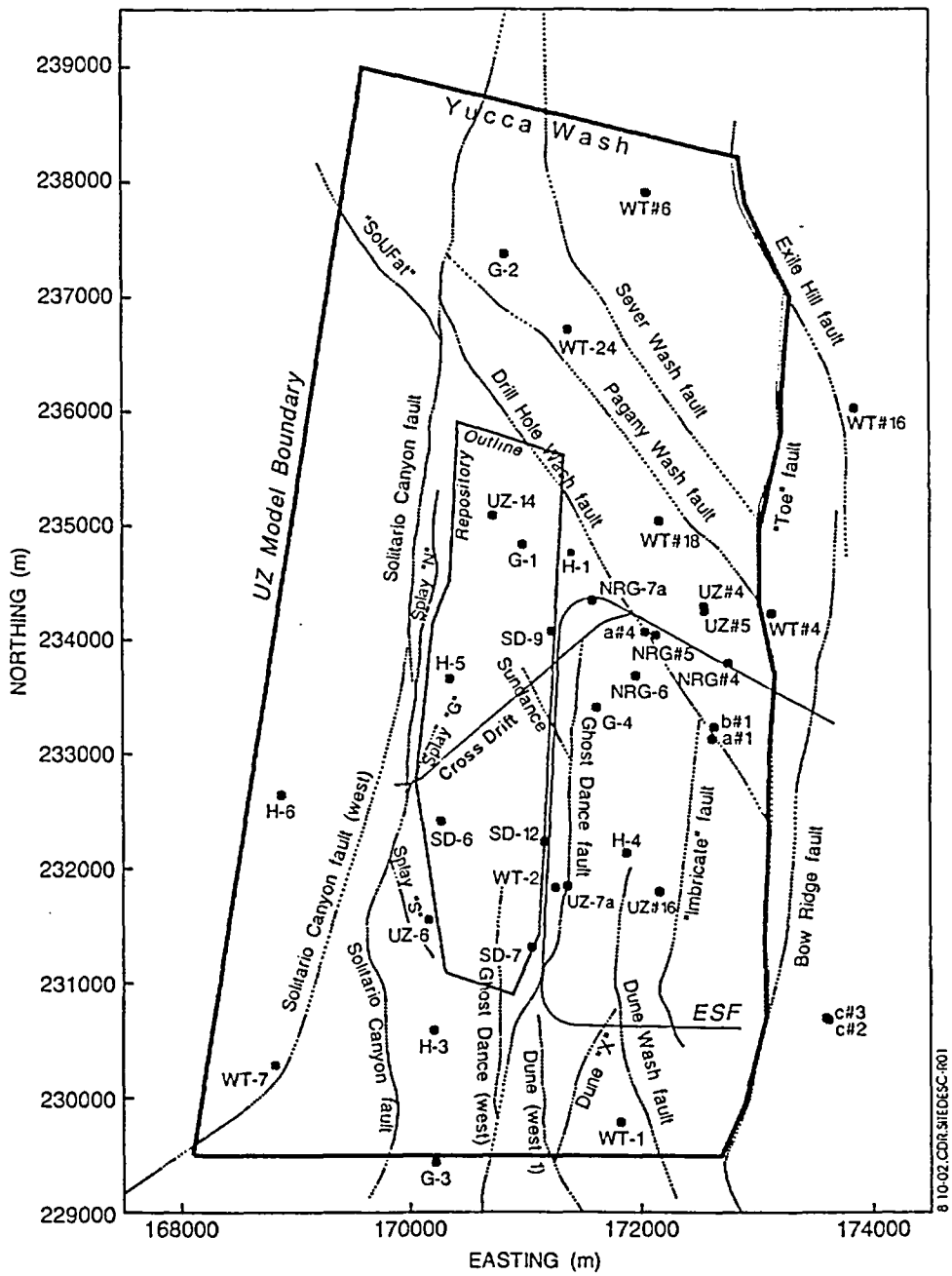

Source: CRWMS M&O (2000e, Figure 1)

Figure 8.10-2. Plan View of the Unsaturated Zone Flow and Transport Model Domain Showing the Model Boundary, the Potential Repository Area, Locations of Major Faults Derived from the Geologic Framework Model Version 3.1, Selected Boreholes, and the Locations of the Exploratory Studies Facility and the Enhanced Characterization of the Repository Block Cross Drift

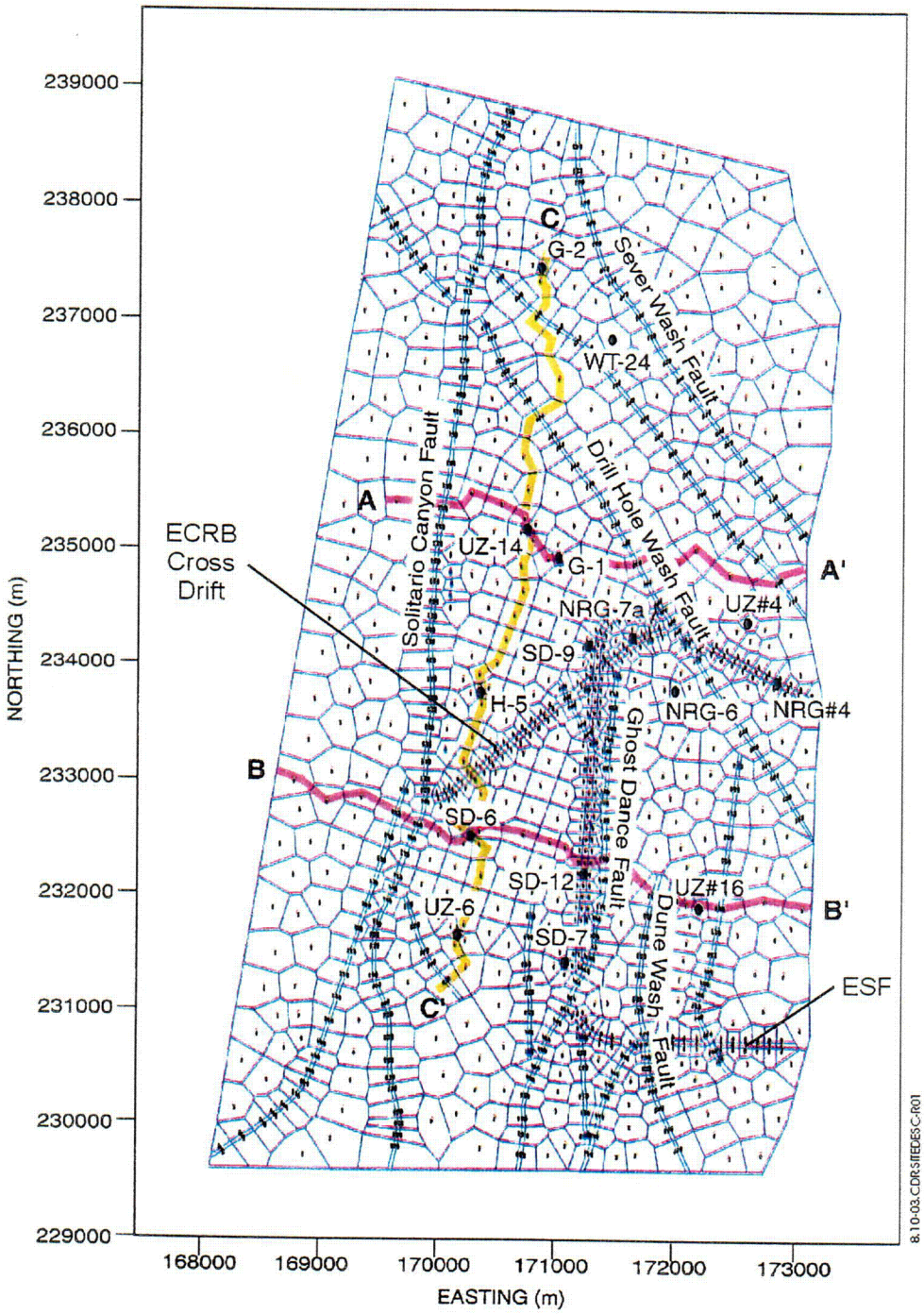

Source: CRWMS M&O (2000e, Figure V-1)

NOTE: Cross section B-B' is illustrated in Figure 8.10-5.

Figure 8.10-3. Two-Dimensional Plan View of Numerical Grid Used for Fiscal Year 1999 Unsaturated Zone Model Calibration

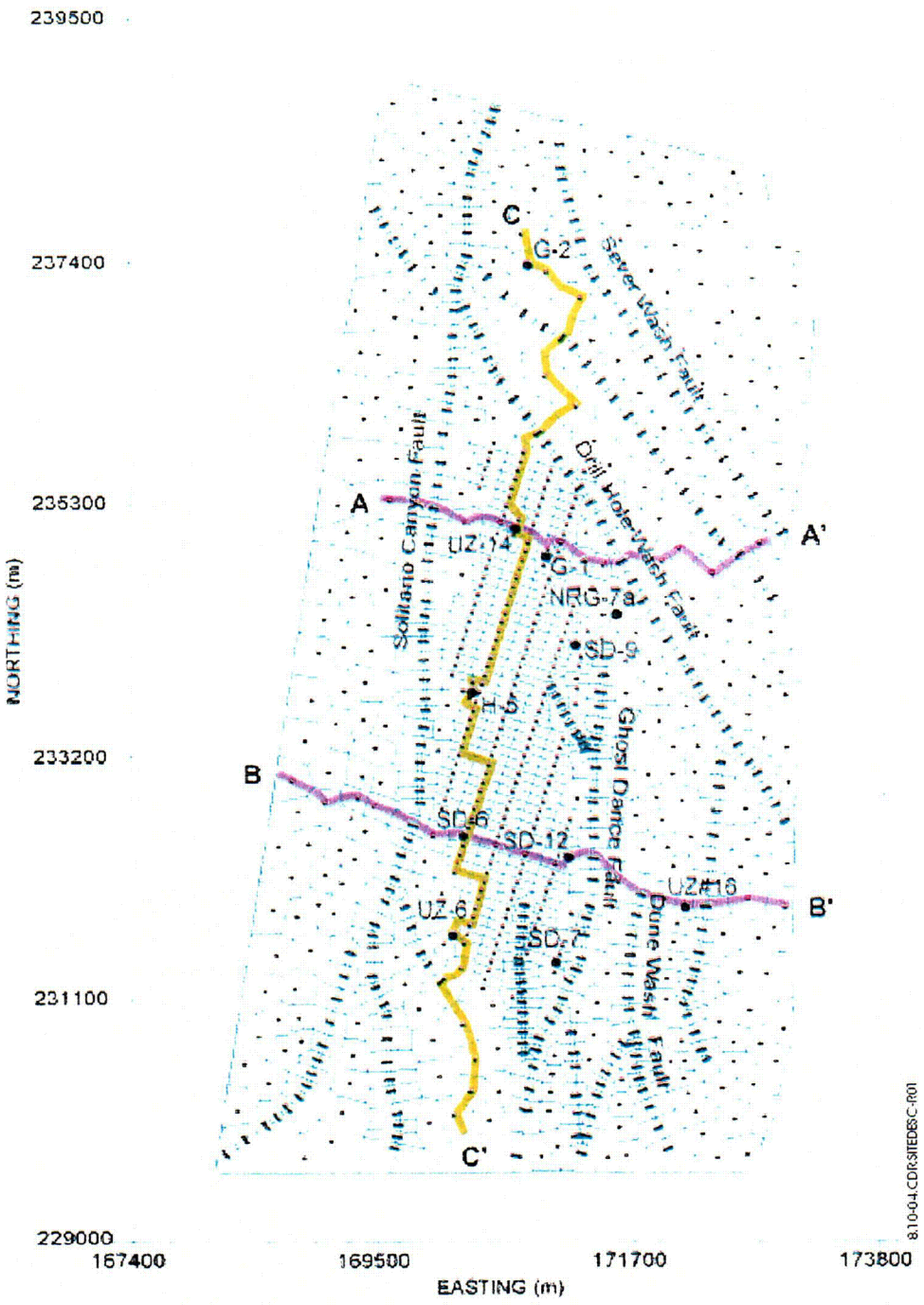

Source: CRWMS M&O (2000e, Figure VI-1)

NOTE: Cross section B-B' is illustrated in Figure 8.10-5.

Figure 8.10-4. Two-Dimensional Plan View of Numerical Grid Used for Fiscal Year 1999 Unsaturated Zone Model Flow-Field Calculations

C081

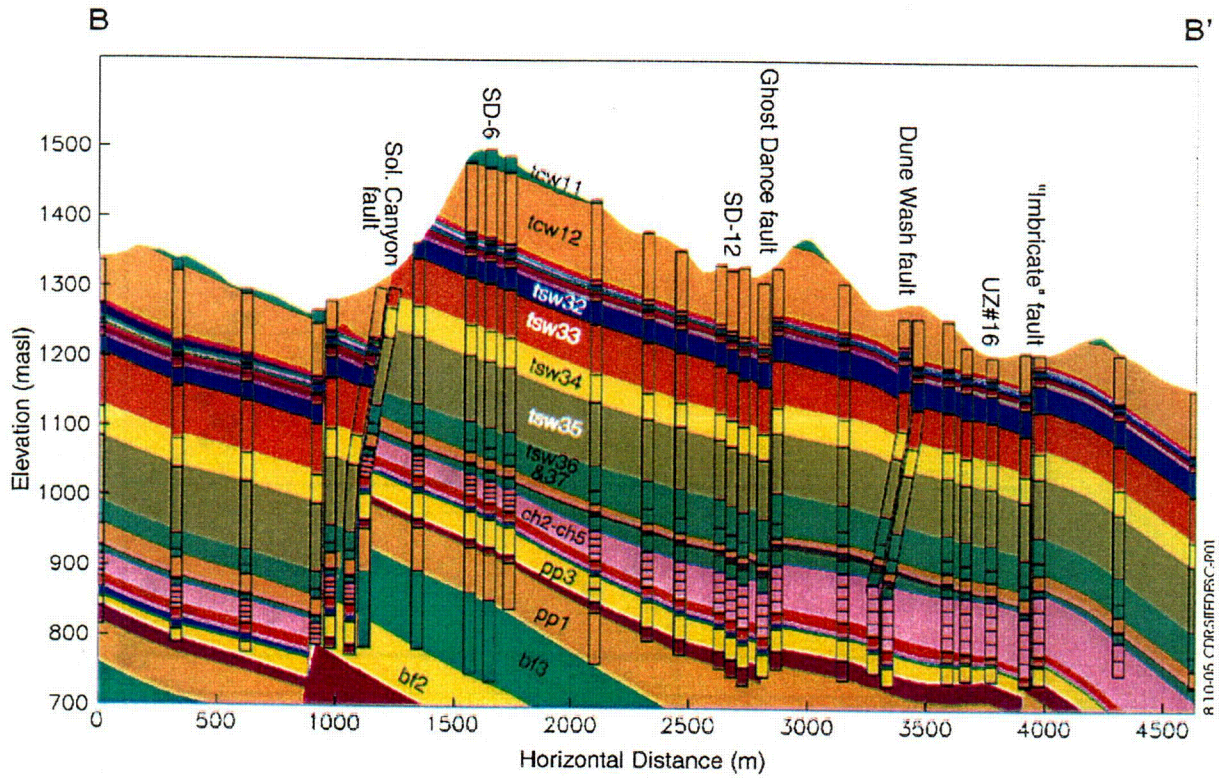

Source: CRWMS M&O (2000e, Figure V-7)

NOTES: Trace of cross section B-B' is shown on Figures 8.10-3 and 8.10-4.
masl = meters above sea level

Figure 8.10-5. East-West Cross Section through Yucca Mountain along B-B' Showing Layers and Selected Columns from the Unsaturated Zone Model Calibration Grid along with the Geologic Framework Model, Version 3.1, Stratigraphy

C082

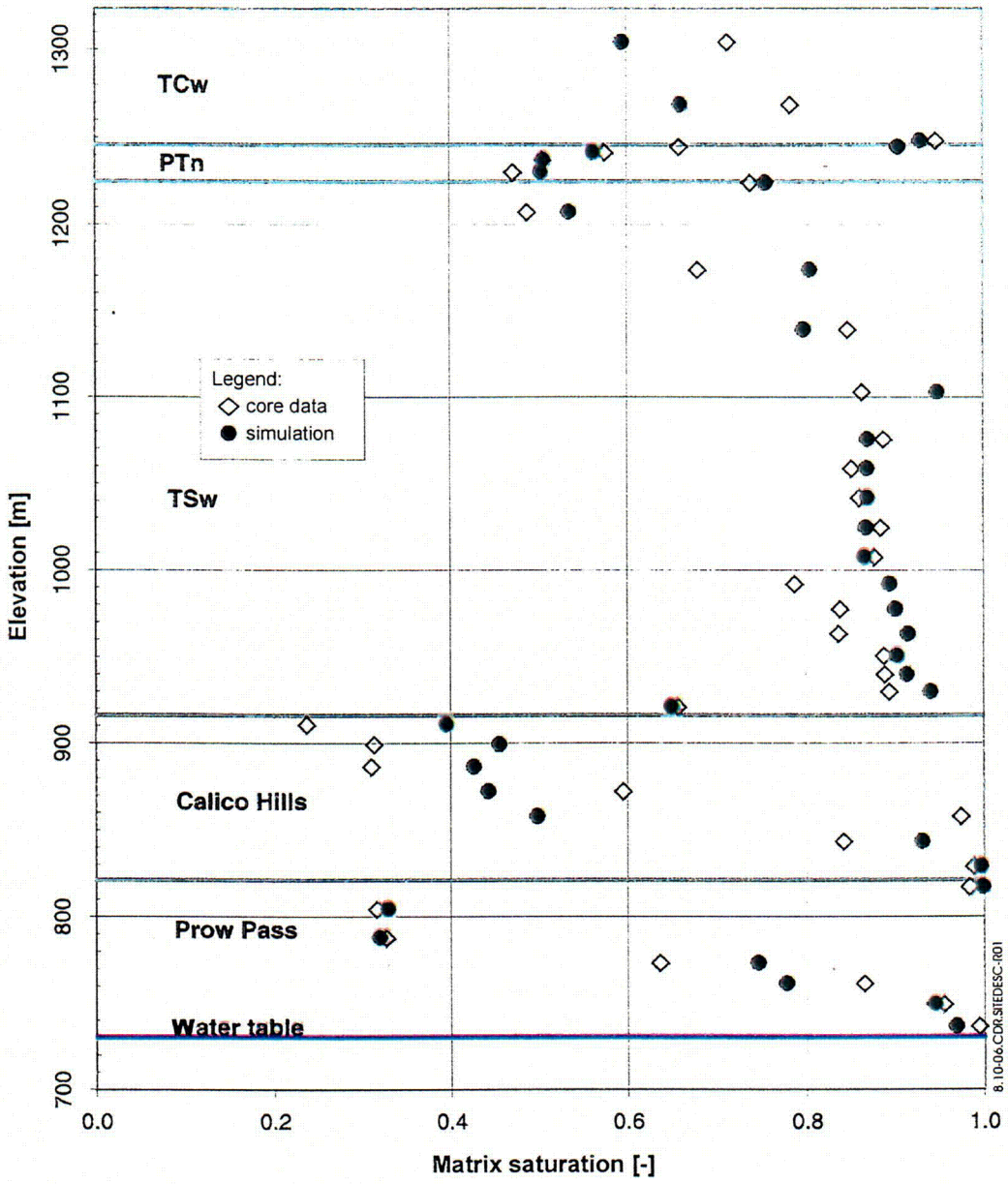

Source: CRWMS M&O (2000f, Figure 2)

Figure 8.10-6. Simulated and Measured Rock Core Saturation at Borehole USW SD-12 Using the Calibrated Parameter Set from the One-Dimensional Mountain-Scale Inversion for Base-Case Infiltration

C083

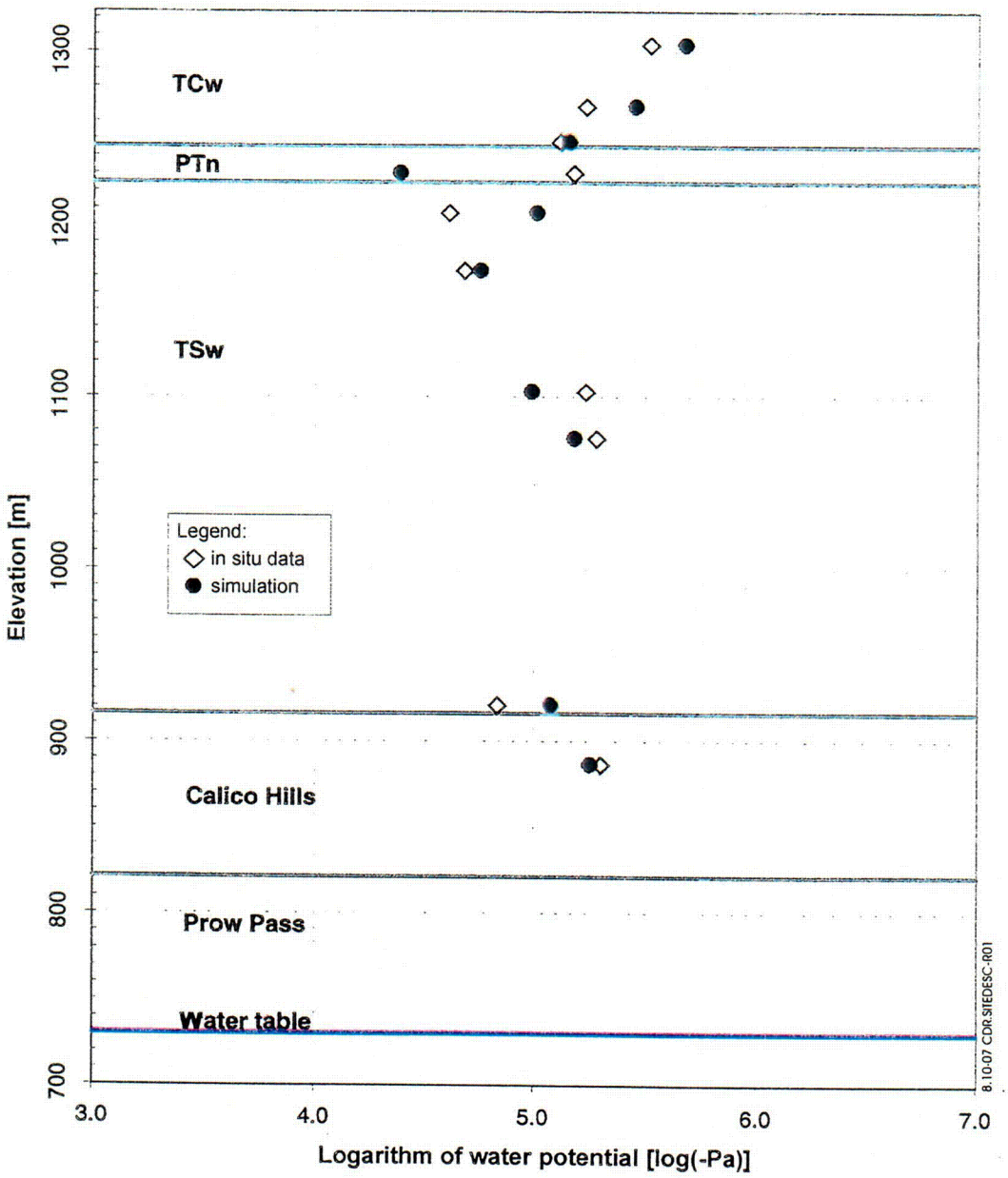

Source: CRWMS M&O (2000f, Figure 3)

Figure 8.10-7. Simulated and Measured In Situ Water Potential at Borehole USW SD-12 Using the Calibrated Parameter Set from the One-Dimensional Mountain-Scale Inversion for Base-Case Infiltration

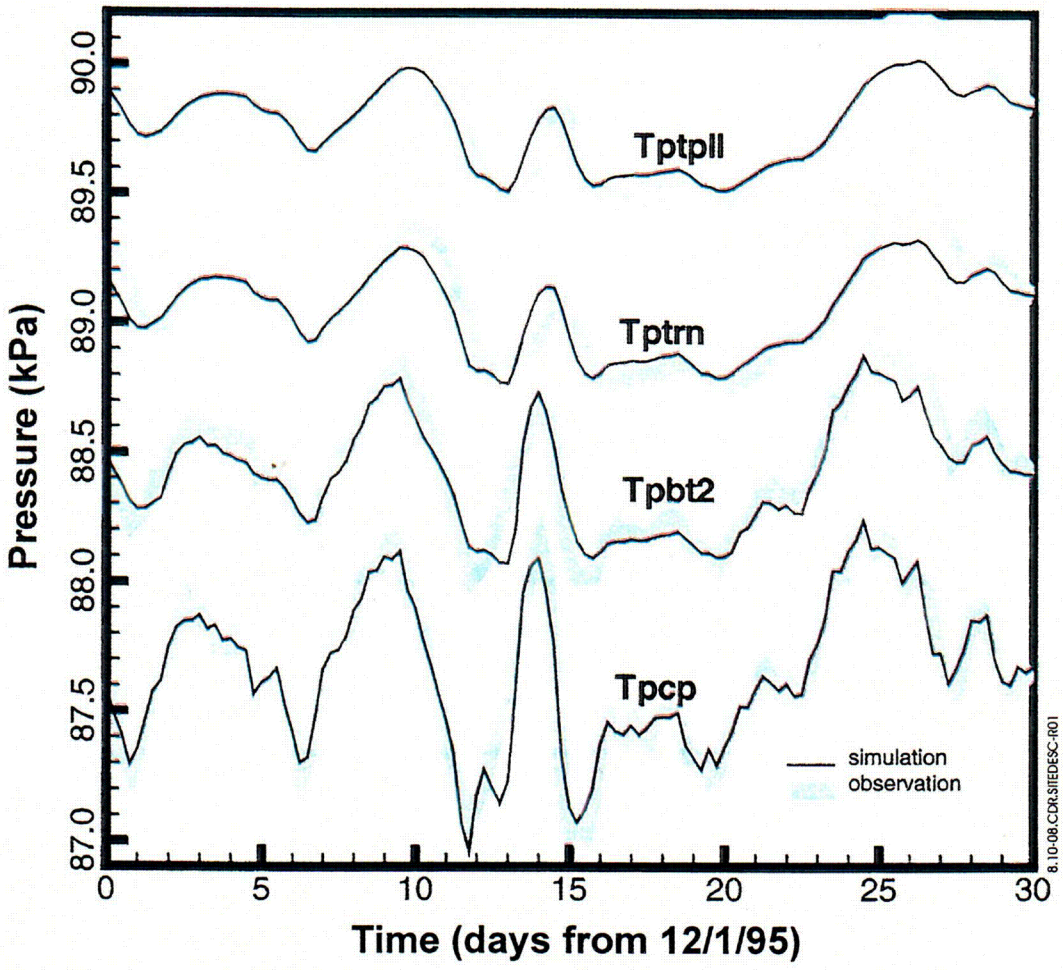

Source: CRWMS M&O (2000f, Figure 4)

Figure 8.10-8. Simulated and Measured Pneumatic Pressure at Borehole USW SD-12 Using the Calibrated Parameter Set from the One-Dimensional Mountain-Scale Inversion for Base-Case Infiltration

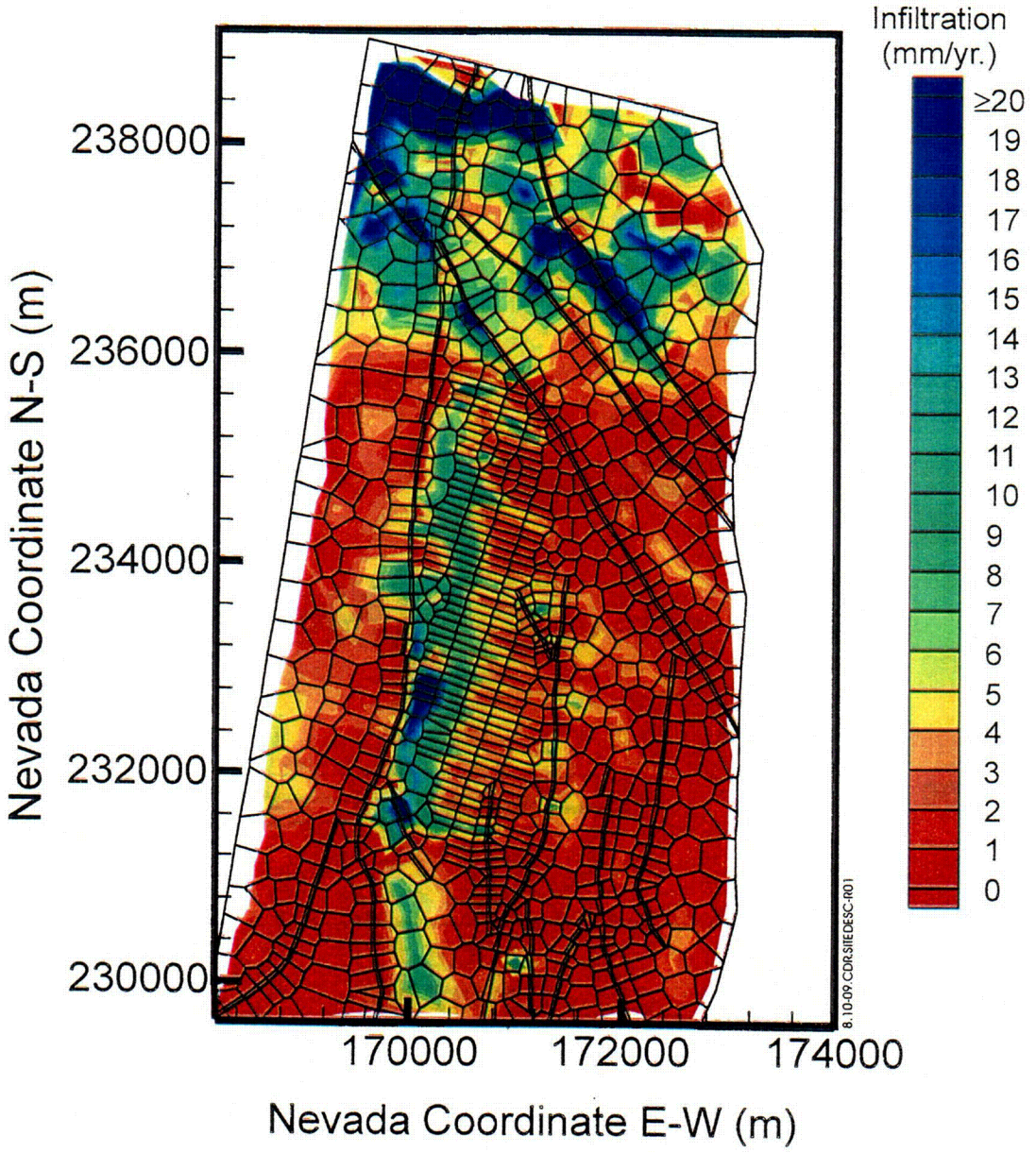

Source: CRWMS M&O (2000d, Figure 6-3)

Figure 8.10-9. Plan View of the Spatial Distribution of Present-Day Mean Infiltration Interpolated onto the Unsaturated Zone Model Flow-Field Grid

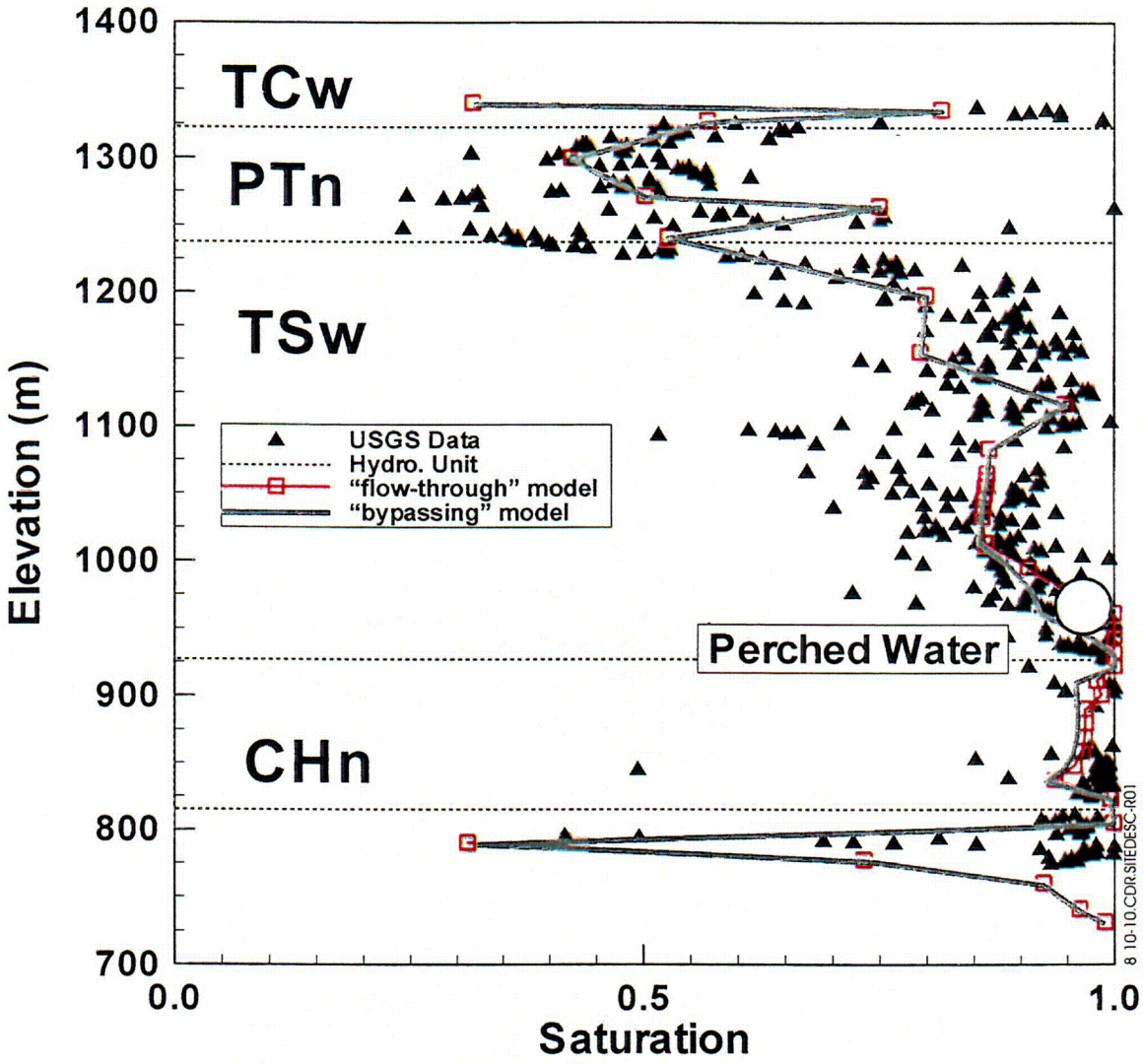

Source: CRWMS M&O (2000d, Figure 6-6)

Figure 8.10-10. Comparison of Measured Matrix Liquid Saturation and Perched-Water Elevation for Borehole UZ-14 and Simulated Saturation for Present-Day Mean Infiltration Using Both the Flow-Through and Bypassing Perched-Water Conceptual Models

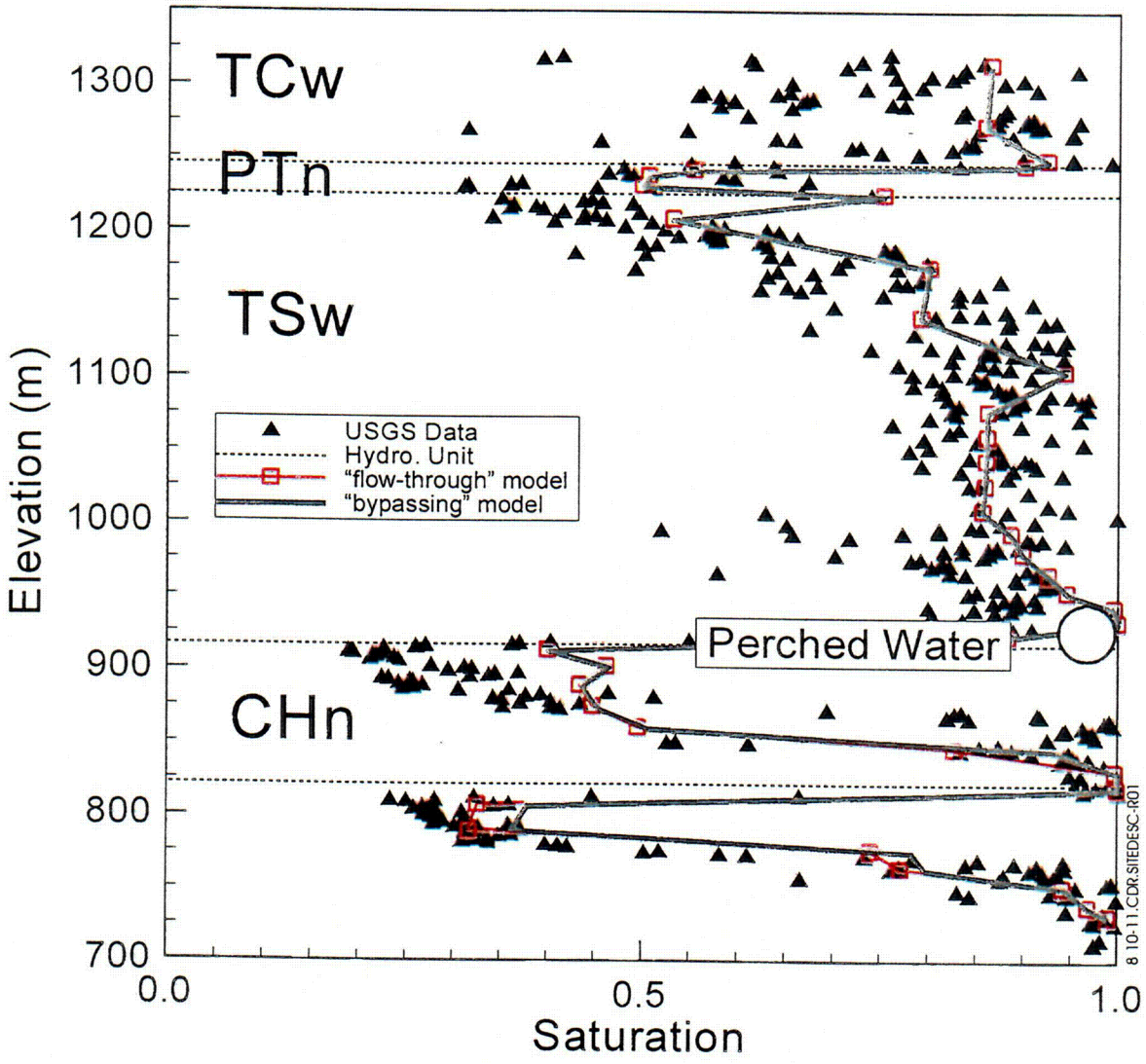

Source: CRWMS M&O (2000d, Figure 6-7)

Figure 8.10-11. Comparison of Measured Matrix Liquid Saturation and Perched-Water Elevation for Borehole USW SD-12 and Simulated Saturation for Present-Day Mean Infiltration Using Both the Flow-Through and Bypassing Perched-Water Conceptual Models

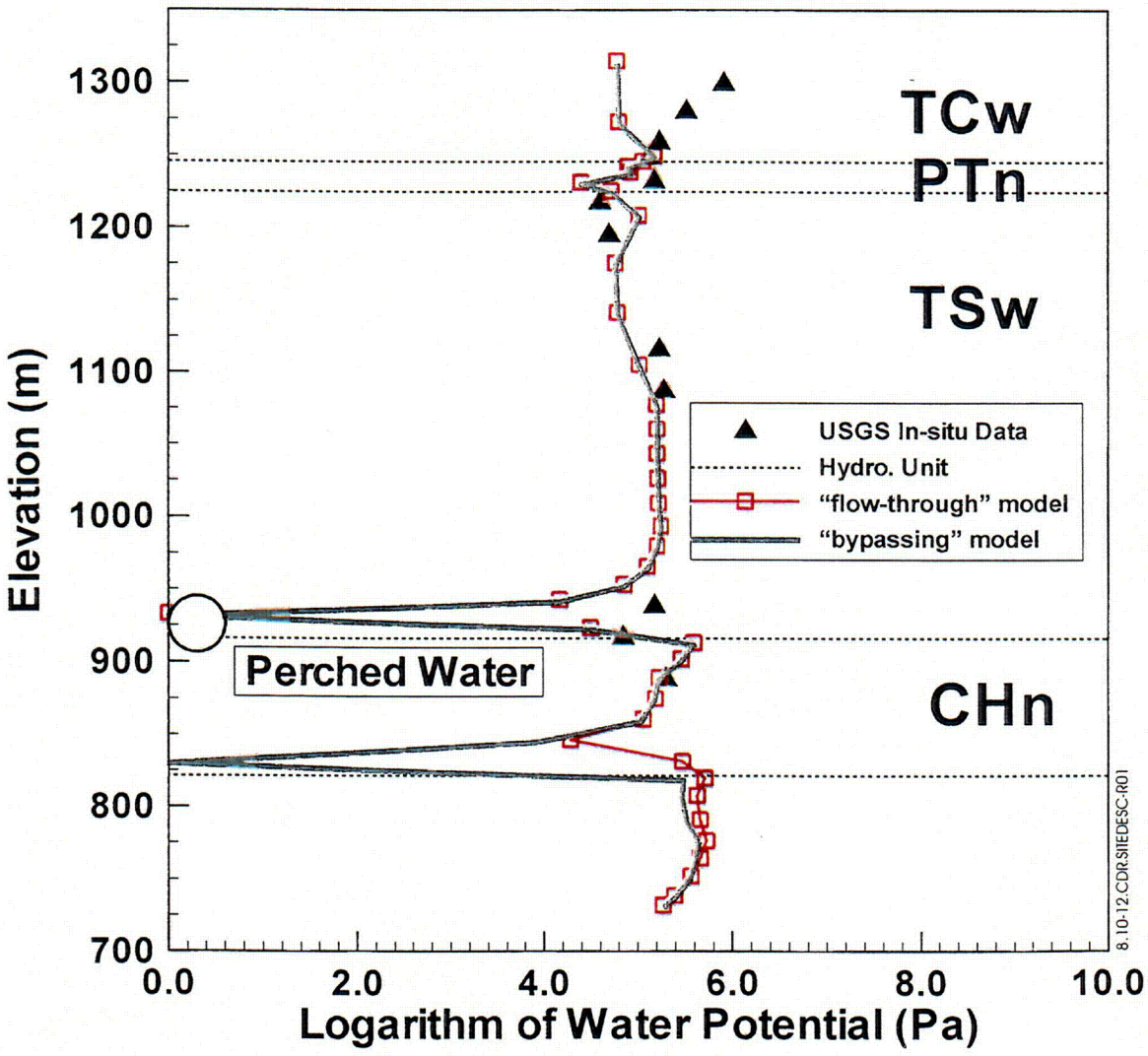

Source: CRWMS M&O (2000d, Figure 6-8)

Figure 8.10-12. Comparison of Measured Matrix Water Potential and Perched-Water Elevation for Borehole USW SD-12 and Simulated Water Potential for Present-Day Mean Infiltration Using Both the Flow-Through and Bypassing Perched-Water Conceptual Models

C089

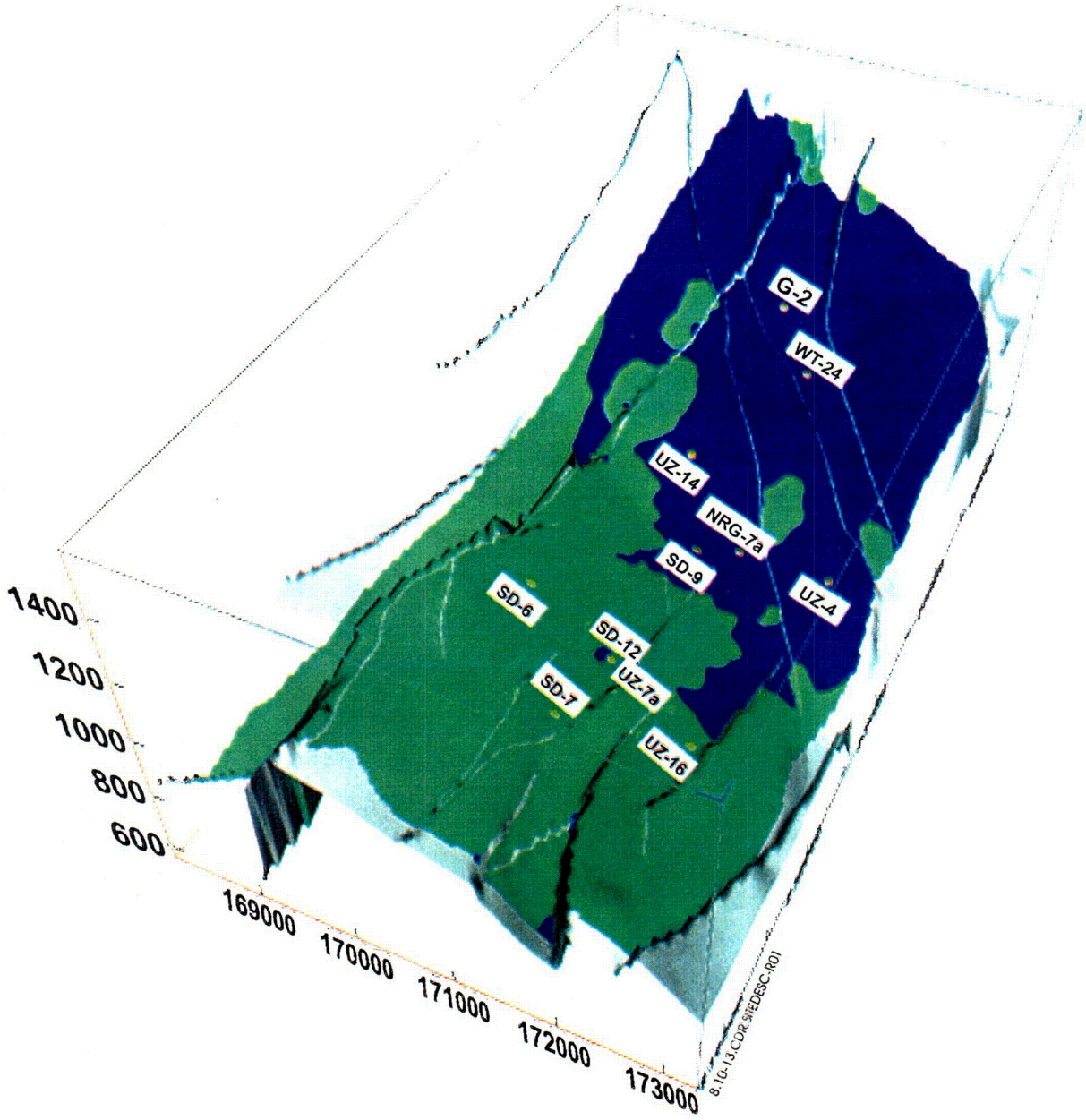

Source: CRWMS M&O (2000d, Figure 6-9)

NOTE: In the dark blue areas, fractures in the lowest layer of the Topopah Spring welded unit have liquid saturations of 100 percent (perched-water zones); in the green areas, fractures have liquid saturations of less than 100 percent.

Figure 8.10-13. Perspective View of Simulated Three-Dimensional Perched Water Bodies within the Unsaturated Zone Flow and Transport Model Domain for the Flow-Through Conceptual Model under Present-Day Mean Infiltration

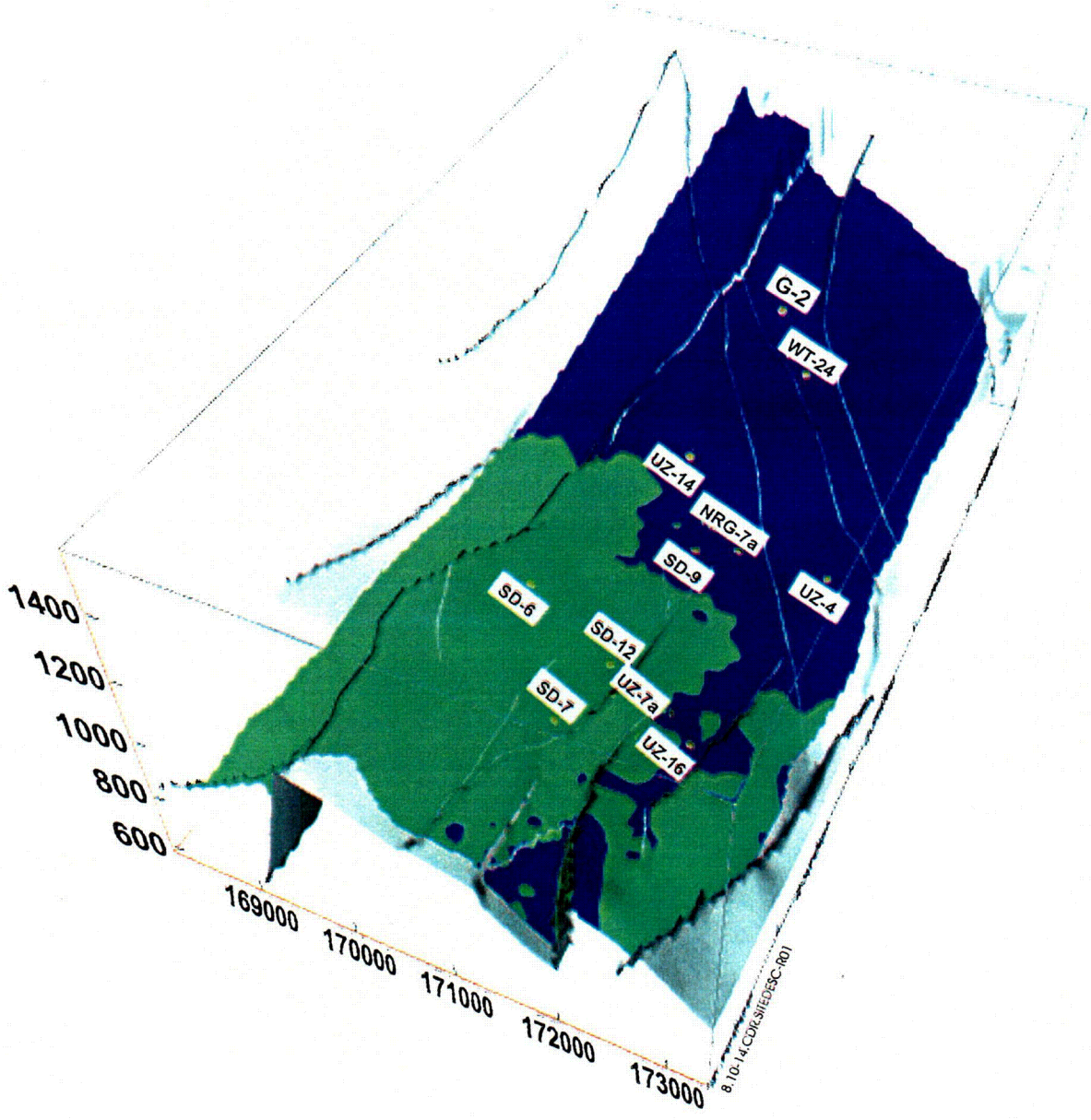

Source: CRWMS M&O (2000d, Figure 6-10)

NOTE: In the dark blue areas, fractures in the uppermost zeolitic layer of the Calico Hills nonwelded unit have liquid saturations of 100 percent (perched-water zones); in the green areas, fractures have liquid saturations of less than 100 percent.

Figure 8.10-14. Perspective View of Simulated Three-Dimensional Perched-Water Bodies within the Unsaturated Zone Flow and Transport Model Domain for the Bypassing Conceptual Model under Present-Day Mean Infiltration

C091

a)

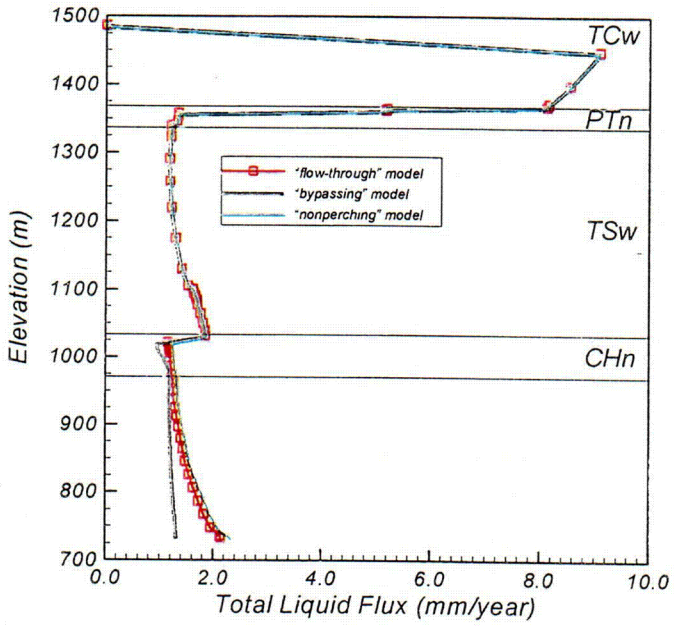

b)

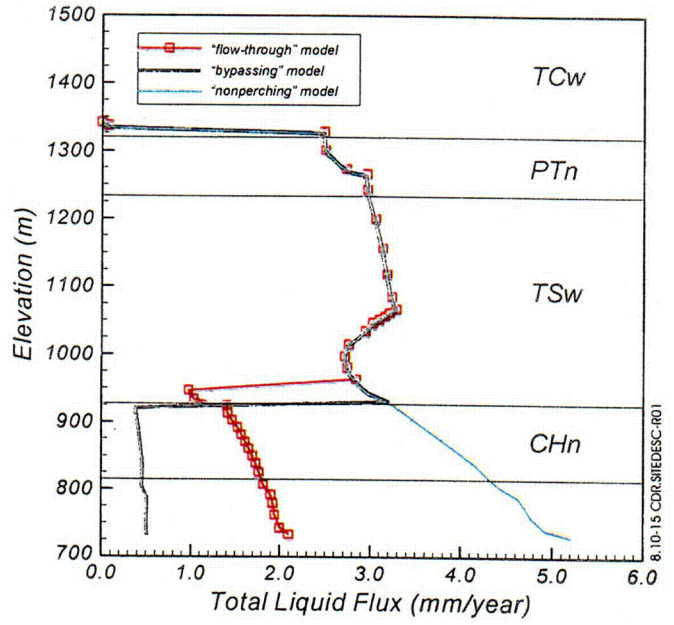

Source: CRWMS M&O (2000d, Figures 6-14b, 6-15b)

NOTE: Part (a) shows simulated vertical percolation flux at borehole USW SD-6. Part (b) shows simulated vertical percolation flux at borehole USW UZ-14.

Figure 8.10-15. Simulated Vertical Percolation Fluxes for the Flow-Through, Bypassing, and Nonperching Conceptual Models under Present-Day Mean Infiltration

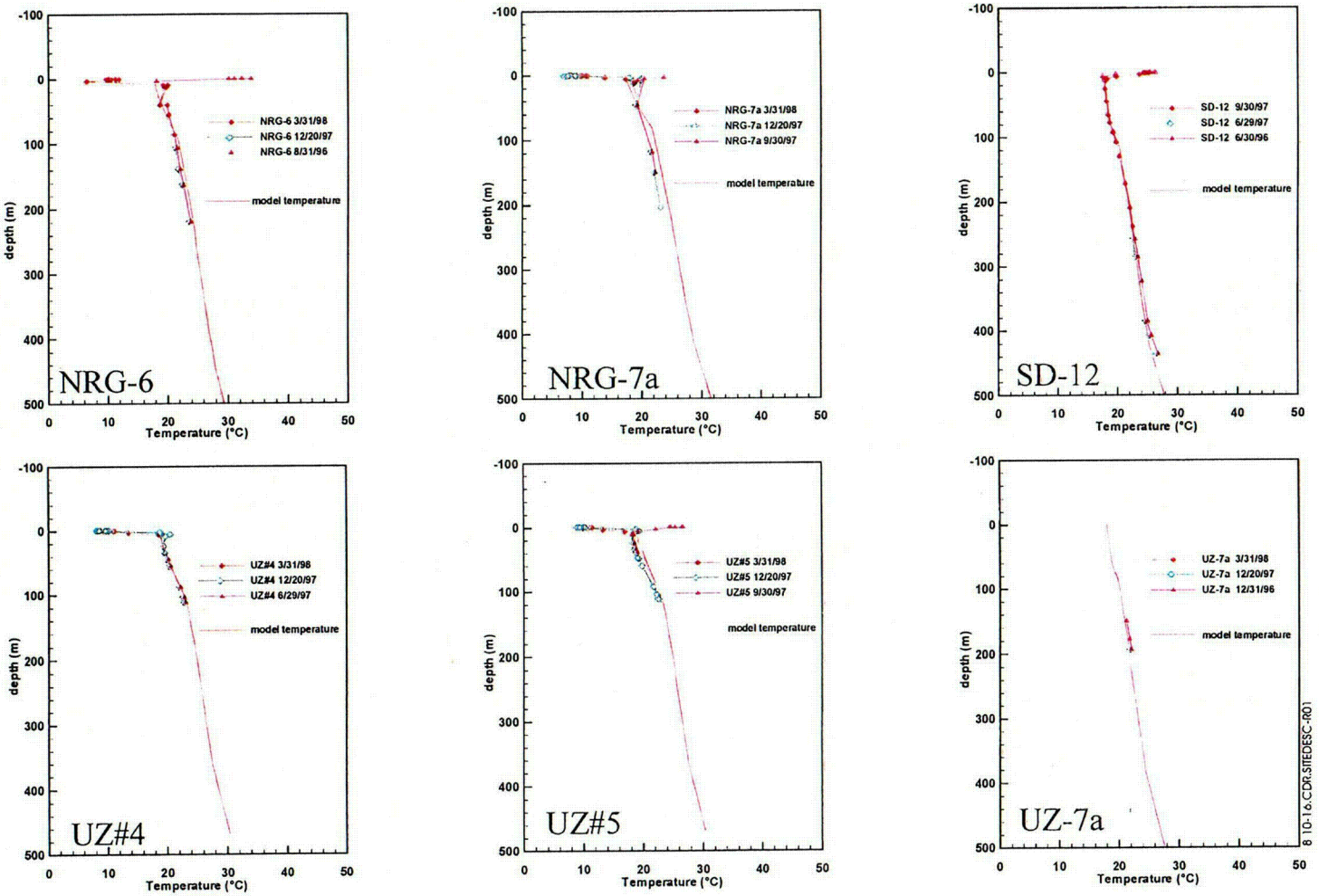

Source: CRWMS M&O (2000d, Figure 6-16)

Figure 8.10-16. Simulated and Measured Ambient Temperature Profiles for Six Boreholes Using the Effective Continuum Model Formulation of the Three-Dimensional Unsaturated Zone Flow and Transport Model, the Calibration Grid, and Present-Day Mean Infiltration

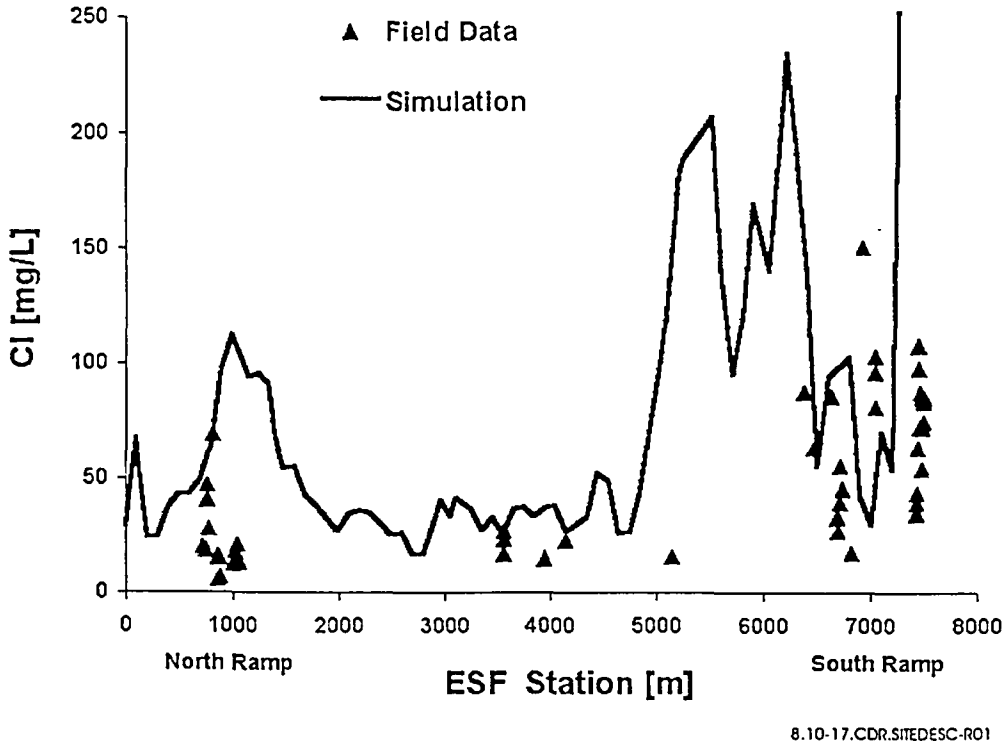

Source: CRWMS M&O (2000d, Figure 6-19)

Figure 8.10-17. Comparison of Measured Chloride Concentrations for Pore Water from the Exploratory Studies Facility, the Enhanced Characterization of the Repository Block Cross Drift, and Borehole UZ#16 and Simulated Chloride Concentrations Using the Geochemical Model and Present-Day Mean Infiltration

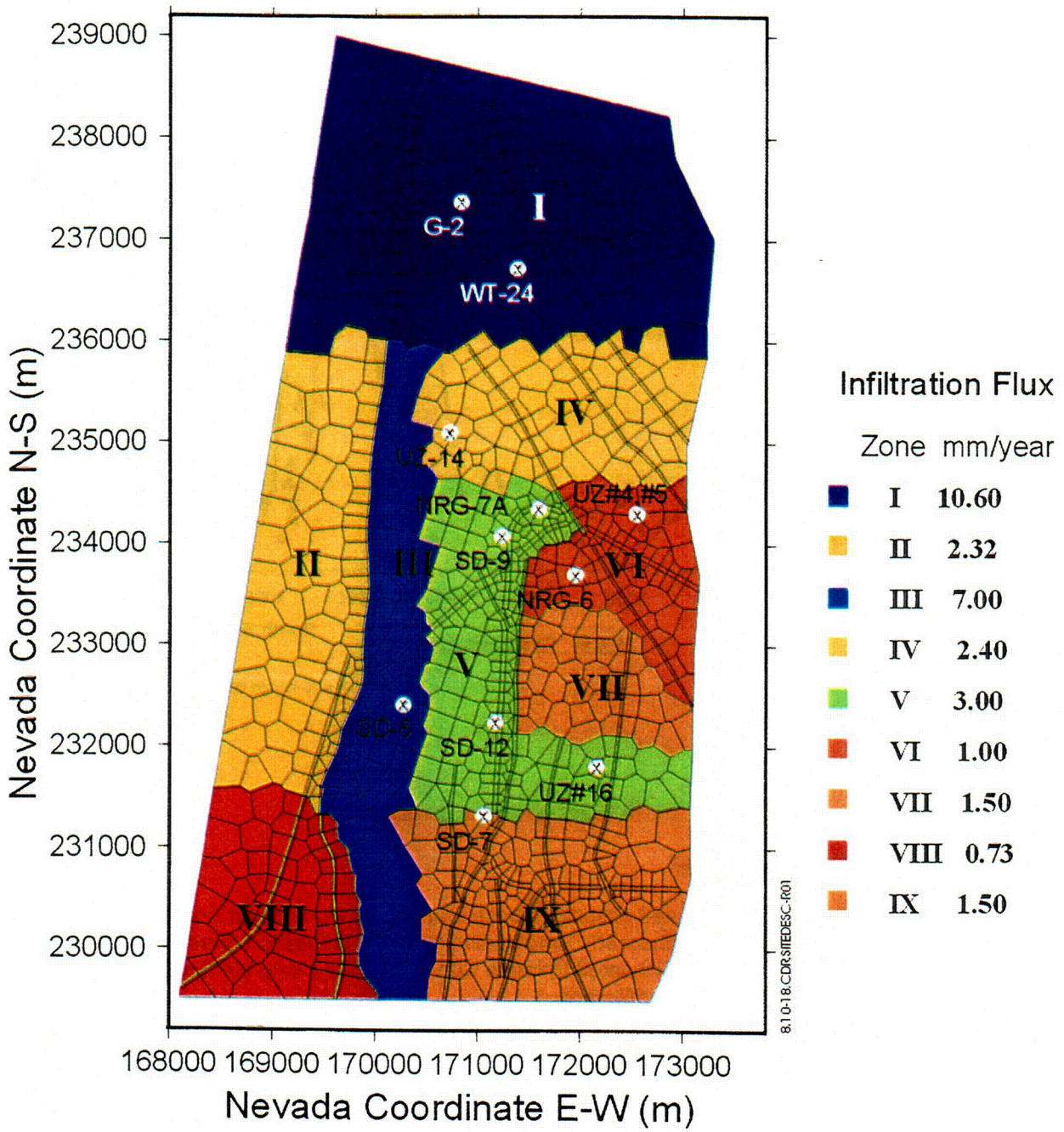

Source: CRWMS M&O (2000d, Figure 6-24)

Figure 8.10-18. Distribution of Net Infiltration Based on Chloride Concentrations Simulated with the Geochemical Model

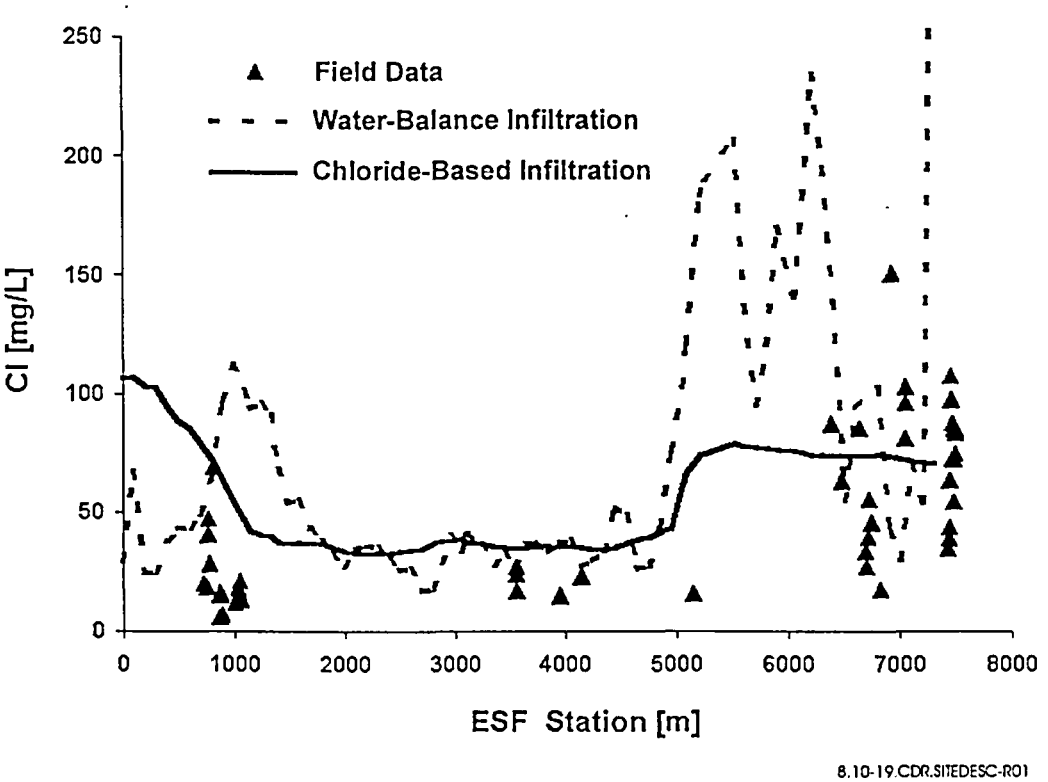

Source: CRWMS M&O (2000d, Figure 6-25)

Figure 8.10-19. Comparison of Measured Chloride Concentrations in Pore Water from the Exploratory Studies Facility and Simulated Concentrations Using Both the Water-Balance and Chloride-Based Infiltration Distributions

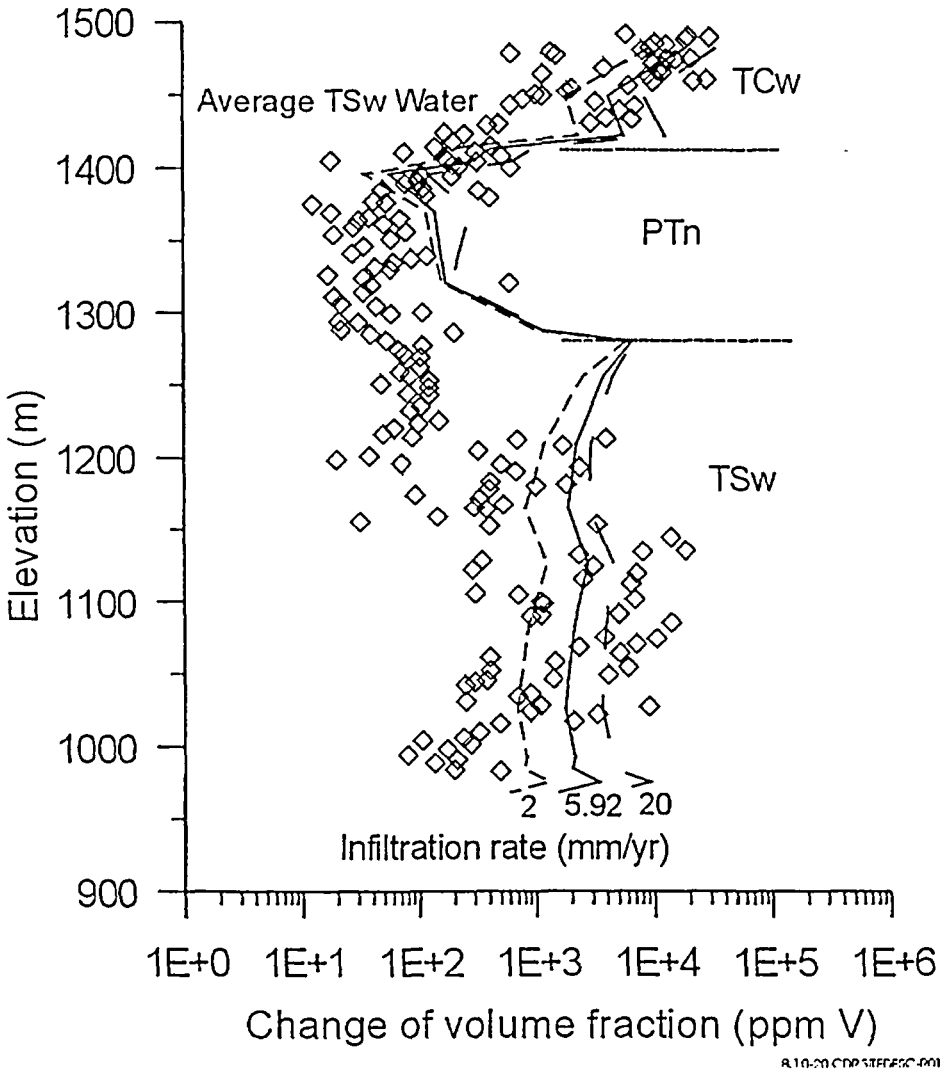

Source: CRWMS M&O (2000d, Figure 6-36)

NOTE: Lines denote the simulated calcite volume fraction changes; diamonds denote the measured calcite deposition data.

Figure 8.10-20. Comparison of Simulated Changes in Calcite Volume Fraction for Three Infiltration Rates after 10 Million Years and Measured Calcite Deposition Data for Borehole WT-24

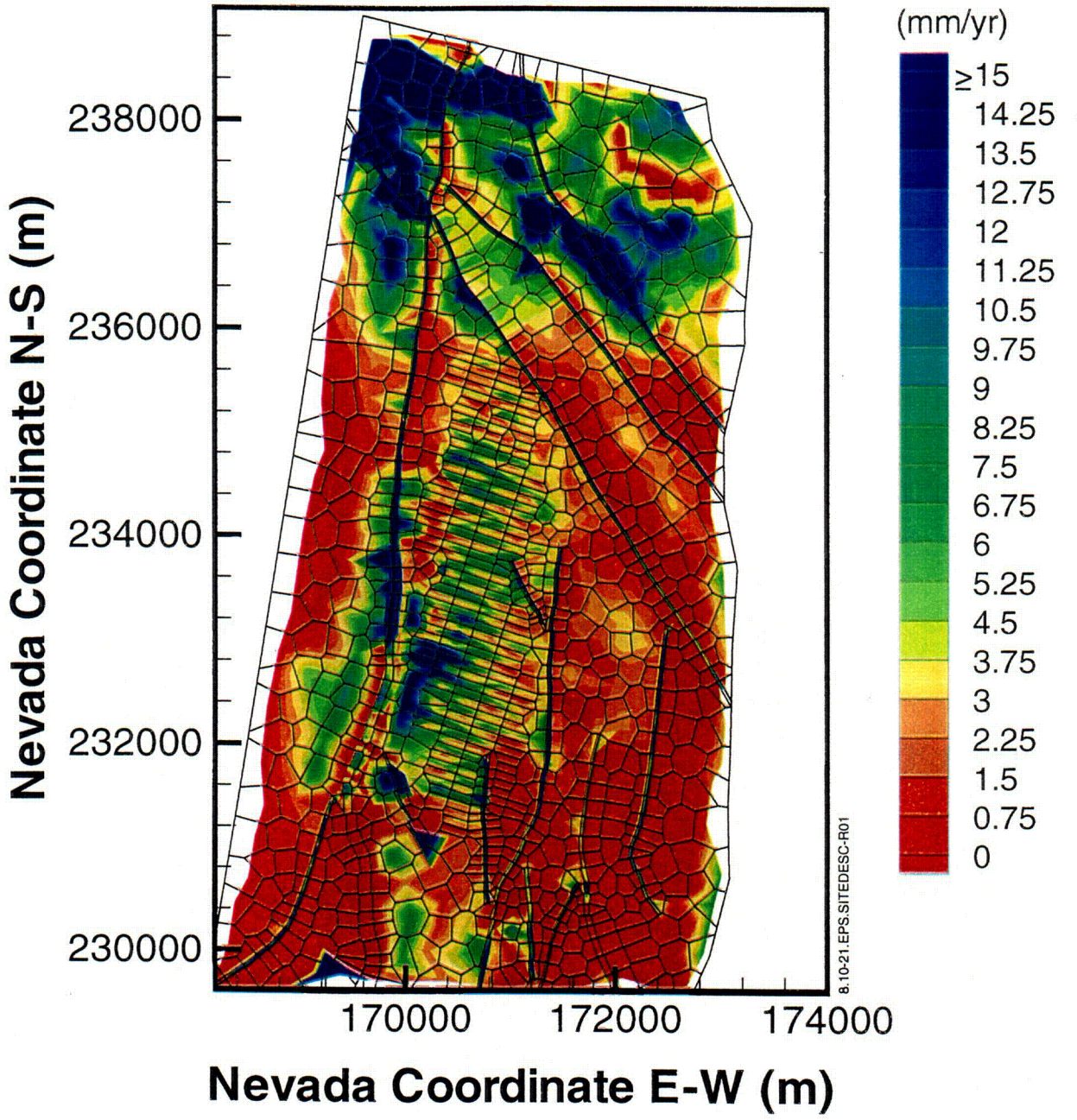

Source: CRWMS M&O (2000d, Figure 6-42)

Figure 8.10-21. Simulated Distribution of Percolation Flux at the Repository Horizon under the Mean Present-Day Infiltration Scenario

C095

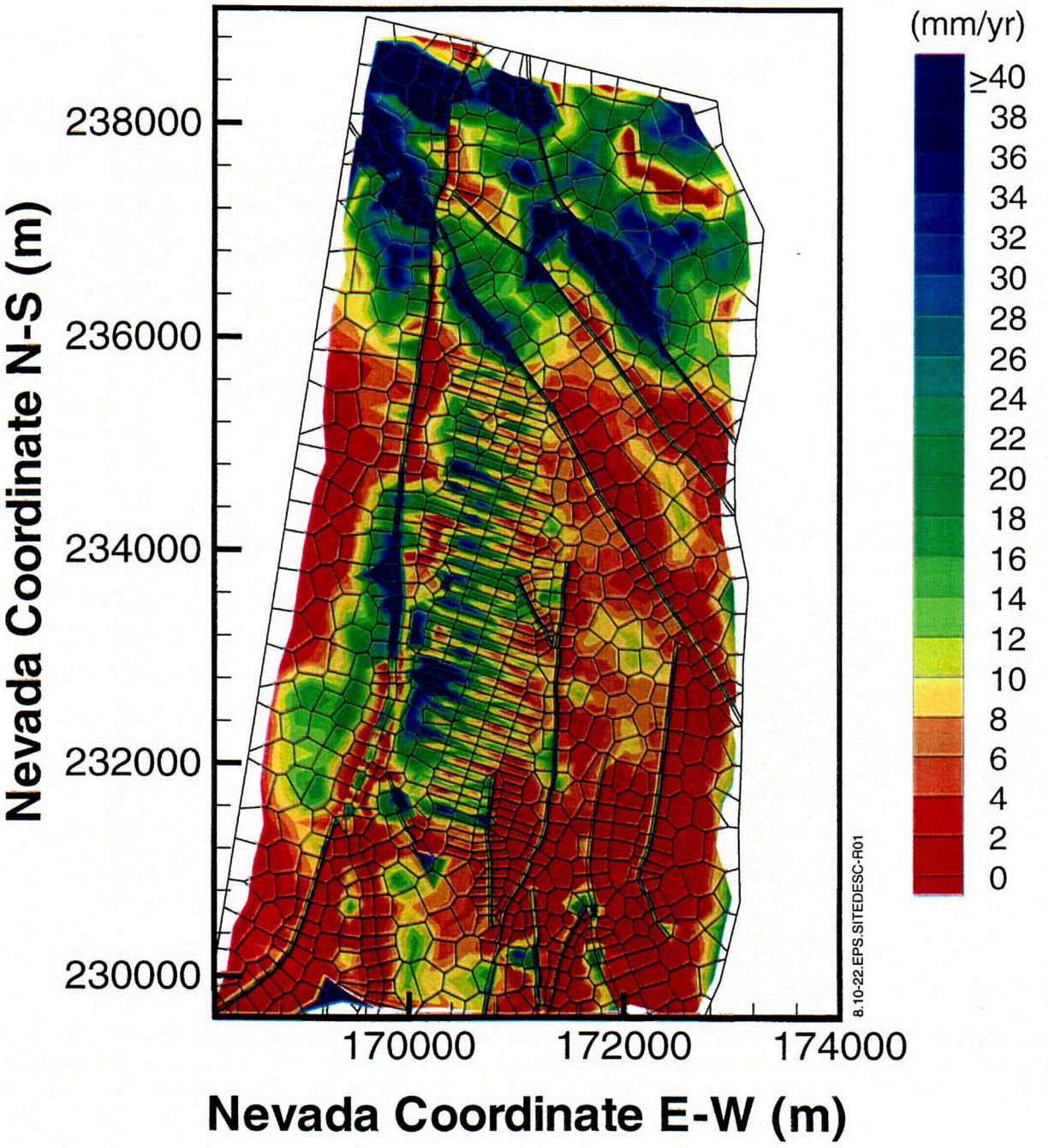

Source: CRWMS M&O (2000d, Figure 6-43)

Figure 8.10-22. Simulated Distribution of Percolation Flux at the Repository Horizon under the Mean Monsoon Infiltration Scenario

C096

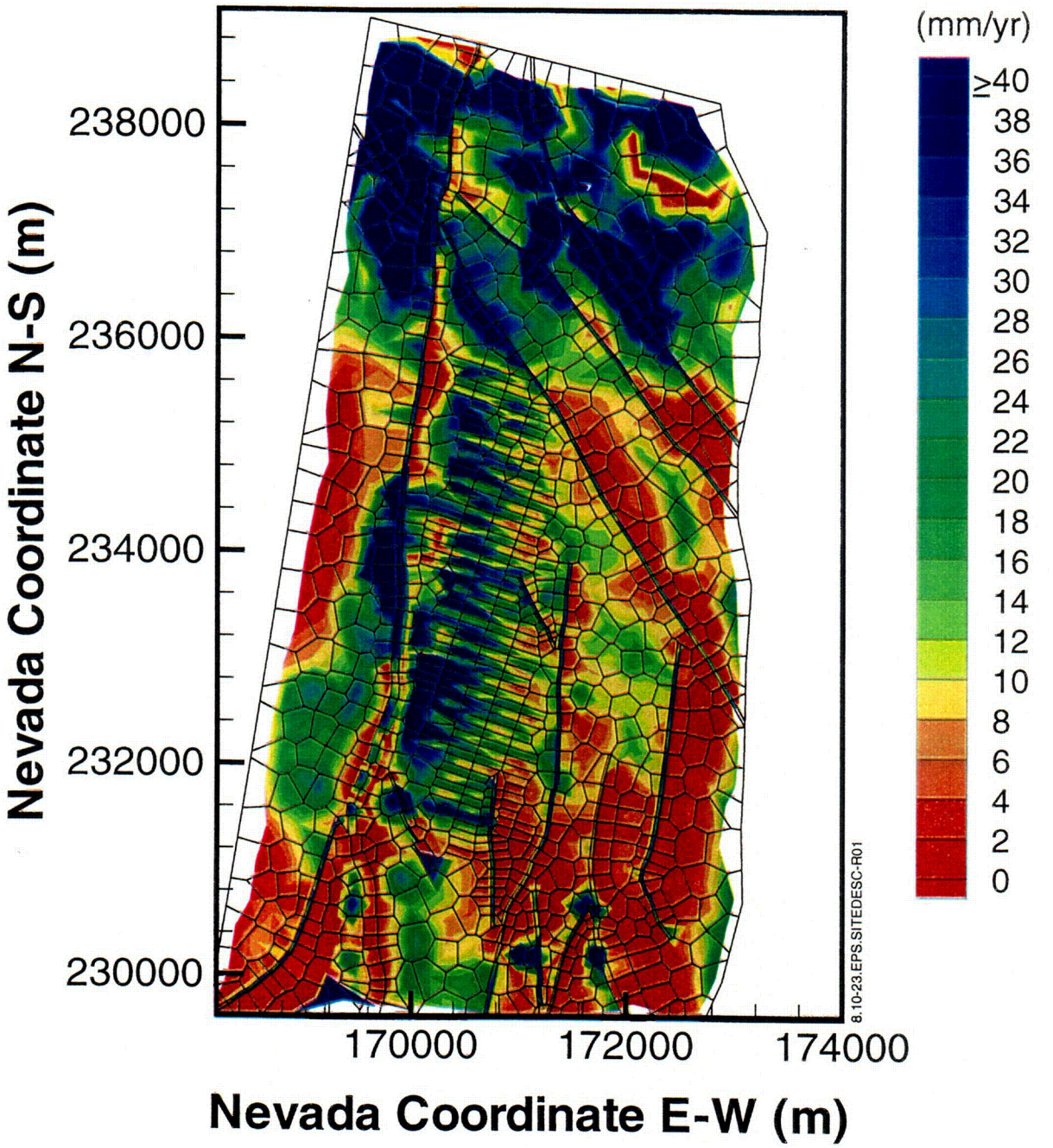

Source: CRWMS M&O (2000d, Figure 6-44)

Figure 8.10-23. Simulated Distribution of Percolation Flux at the Repository Horizon under the Mean Glacial Transition Infiltration Scenario

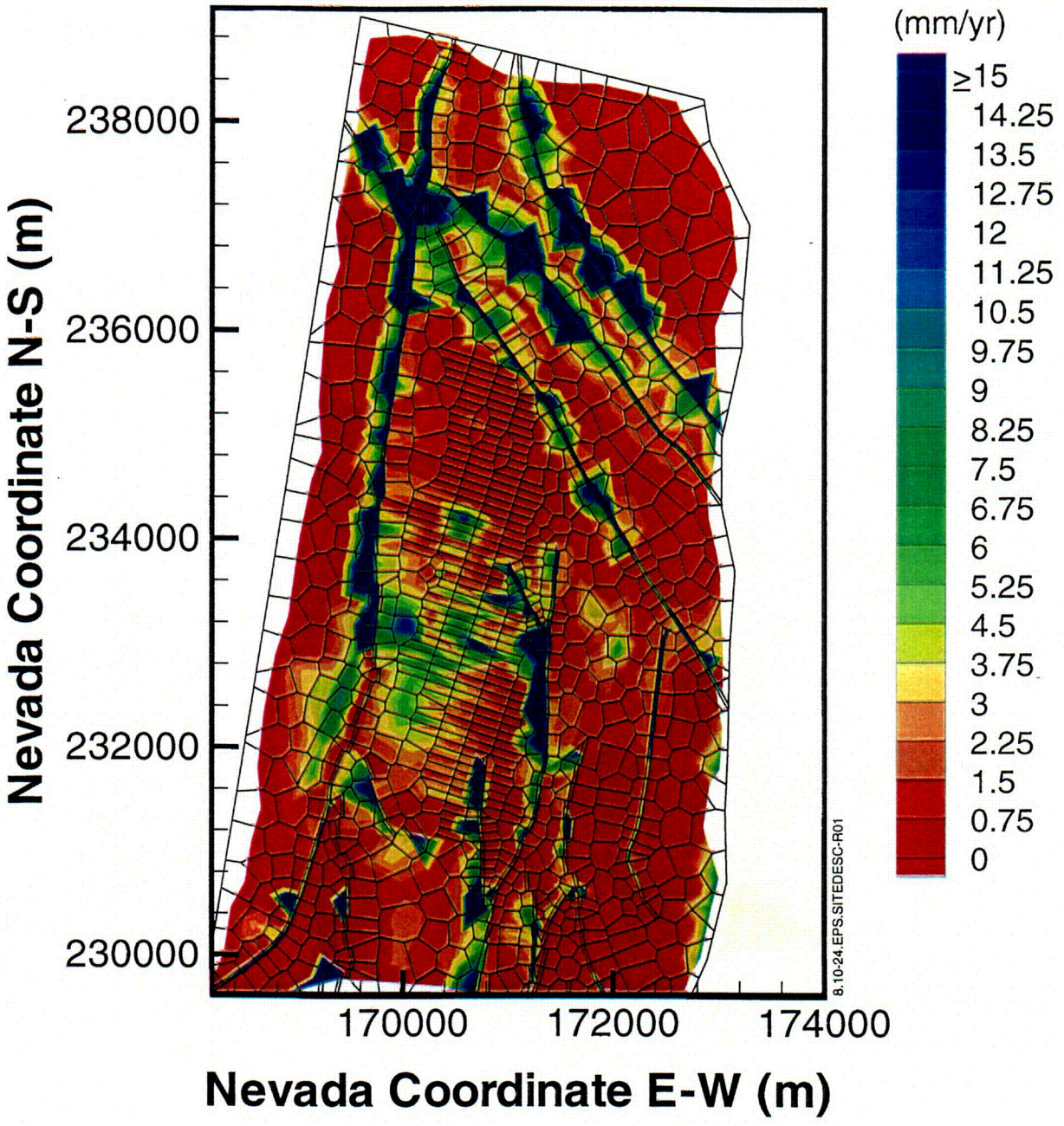

Source: CRWMS M&O (2000d, Figure 6-45)

Figure 8.10-24. Simulated Distribution of Percolation Flux at the Water Table under the Mean Present-Day Infiltration Scenario for the Flow-Through Perched-Water Conceptual Model

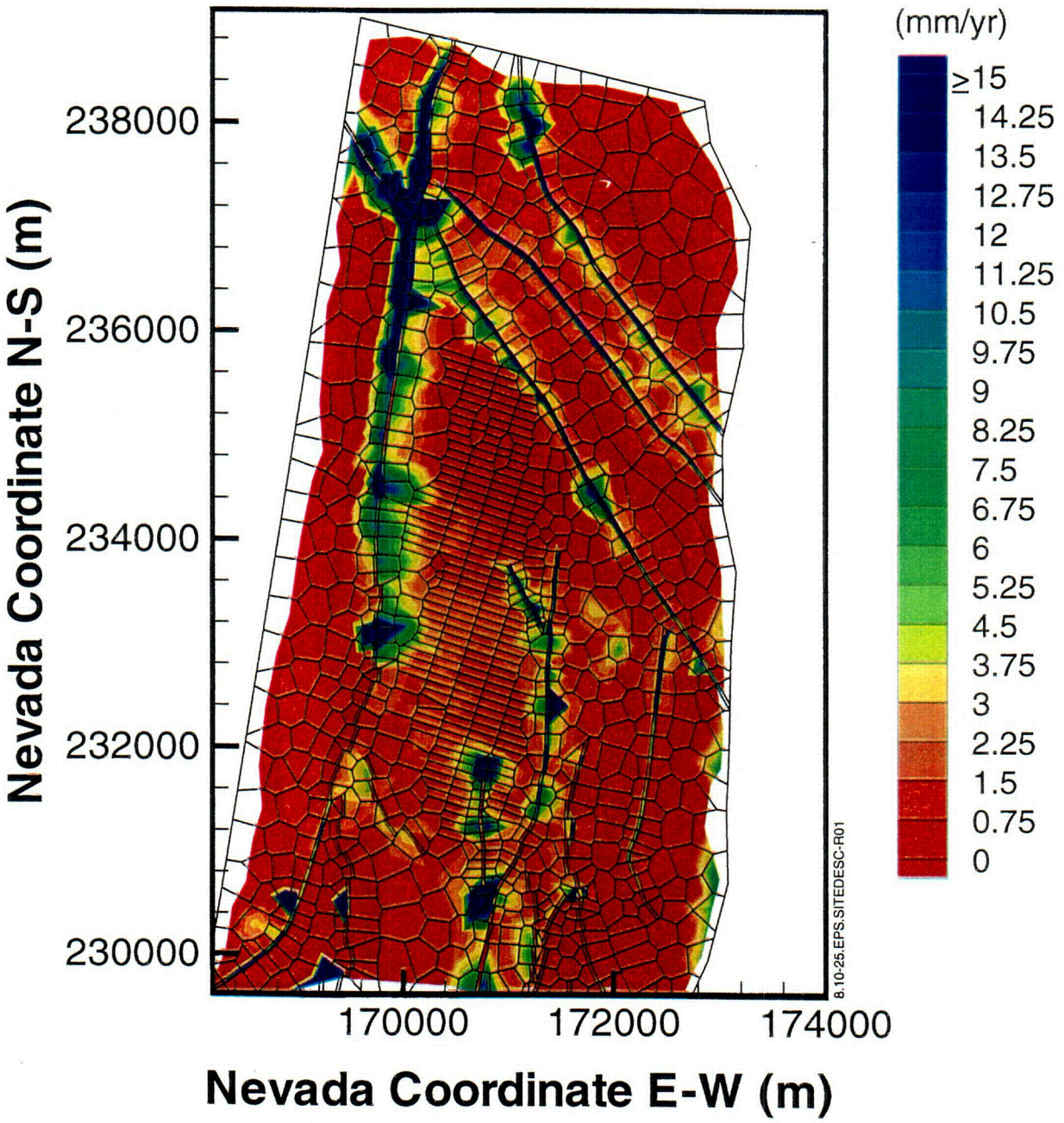

Source: CRWMS M&O (2000d, Figure 6-46)

Figure 8.10-25. Simulated Distribution of Percolation Flux at the Water Table under the Mean Present-Day Infiltration Scenario for the Bypassing Perched-Water Conceptual Model

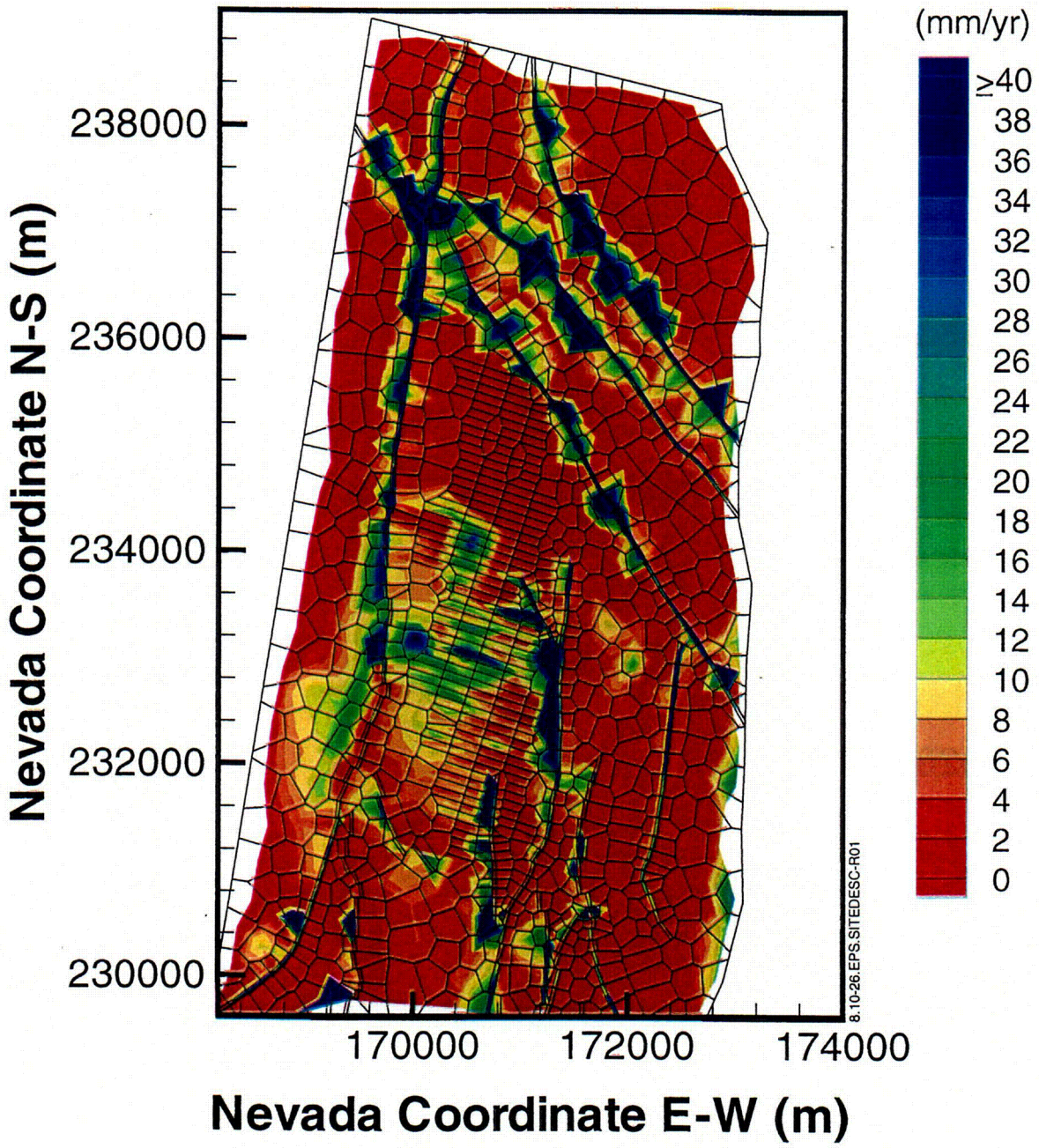

Source: CRWMS M&O (2000d, Figure 6-48)

Figure 8.10-26. Simulated Distribution of Percolation Flux at the Water Table under the Mean Monsoon Infiltration Scenario for the Flow-Through Perched-Water Conceptual Model

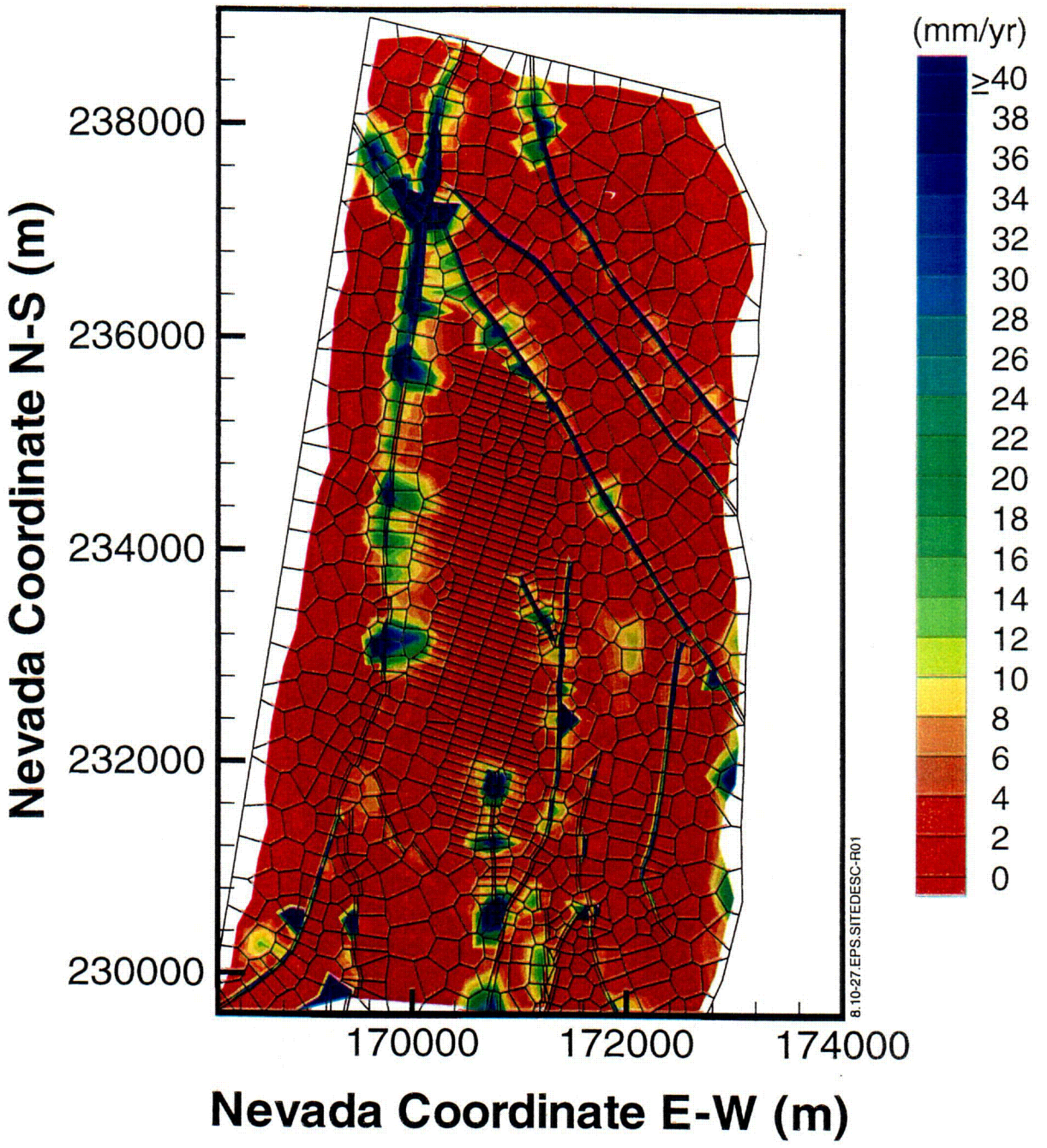

Source: CRWMS M&O (2000d, Figure 6-49)

Figure 8.10-27. Simulated Distribution of Percolation Flux at the Water Table under the Mean Monsoon Infiltration Scenario for the Bypassing Perched-Water Conceptual Model

C101

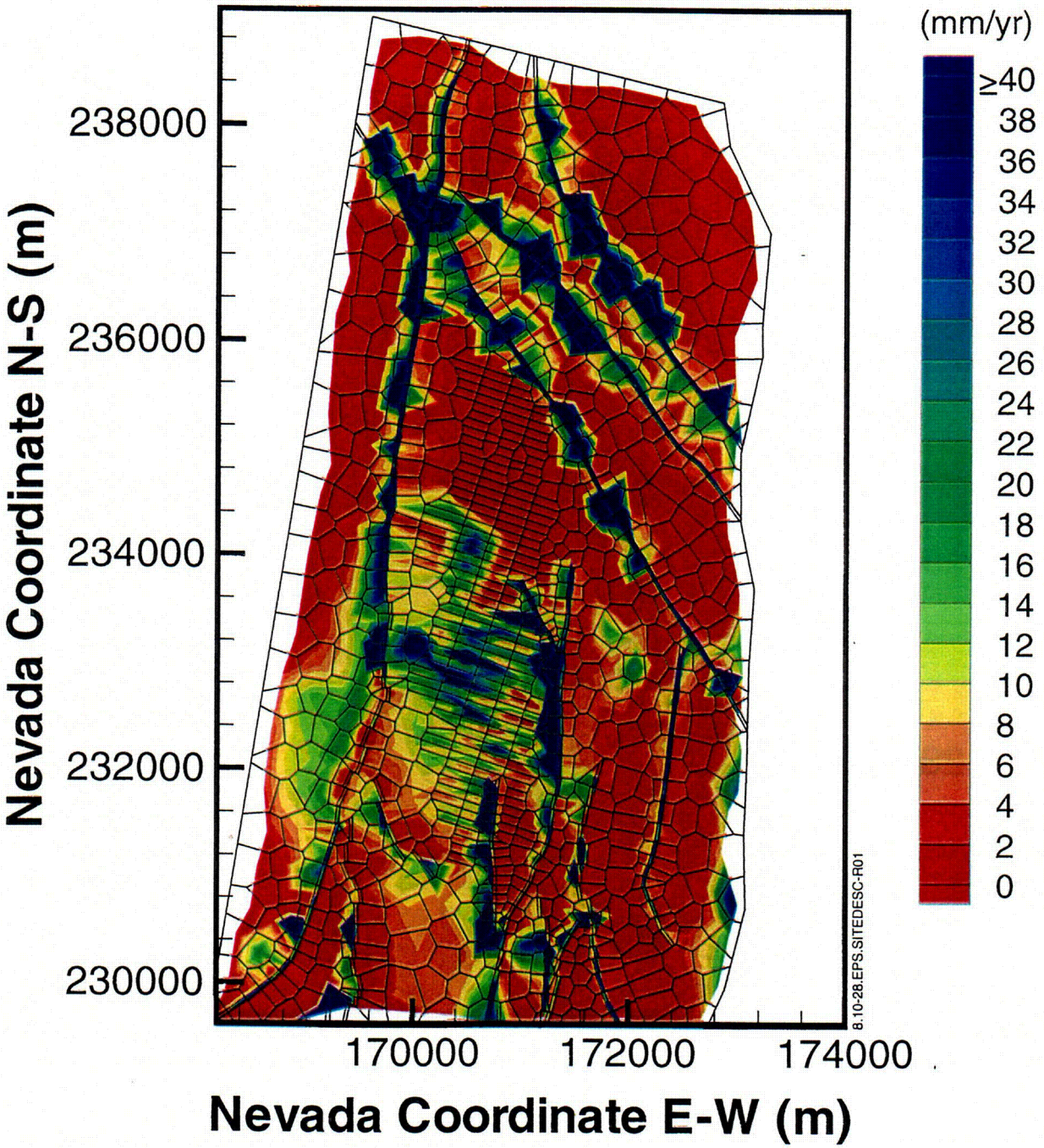

Source: CRWMS M&O (2000d, Figure 6-51)

Figure 8.10-28. Simulated Distribution of Percolation Flux at the Water Table under the Mean Glacial Transition Infiltration Scenario for the Flow-Through Perched-Water Conceptual Model

C102

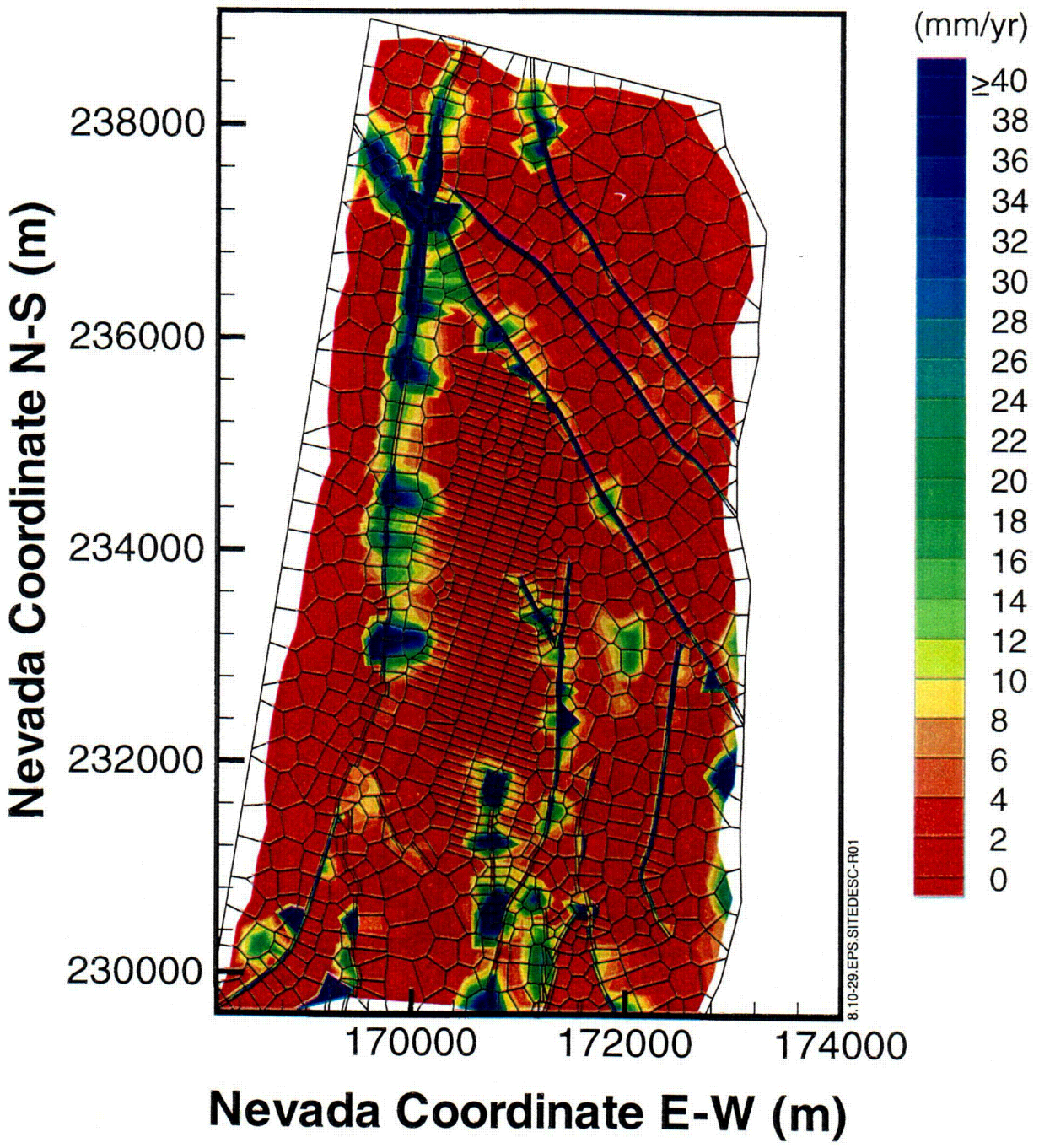

Source: CRWMS M&O (2000d, Figure 6-52)

Figure 8.10-29. Simulated Distribution of Percolation Flux at the Water Table under the Mean Glacial Transition Infiltration Scenario for the Bypassing Perched-Water Conceptual Model

C103

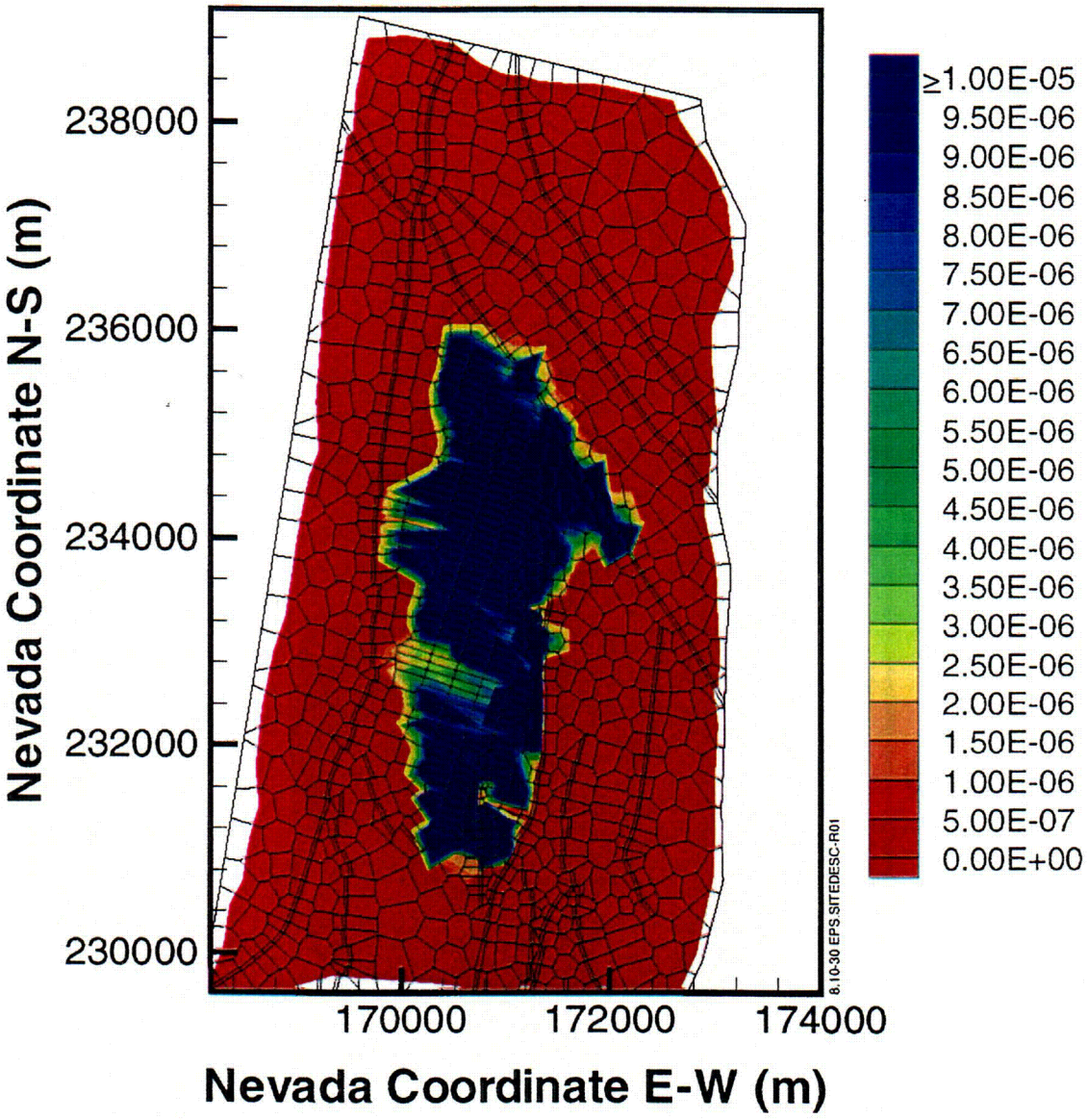

Source: CRWMS M&O (2000d, Figure 6-58)

Figure 8.10-30. Simulated Distribution of Mass Fraction of a Conservative Tracer and Potential Breakthrough Locations at the Water Table after 1,000 Years under the Mean Present-Day Infiltration Scenario and the Flow-Through Perched-Water Conceptual Model

C104

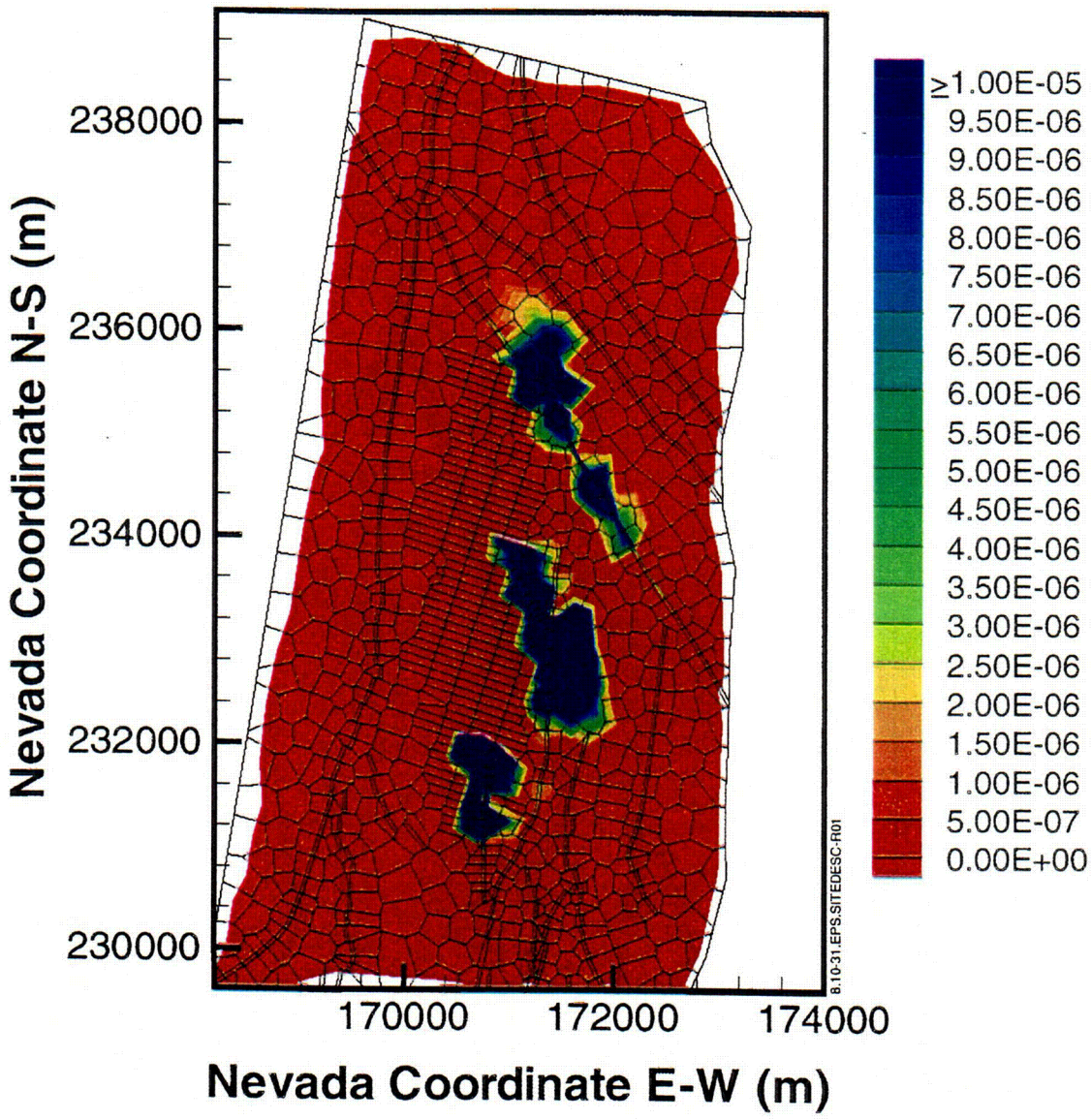

Source: CRWMS M&O (2000d, Figure 6-59)

Figure 8.10-31. Simulated Distribution of Mass Fraction of a Conservative Tracer and Potential Breakthrough Locations at the Water Table after 1,000 Years under the Mean Present-Day Infiltration Scenario and the Bypassing Perched-Water Conceptual Model

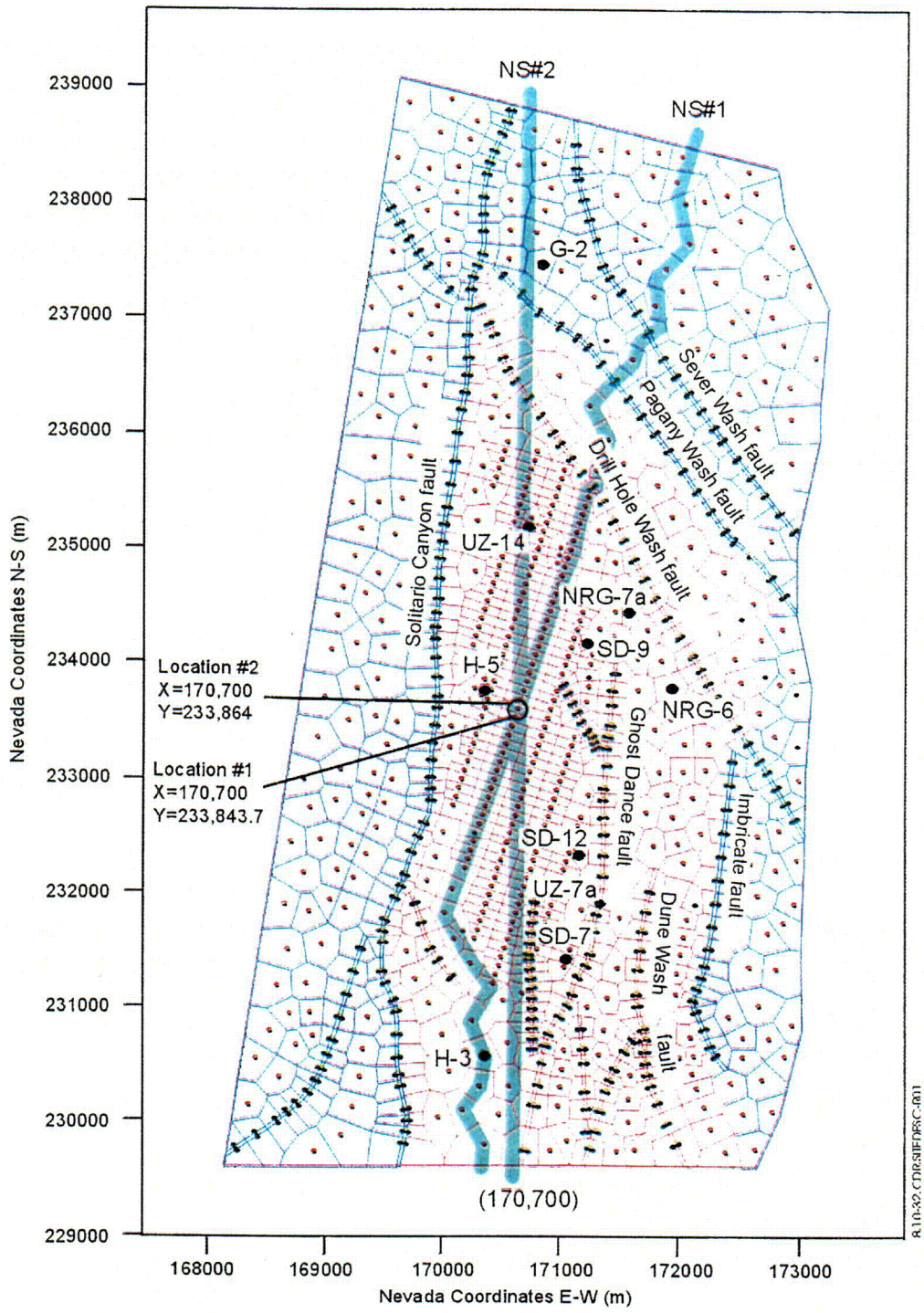

Source: CRWMS M&O (2000i, Figure 1)

NOTE: The locations of the potential repository submodel domain are shown in red.

Figure 8.10-32. Plan View of the Mountain-Scale Thermohydrologic Model Grid Showing the Locations of the Potential Repository Submodel Domain and Cross Sections NS#1 and NS#2

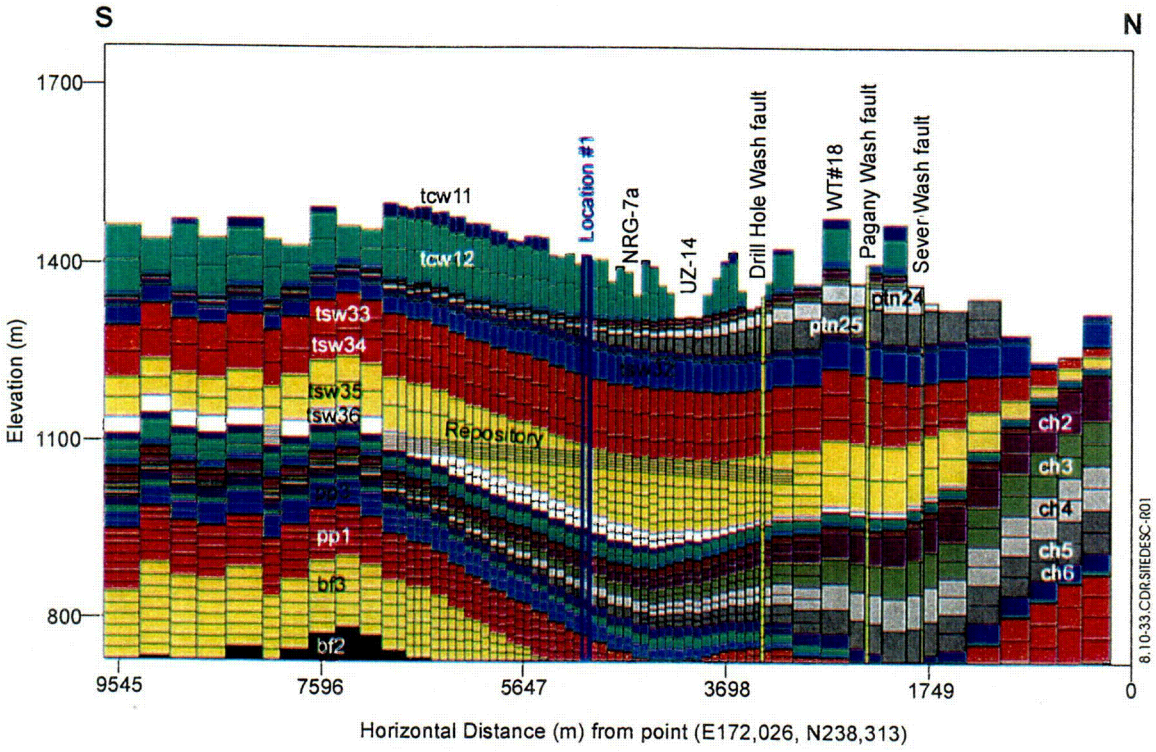

Source: CRWMS M&O (2000i, Figure 2)

Figure 8.10-33. Lateral and Vertical Discretization of the Thermohydrologic Model along Cross Section NS#1 Showing Model Layers and Locations of Boreholes, Faults, and the Potential Repository

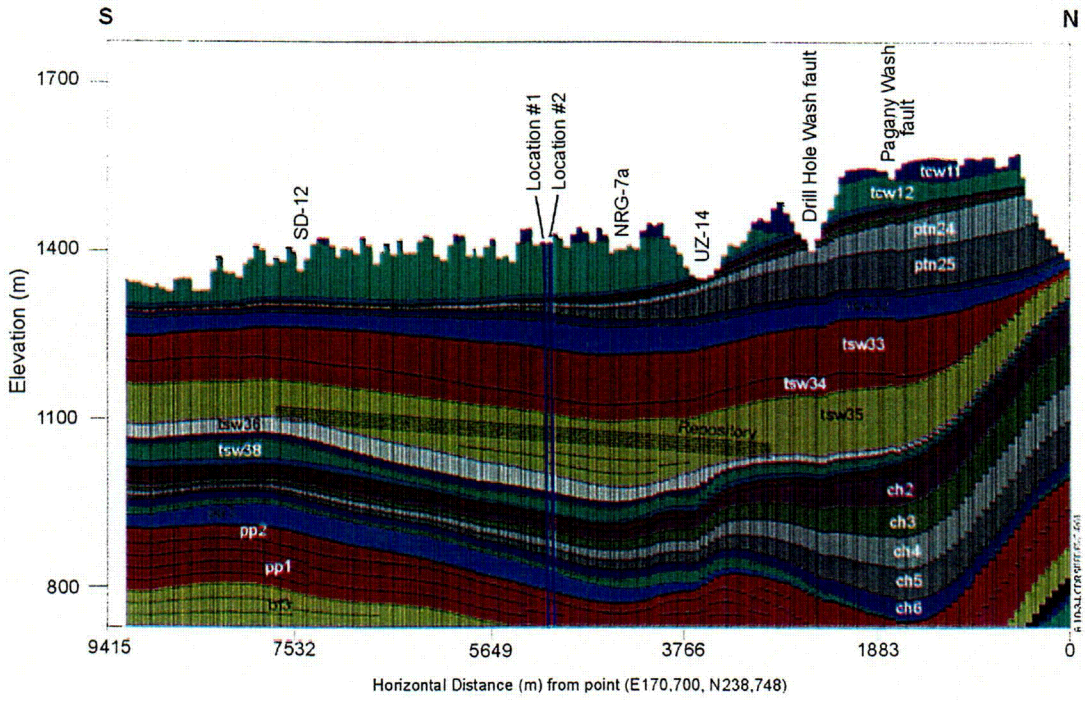

Source: CRWMS M&O (2000i, Figure 3)

Figure 8.10-34. Lateral and Vertical Discretization of the Thermohydrologic Model along Cross Section NS#2 Showing Model Layers and Locations of Boreholes, Faults, and the Potential Repository

C108

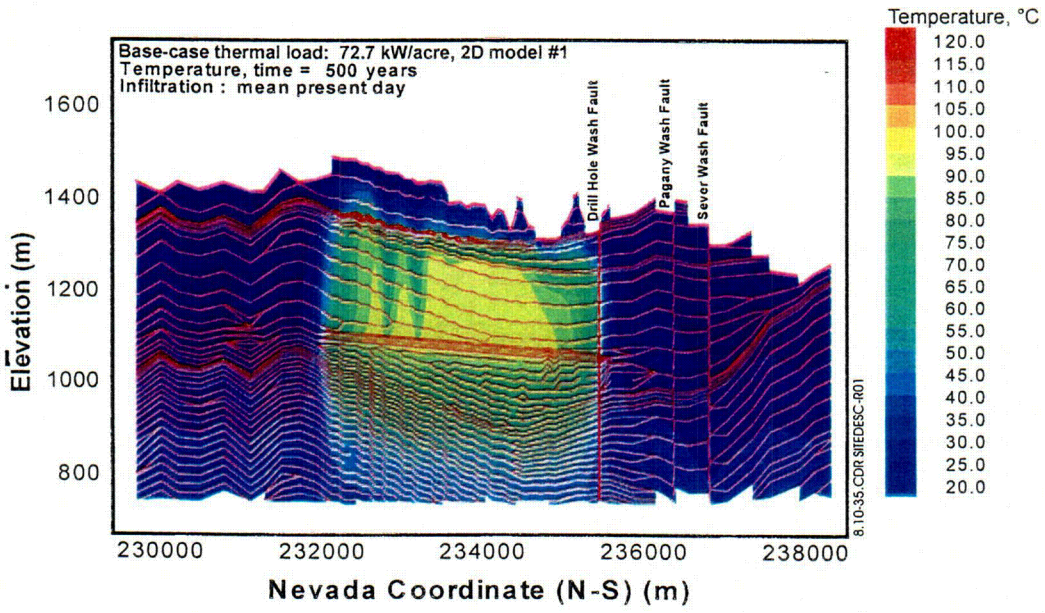

Source: CRWMS M&O (2000i, Figure 7)

Figure 8.10-35. Distribution of Temperature along Cross Section NS#1 for the Three-Dimensional, Repository-Area Submodel Simulation after 500 Years

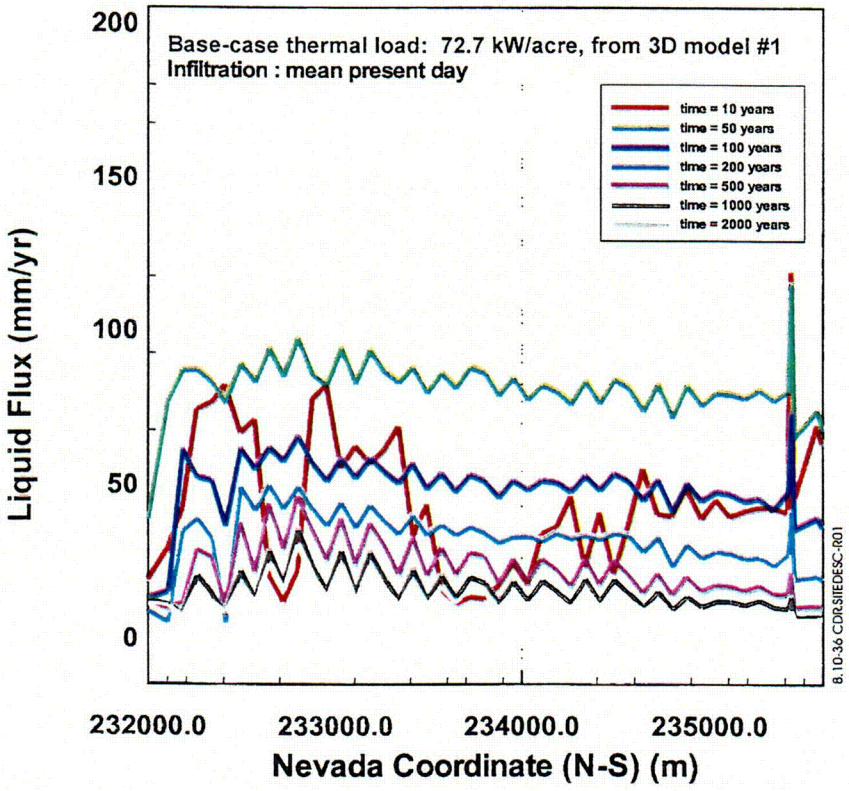

Source: CRWMS M&O (2000i, Figure 18)

Figure 8.10-36. Fracture Liquid Flux over Time at the Potential Repository Horizon along Cross Section NS#1 for the Three-Dimensional, Repository-Area Submodel Simulation

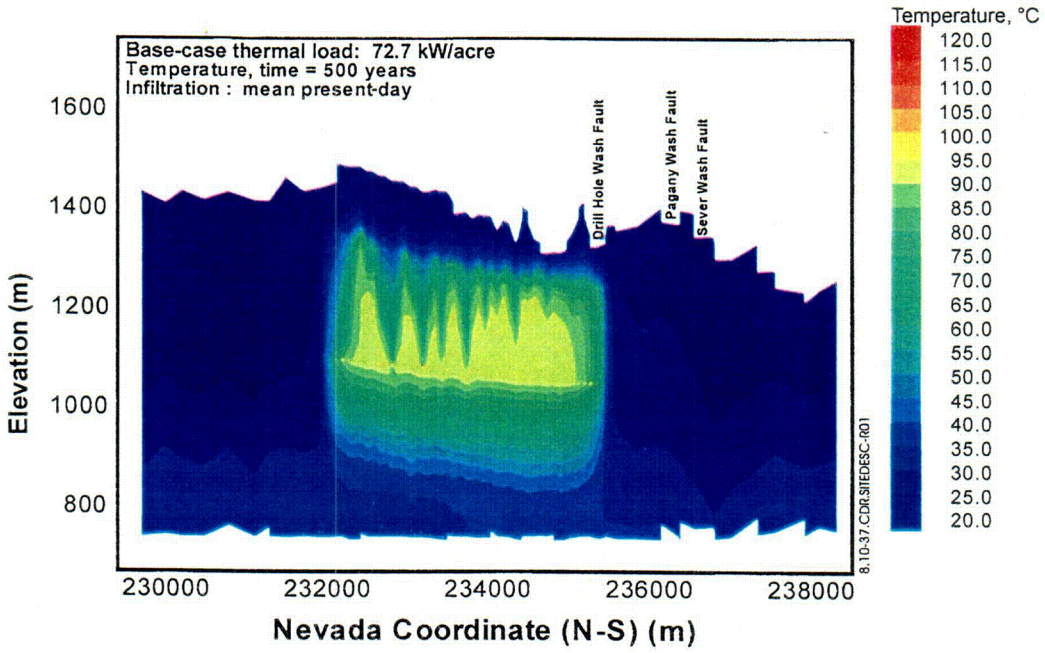

Source: CRWMS M&O (2000i, Figure 33)

Figure 8.10-37. Distribution of Temperature along Cross Section NS#1 for the Two-Dimensional Simulation after 500 Years

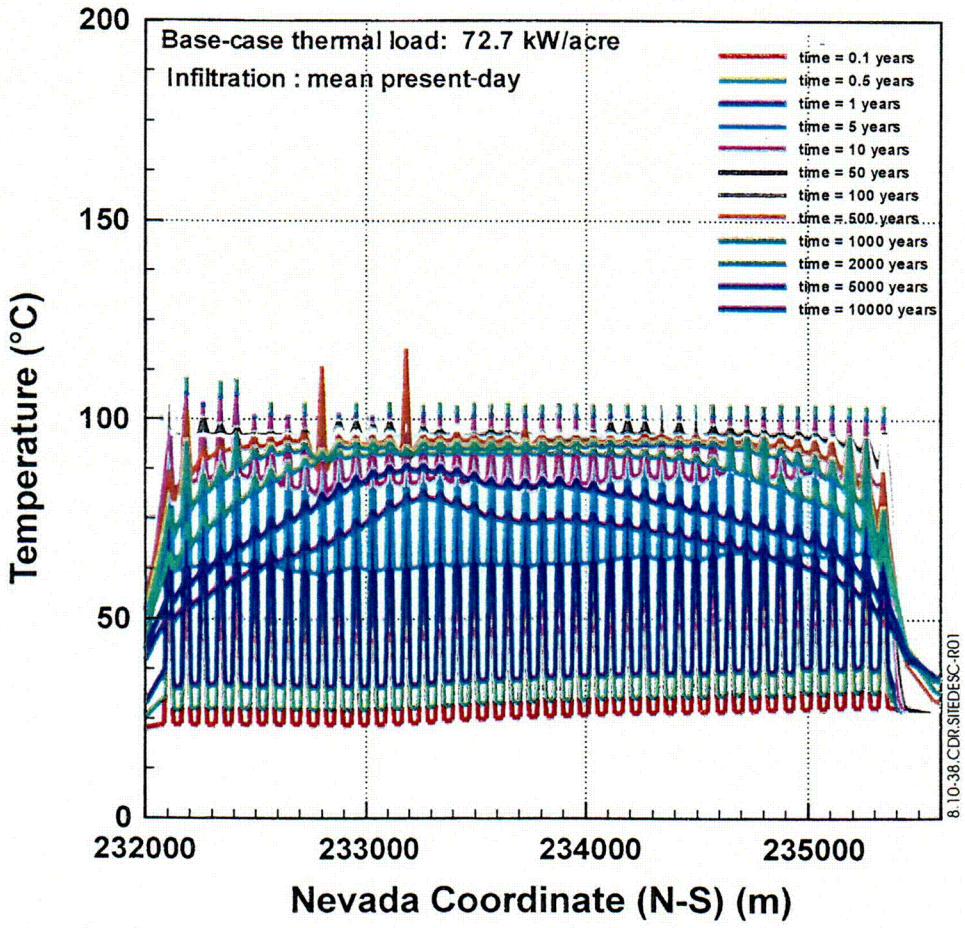

Source: CRWMS M&O (2000i, Figure 36)

Figure 8.10-38. Distribution of Temperature over Time at the Potential Repository Horizon along Cross Section NS#1 for the Two-Dimensional Simulation

C112

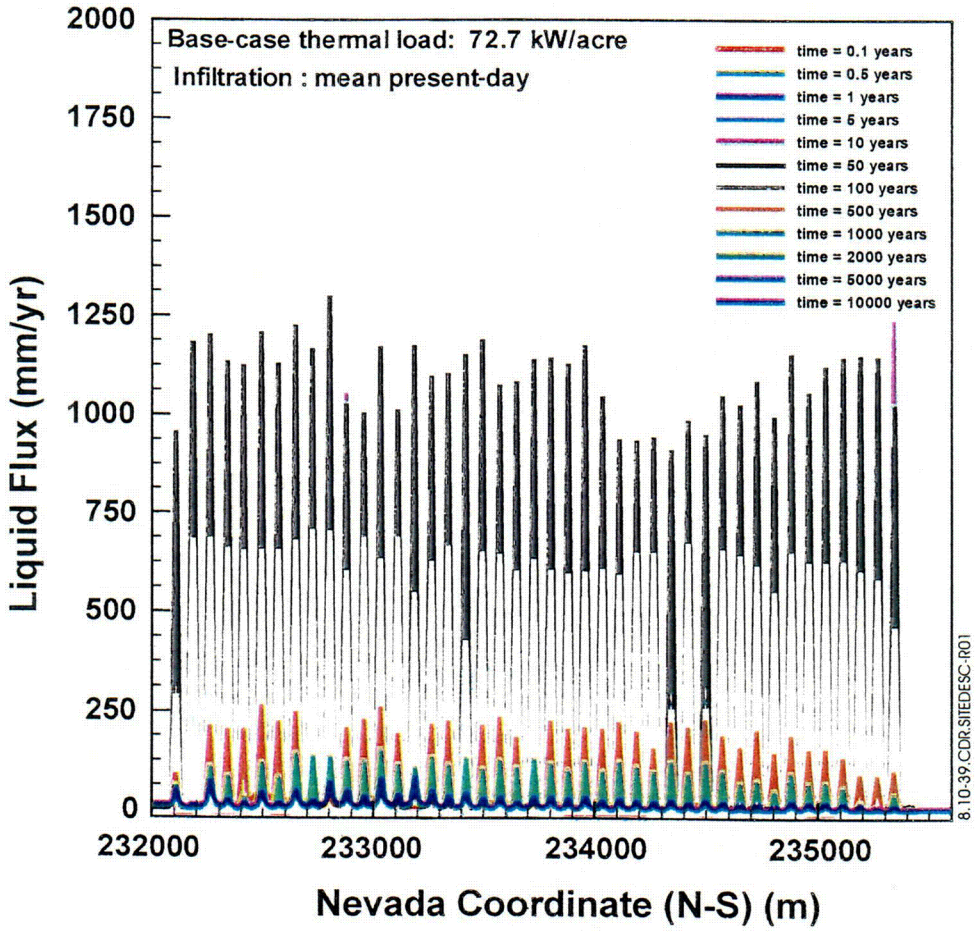

Source: CRWMS M&O (2000i, Figure 42)

Figure 8.10-39. Fracture Liquid Flux over Time at the Potential Repository Horizon along Cross Section NS#1 for the Two-Dimensional Simulation

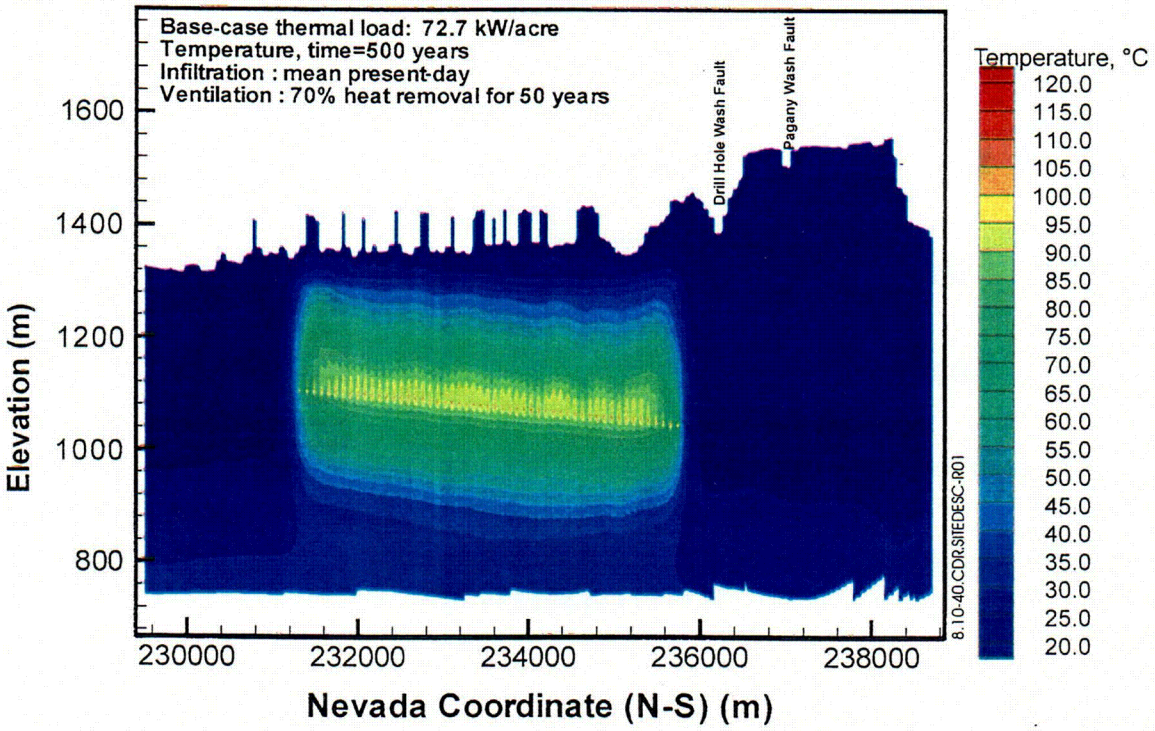

Source: CRWMS M&O (2000i, Figure 58)

Figure 8.10-40. Distribution of Temperature along Cross Section NS#2 for the Two-Dimensional Simulation after 500 Years

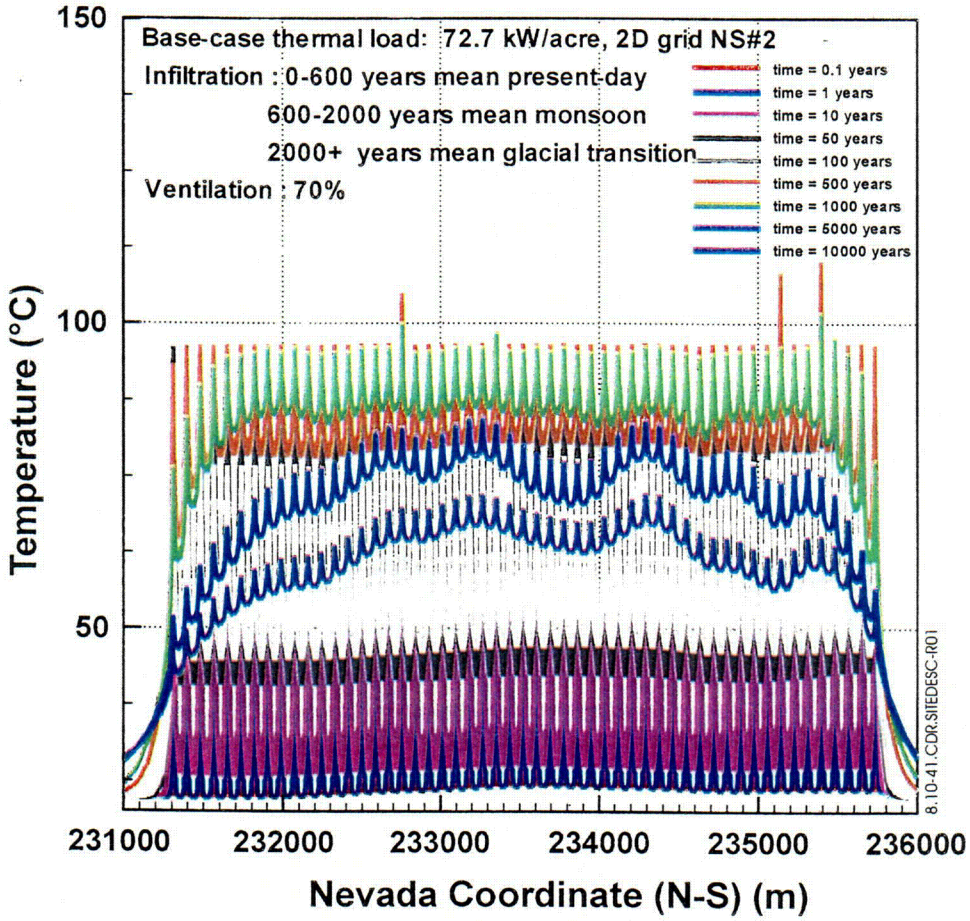

Source: CRWMS M&O (2000i, Figure 62)

Figure 8.10-41. Distribution of Temperature over Time at the Potential Repository Horizon along Cross Section NS#2 for the Two-Dimensional Simulation

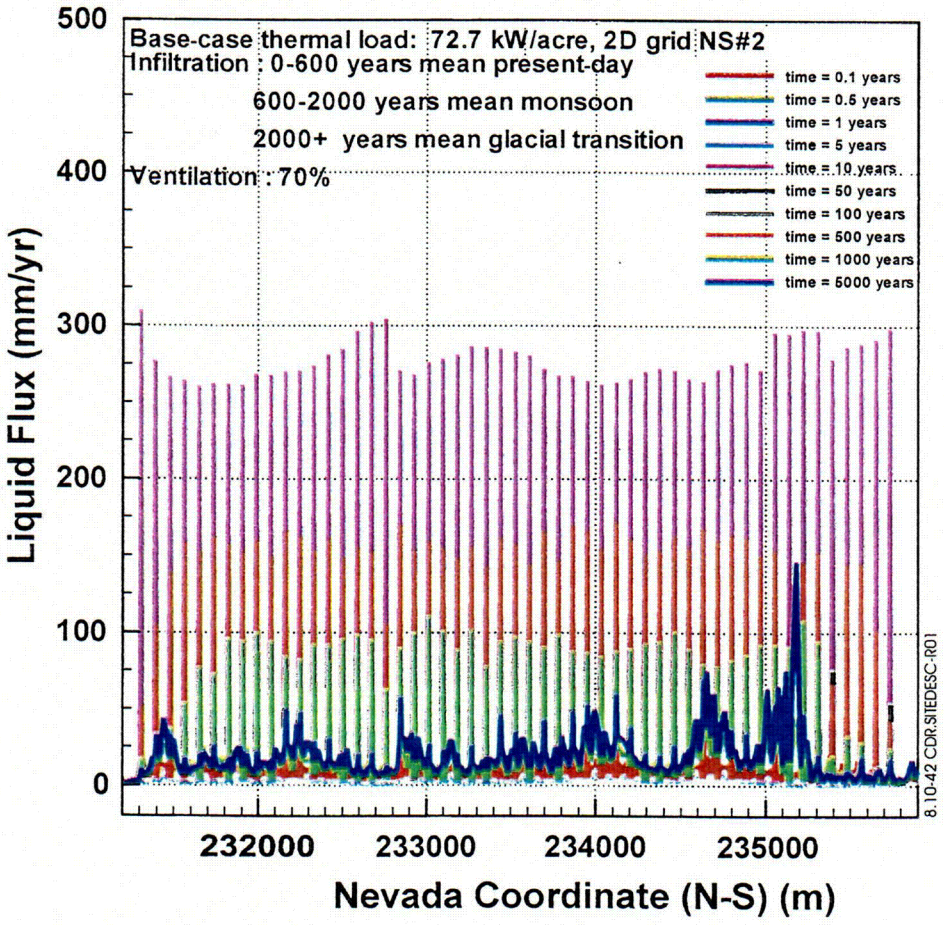

Source: CRWMS M&O (2000i, Figure 68)

Figure 8.10-42. Fracture Liquid Flux over Time at the Potential Repository Horizon along Cross Section NS#2 for the Two-Dimensional Simulation

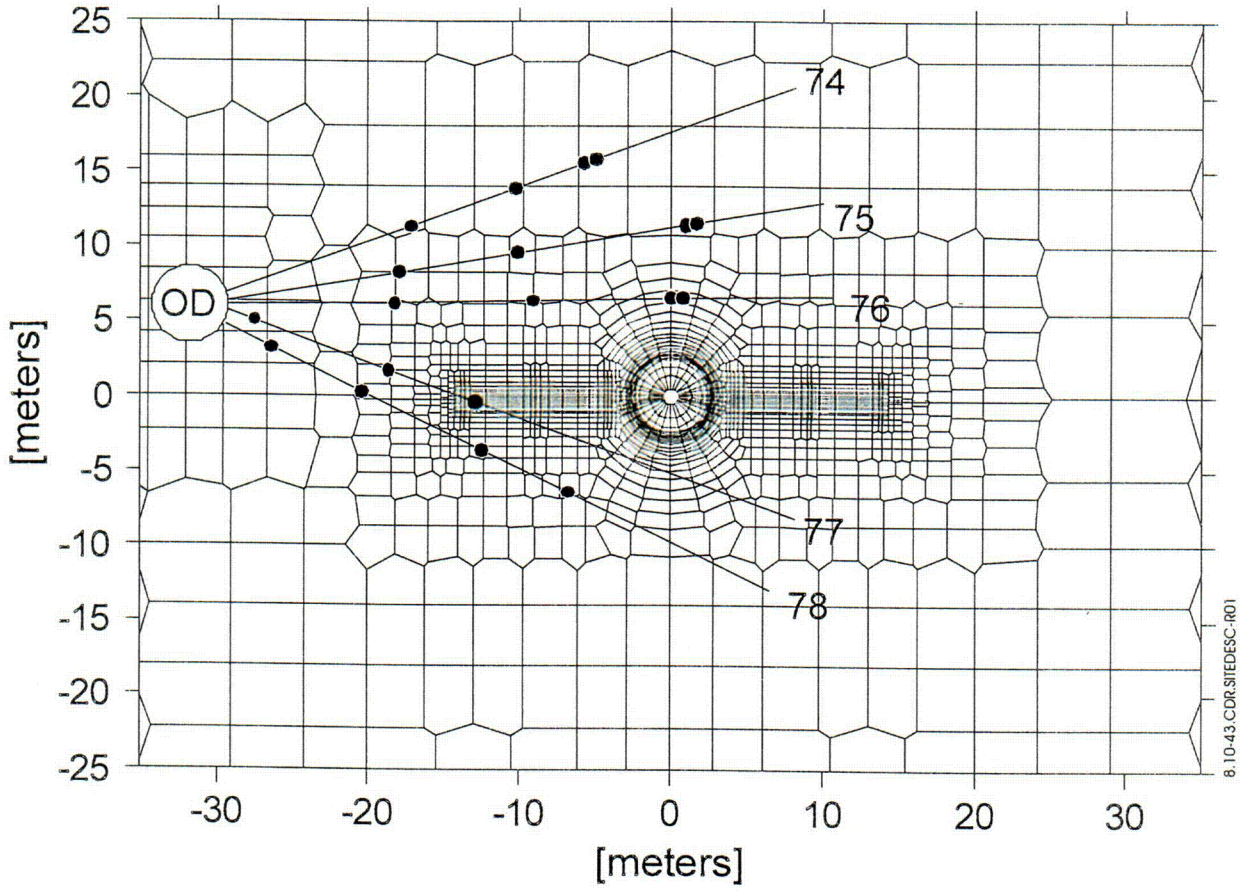

Source: CRWMS M&O (2000j, Figure 3)

NOTE: Boreholes are numbered 74 through 78. Solid circles along boreholes show locations of temperature sensors near the end of packed-off borehole intervals. Borehole intervals are numbered sequentially away from the wall of the observation drift (OD).

Figure 8.10-43. Two-Dimensional Numerical Grid for the Drift-Scale Test Thermohydrologic-Chemical Model

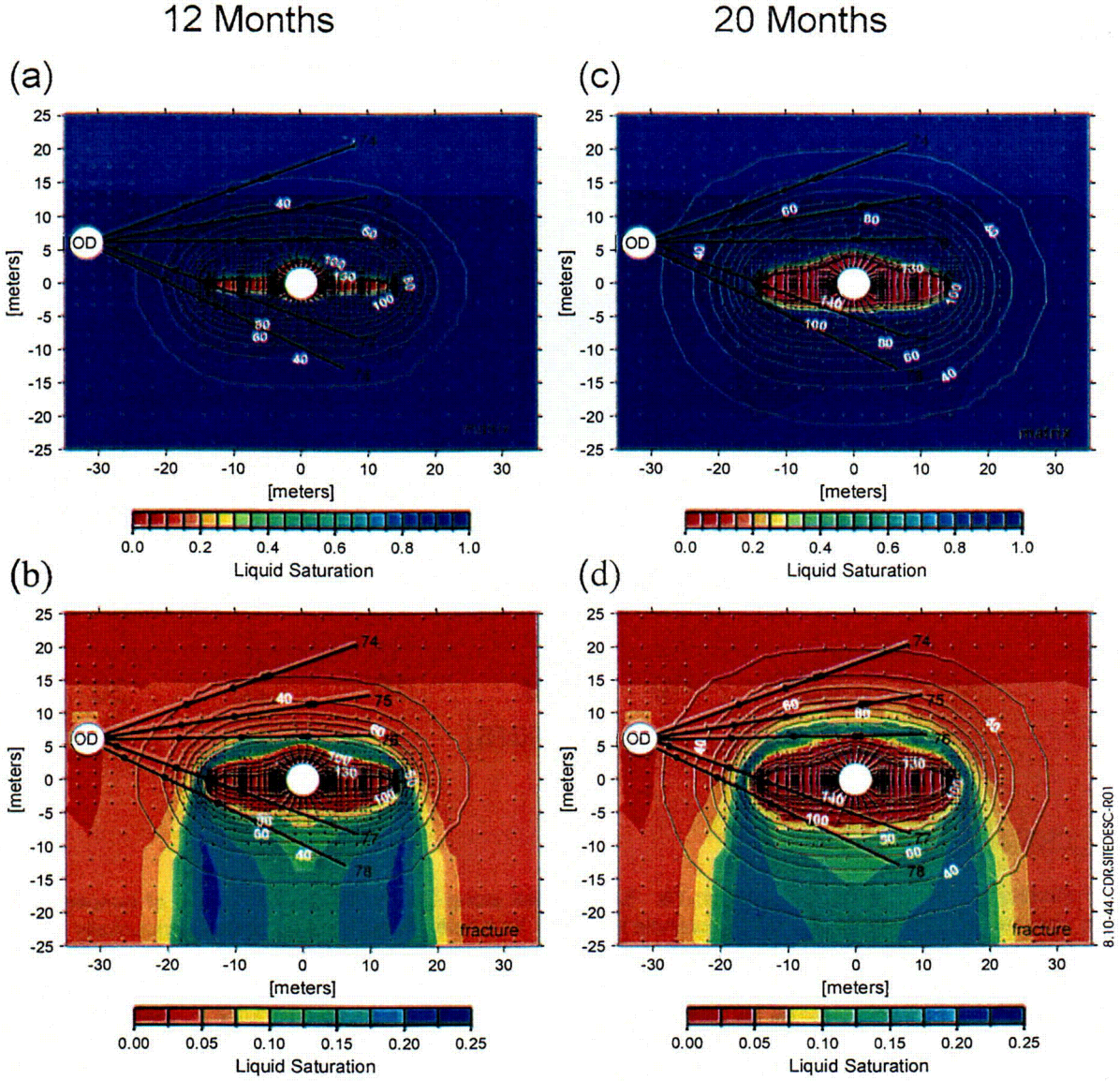

Source: CRWMS M&O (2000j, Figure 4)

NOTE: Simulated liquid saturations (colors) and temperatures (contour lines) are shown after 12 mo. for (a) matrix and (b) fractures, and after 20 mo. for (c) matrix and (d) fractures.

Figure 8.10-44. Simulated Liquid Saturations and Temperatures for the Drift-Scale Test for the Calcite-Silica-Gypsum Geochemical System after 12 Months and after 20 Months

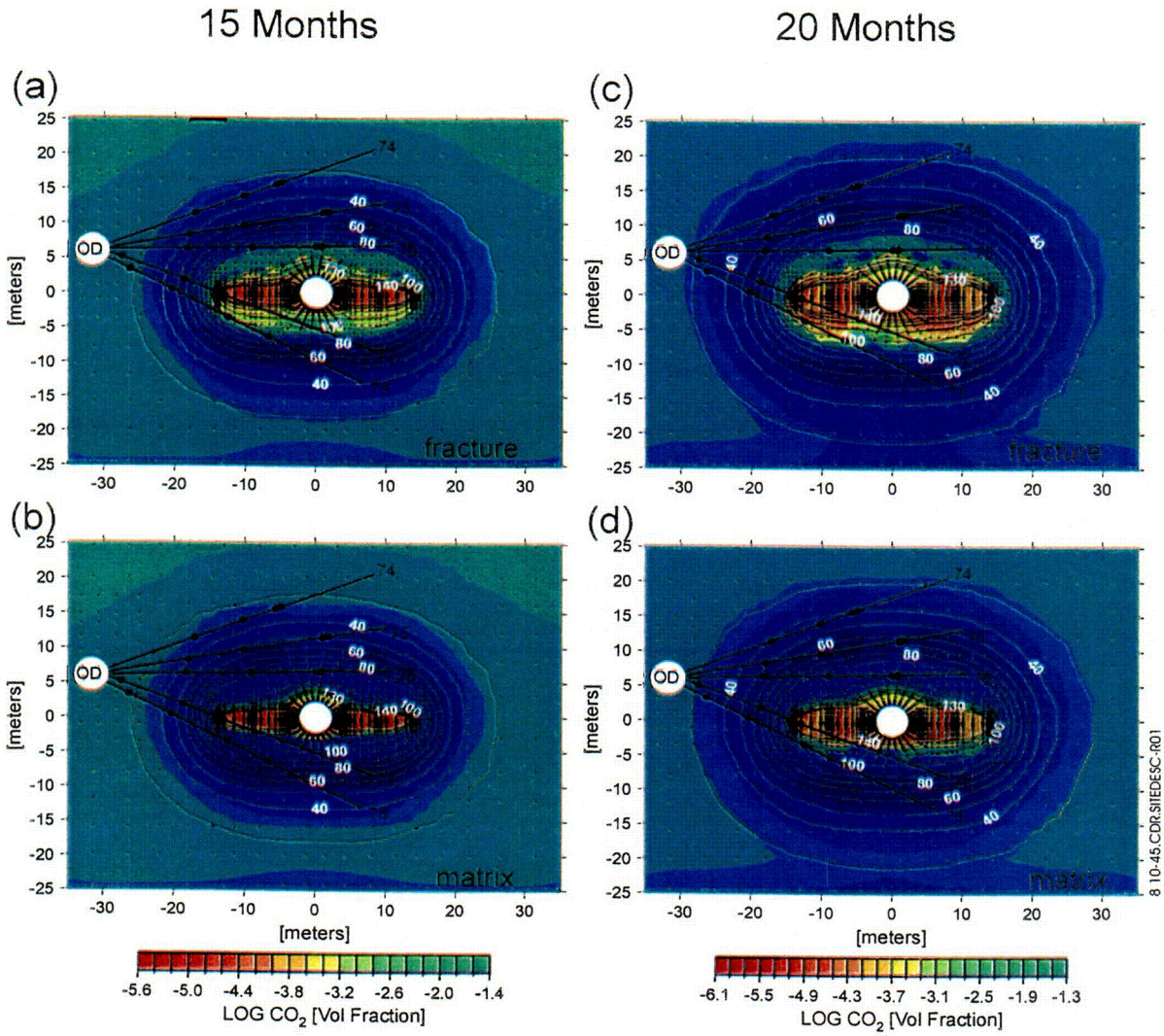

Source: CRWMS M&O (2000j, Figure 6)

NOTE: Simulated carbon dioxide concentrations (colors) and temperatures (contour lines) are shown after 15 mo. for (a) fractures and (b) matrix, and after 20 mo. for (c) fractures and (d) matrix.

Figure 8.10-45. Simulated Carbon Dioxide Concentration and Temperature for the Drift-Scale Test for the Calcite-Silica-Gypsum Geochemical System after 15 Months and after 20 Months

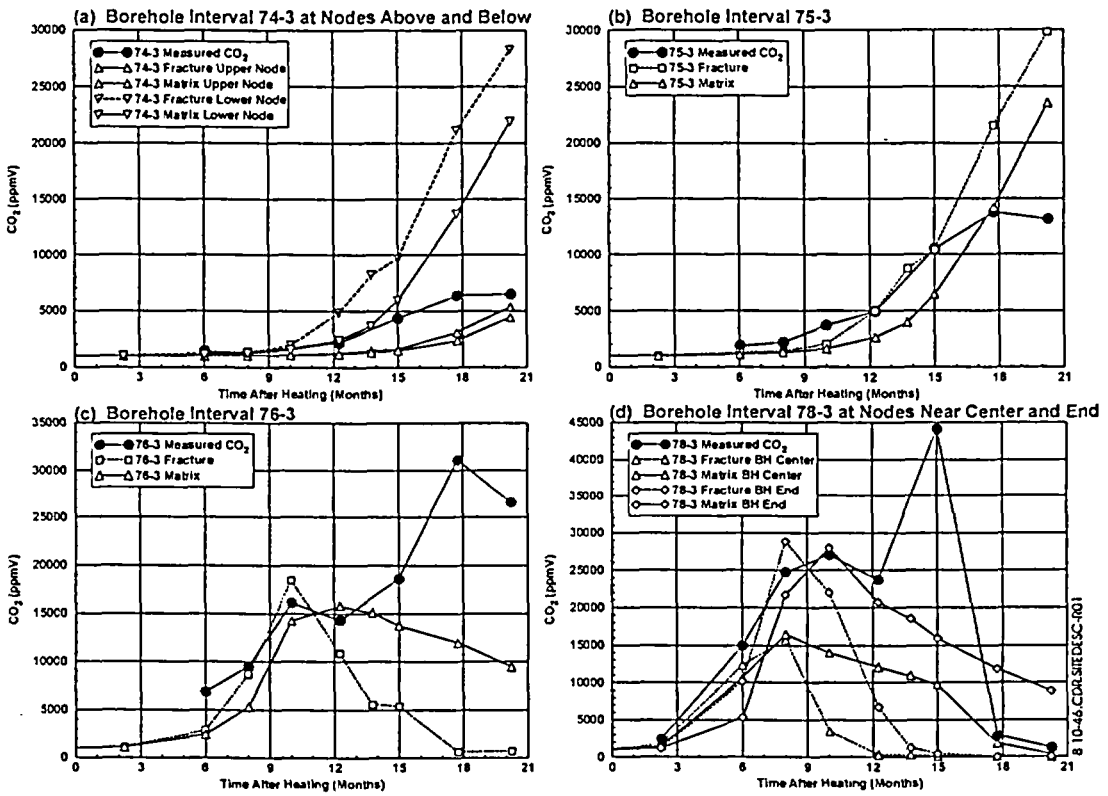

Source: CRWMS M&O (2000j, Figure 10)

Figure 8.10-46. Time-Series Comparison of Simulated Carbon Dioxide Concentrations in Fractures and Matrix for the Drift-Scale Test for the Calcite-Silica-Gypsum Geochemical System to Measured Concentrations in Various Borehole Intervals

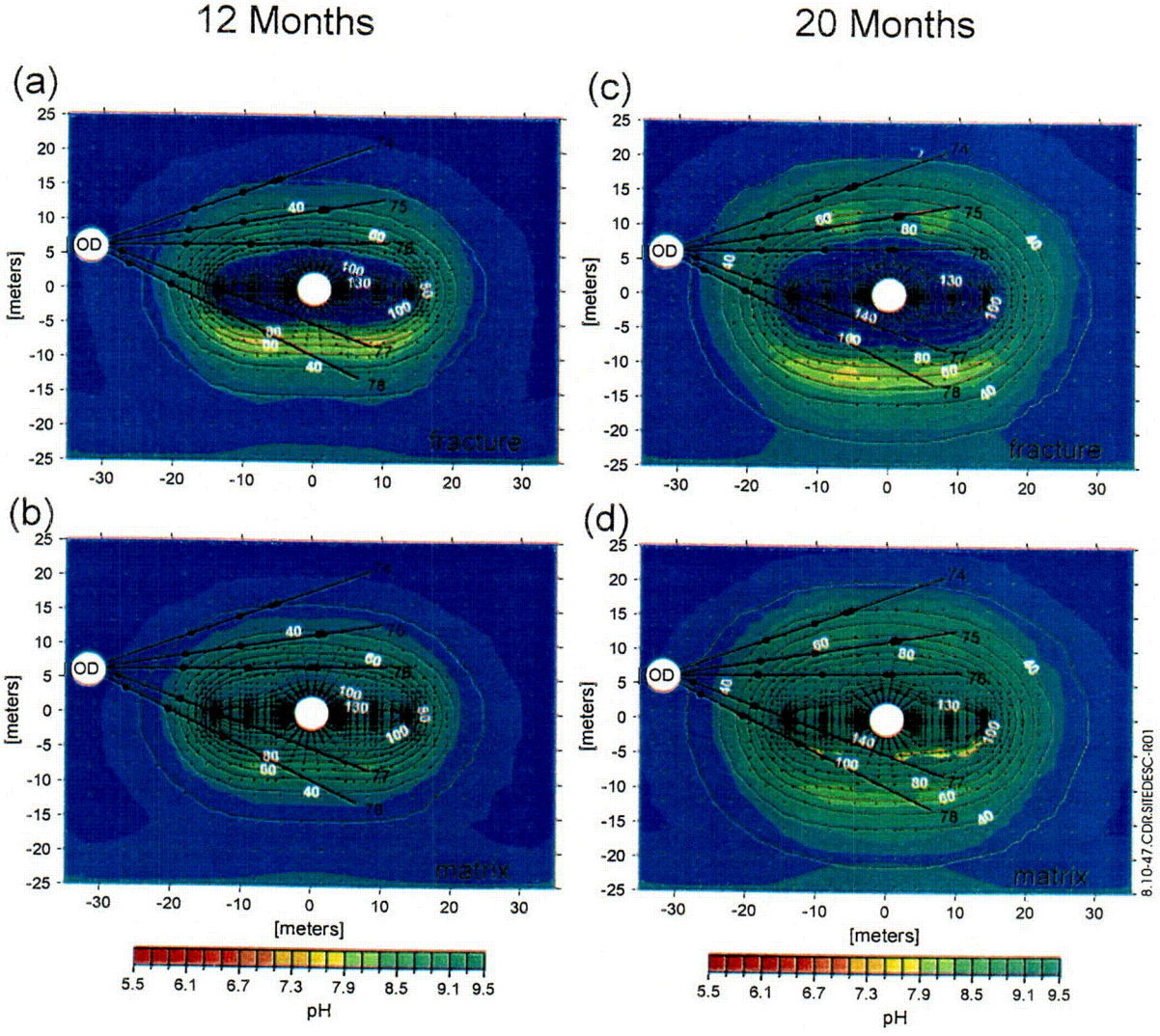

Source: CRWMS M&O (2000j, Figure 13)

NOTE: Simulated pH (colors) and temperatures (contour lines) are shown after 12 mo. for (a) fractures and (b) matrix, and after 20 mo. for (c) fractures and (d) matrix.

Figure 8.10-47. Simulated pH and Temperature for the Drift-Scale Test for the Calcite-Silica-Gypsum Geochemical System after 12 Months and after 20 Months

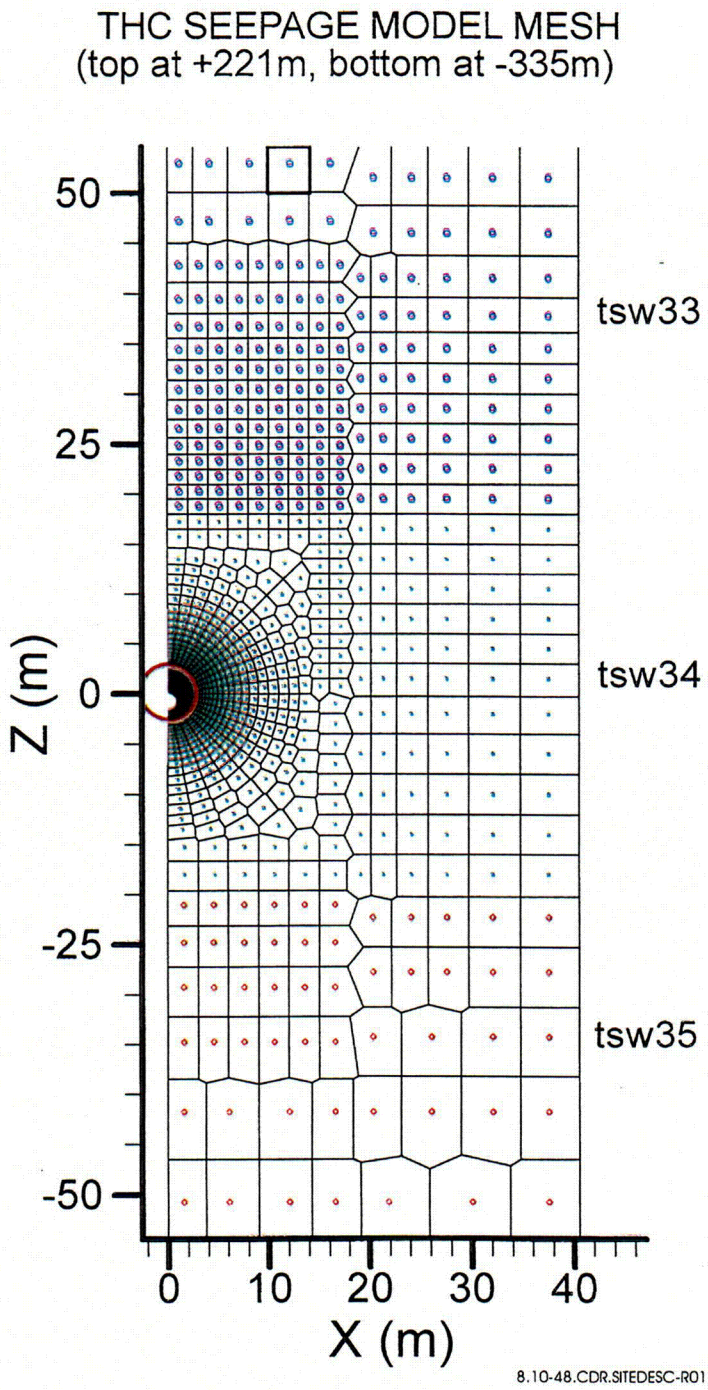

Source: CRWMS M&O (2000j, Figure 18)

Figure 8.10-48. Two-Dimensional Numerical Grid for the Thermohydrologic-Chemical Seepage Model Showing Model Layers tsw33, tsw34, and tsw35

C/21

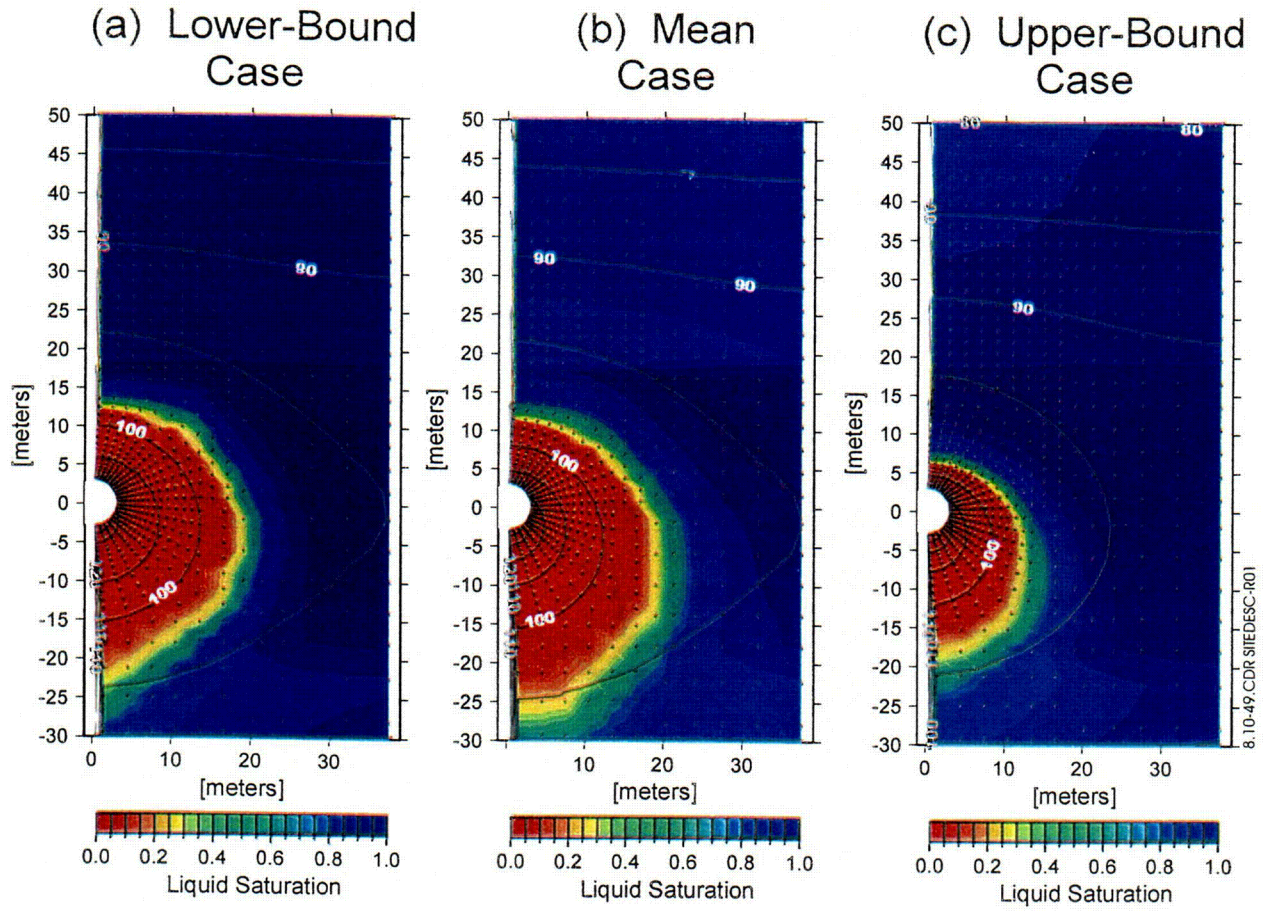

Source: CRWMS M&O (2000j, Figure 26)

NOTE: Colors show simulated liquid saturation values, contour lines indicate temperature.

Figure 8.10-49. Simulated Liquid Saturation and Temperature for the Thermohydrologic-Chemical Seepage Model after 600 Years for the Full Geochemical System

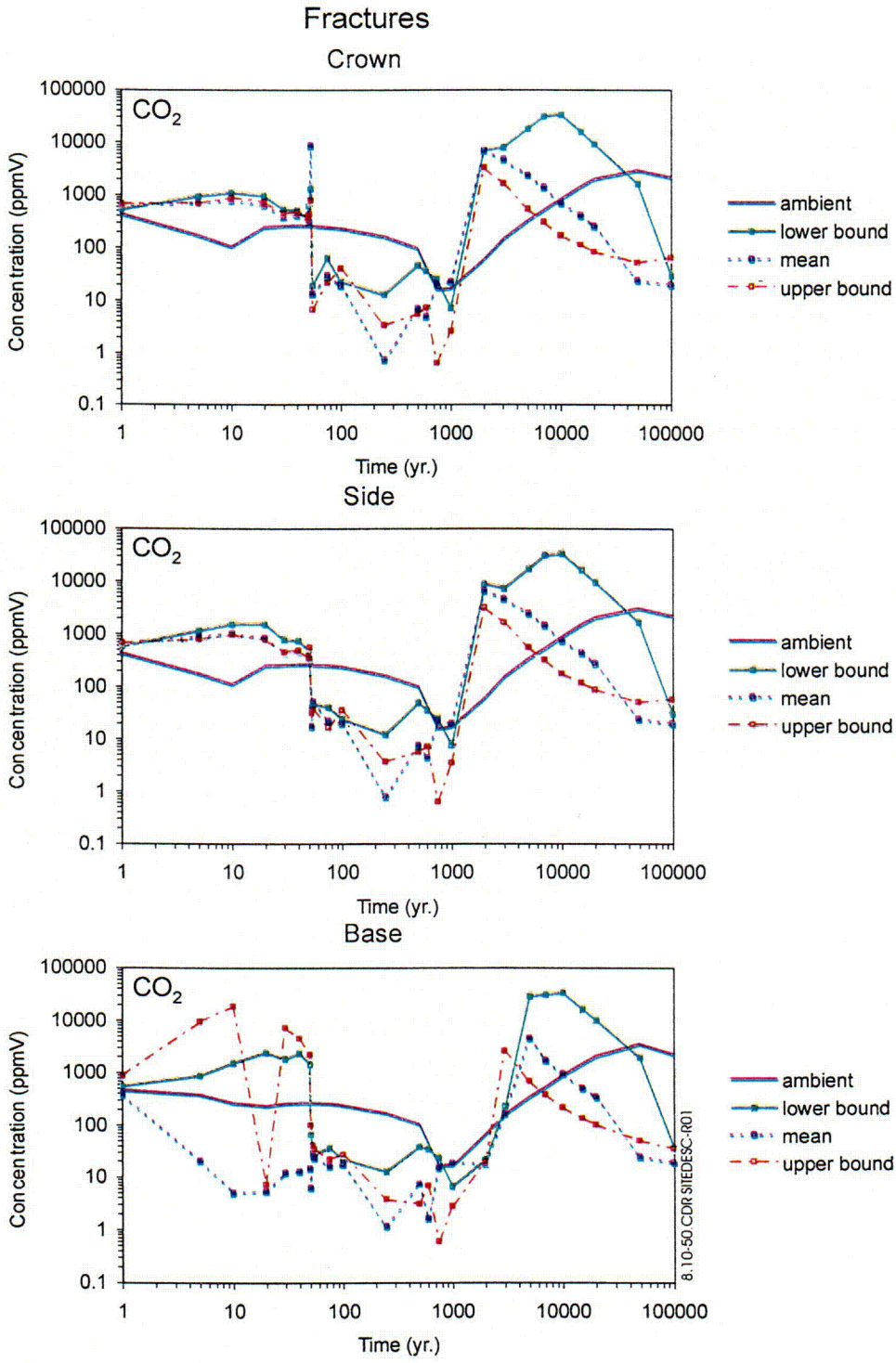

Source: CRWMS M&O (2000j, Figure 28)

Figure 8.10-50. Simulated Time-Series Carbon Dioxide Concentrations in the Gas Phase in Fractures for the Thermohydrologic-Chemical Seepage Model for the Full Geochemical System at Three Drift Wall Locations for Different Infiltration Rates

C123

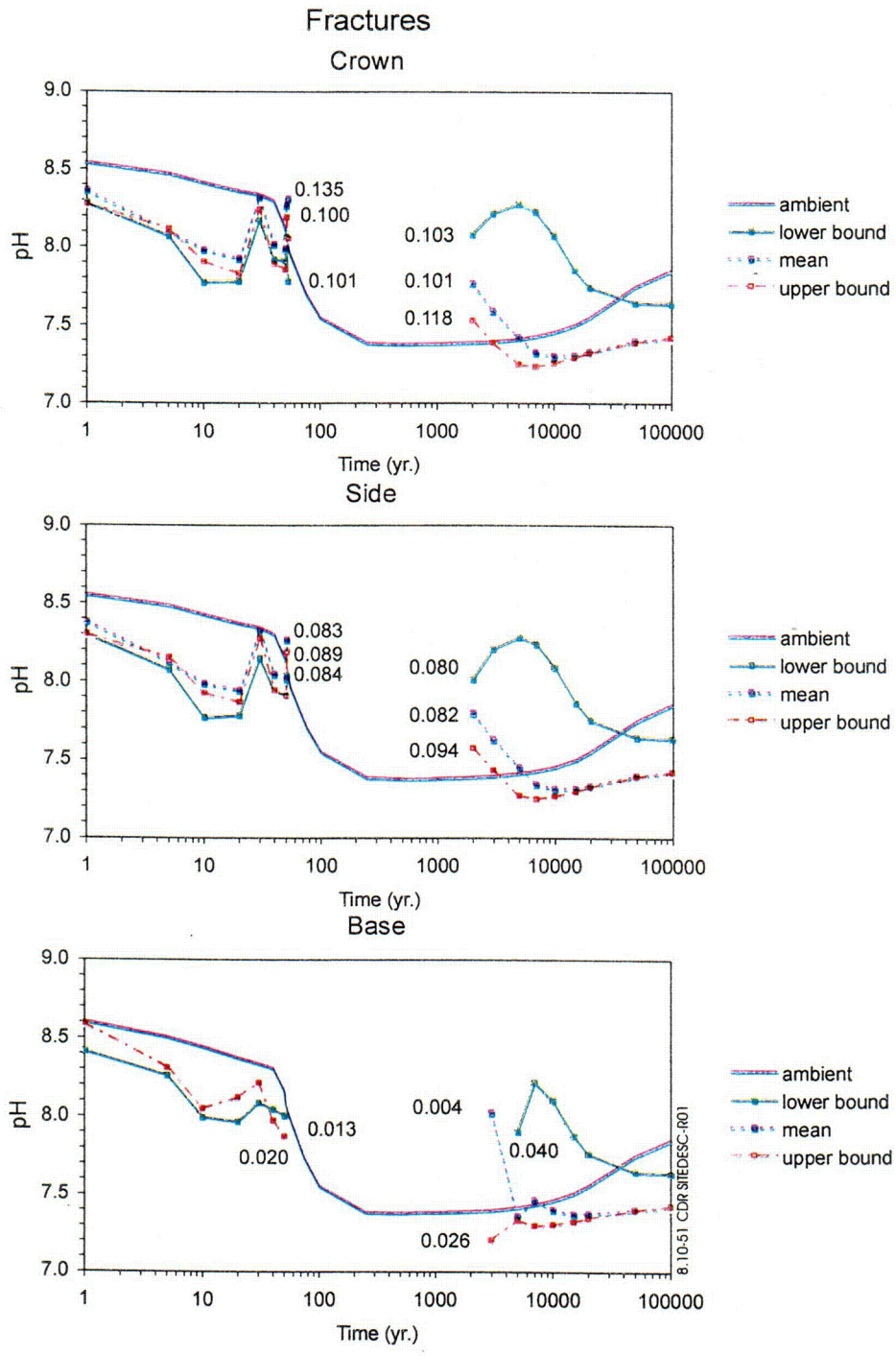

Source: CRWMS M&O (2000j, Figure 31)

NOTE: Numbers by each curve indicate the last calculated liquid saturation before dryout and the first calculated liquid saturation during rewetting.

Figure 8.10-51. Simulated Time-Series pH of Fracture Water for the Thermohydrologic-Chemical Seepage Model for the Calcite-Silica-Gypsum Geochemical System at Three Drift Wall Locations for Different Infiltration Rates

C124

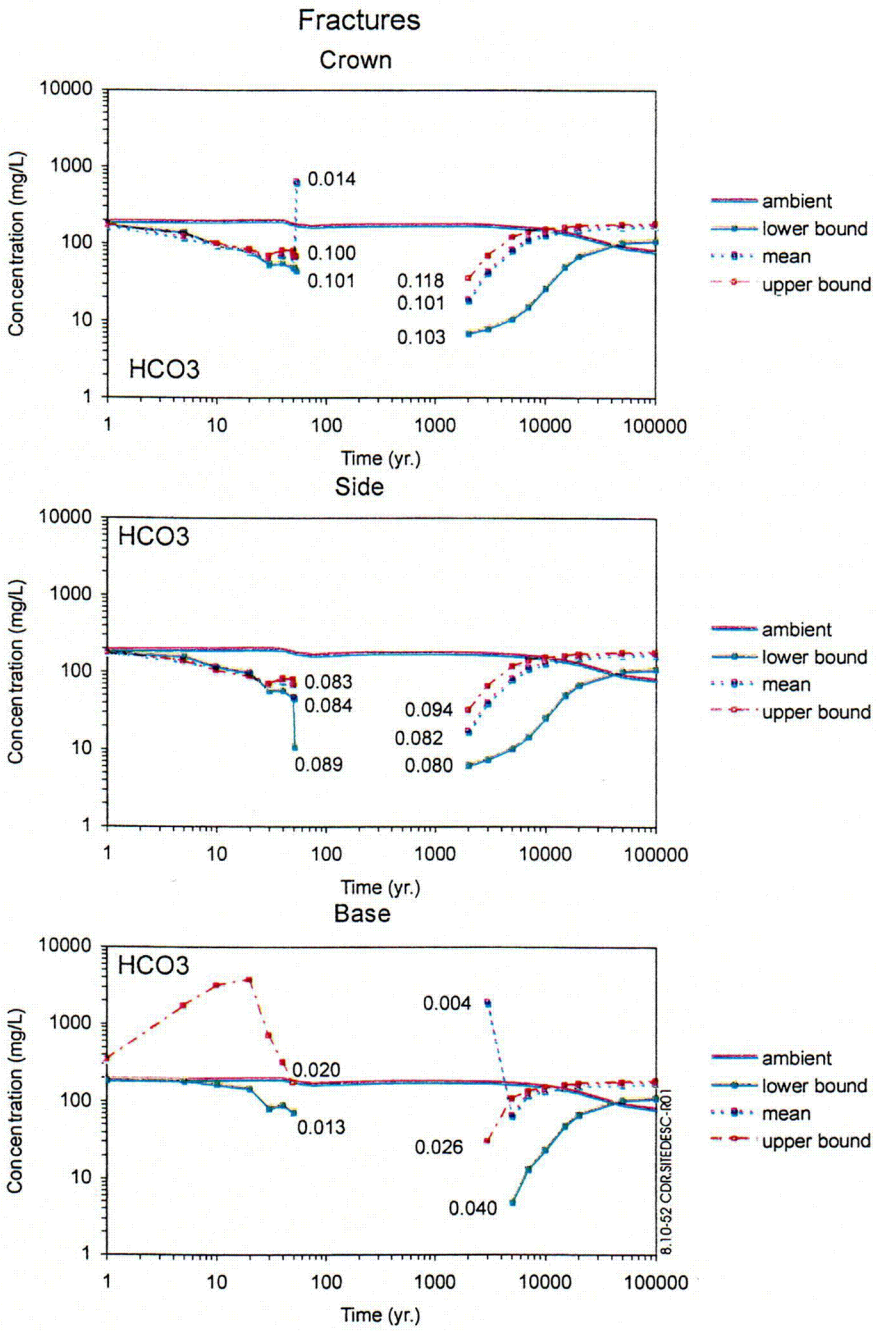

Source: CRWMS M&O (2000j, Figure 33)

NOTE: Numbers by each curve indicate the last calculated liquid saturation before dryout and the first calculated liquid saturation during rewetting.

Figure 8.10-52. Simulated Time-Series Total Aqueous Carbonate Concentrations (as Bicarbonate) in Fracture Water for the Thermohydrologic-Chemical Seepage Model for the Calcite-Silica-Gypsum Geochemical System at Three Drift Wall Locations for Different Infiltration Rates

C125

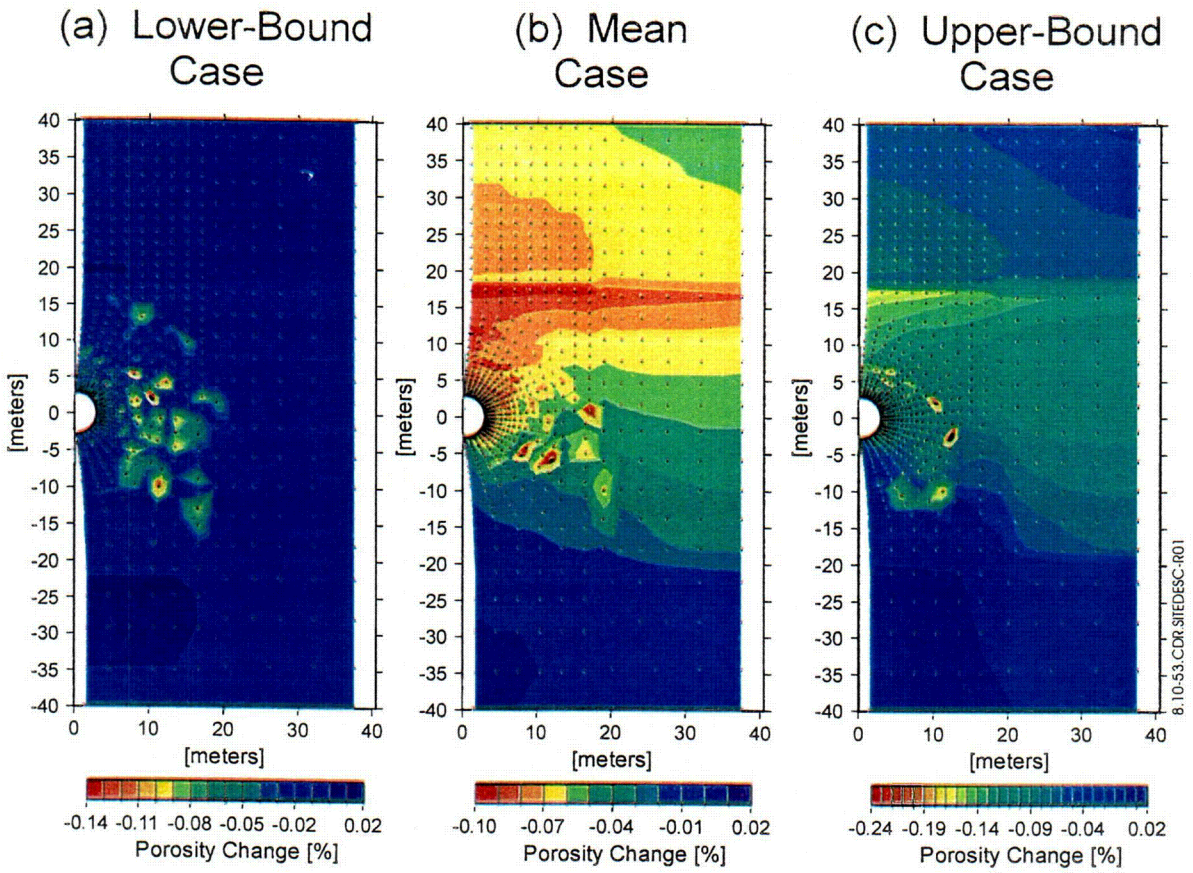

Source: CRWMS M&O (2000j, Figure 42)

Figure 8.10-53. Simulated Total Change in Fracture Porosity for the Thermohydrologic-Chemical Seepage Model after 10,000 Years for the Calcite-Silica-Gypsum Geochemical System

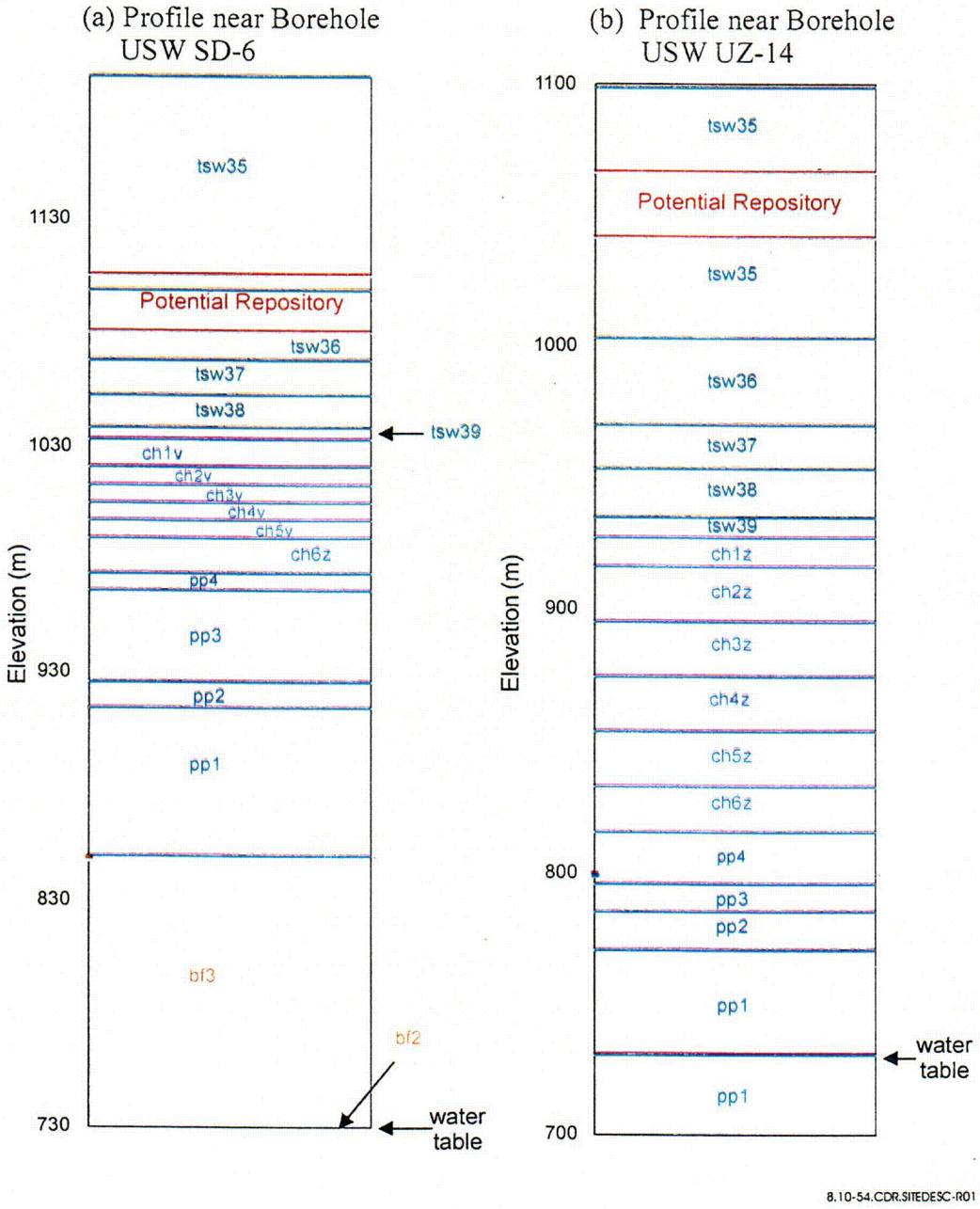

Source: CRWMS M&O (2000l, Figures 6.5.2 and 6.5.4)

Figure 8.10-54. Hydrogeologic Profiles of Model Layers from the Potential Repository to the Water Table Used for Simulation of Radionuclide Transport in Cross-Sectional Simulations

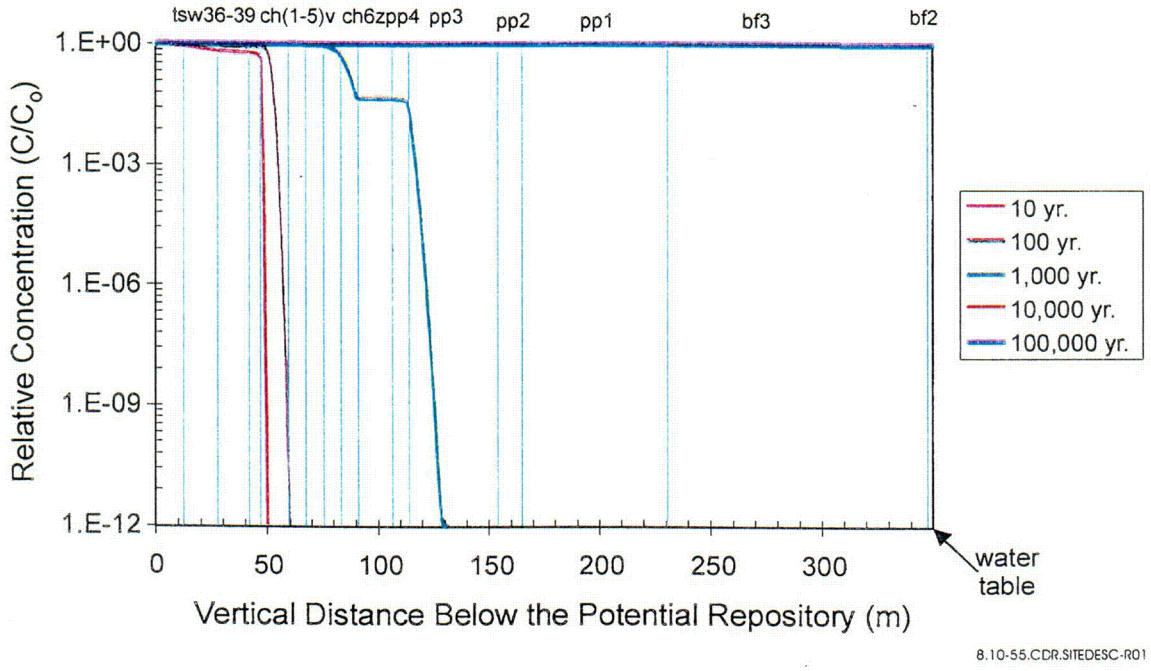

Source: CRWMS M&O (2000l, Figure V.1)

NOTE: The 10,000-yr. and 100,000-yr. concentration lines both plot along the upper horizontal axis.

Figure 8.10-55. Simulated Time-Series Concentration Profile for Technetium-99 under the Potential Repository in the SD-6 Cross Section for Mean Present-Day Infiltration

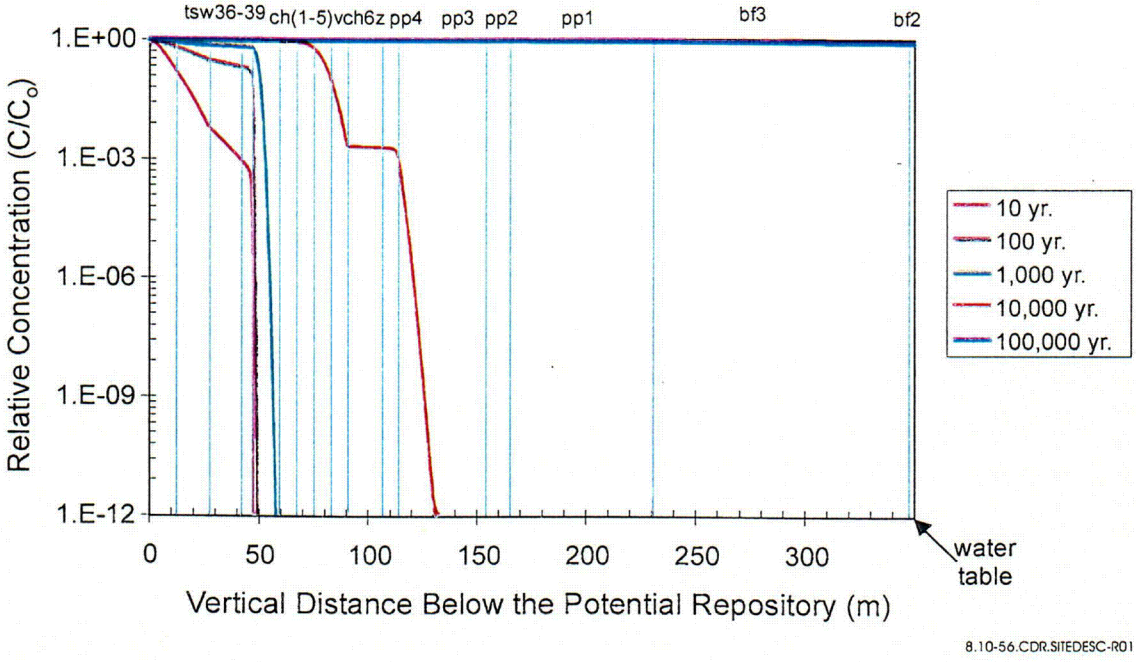

Source: CRWMS M&O (2000l, Figure V.2)

NOTE: The 100,000-yr. concentration line plots along the upper horizontal axis.

Figure 8.10-56. Simulated Time-Series Concentration Profile for Neptunium-237 under the Potential Repository in the SD-6 Cross Section for Mean Present-Day Infiltration

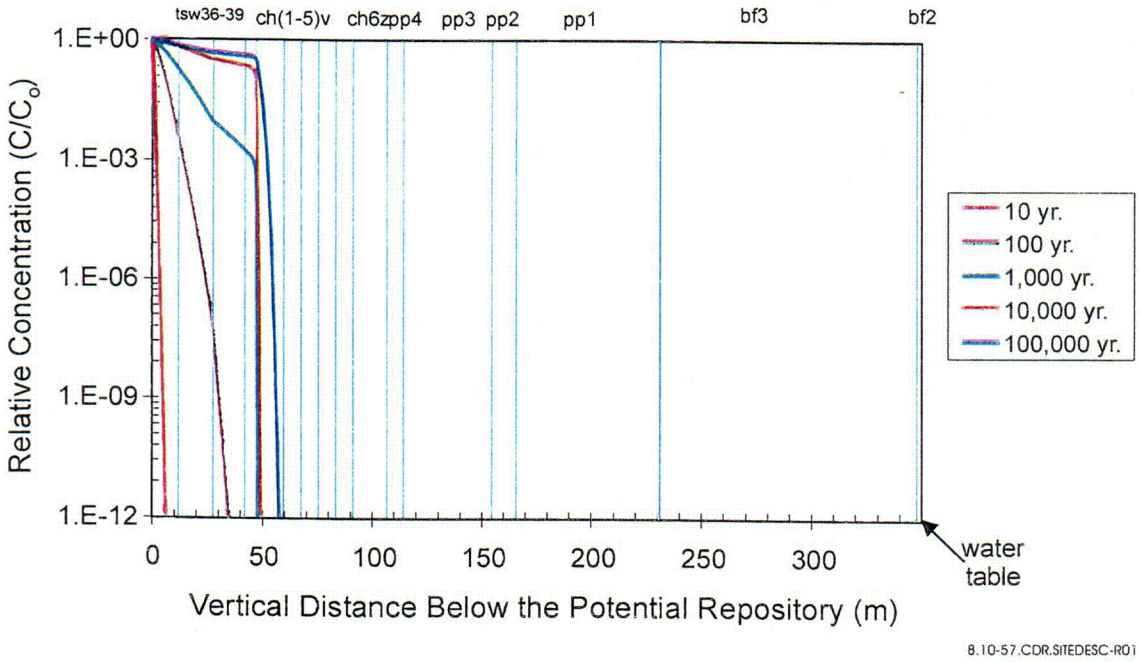

Source: CRWMS M&O (2000I, Figure V.3)

Figure 8.10-57. Simulated Time-Series Concentration Profile for Plutonium-239 under the Potential Repository in the SD-6 Cross Section for Mean Present-Day Infiltration

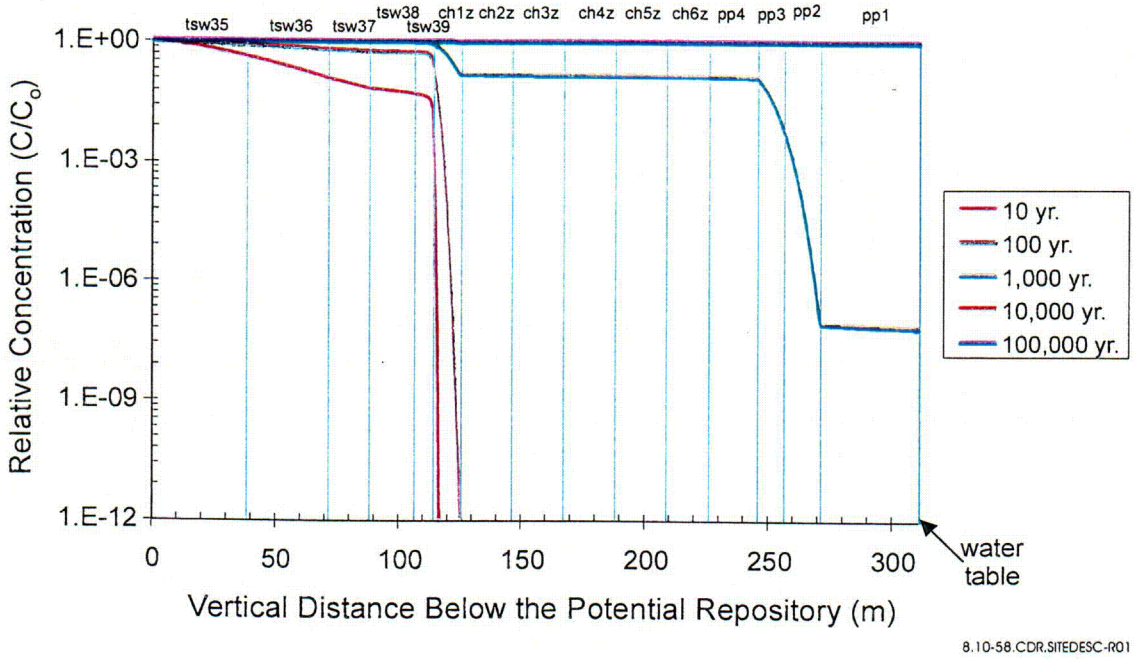

Source: CRWMS M&O (2000l, Figure V.19)

NOTE: The 10,000-yr. and 100,000-yr. concentration lines both plot along the upper horizontal axis.

Figure 8.10-58. Simulated Time-Series Concentration Profile for Technetium-99 under the Potential Repository in the UZ-14 Cross Section for Mean Present-Day Infiltration and a Perched-Water Regime

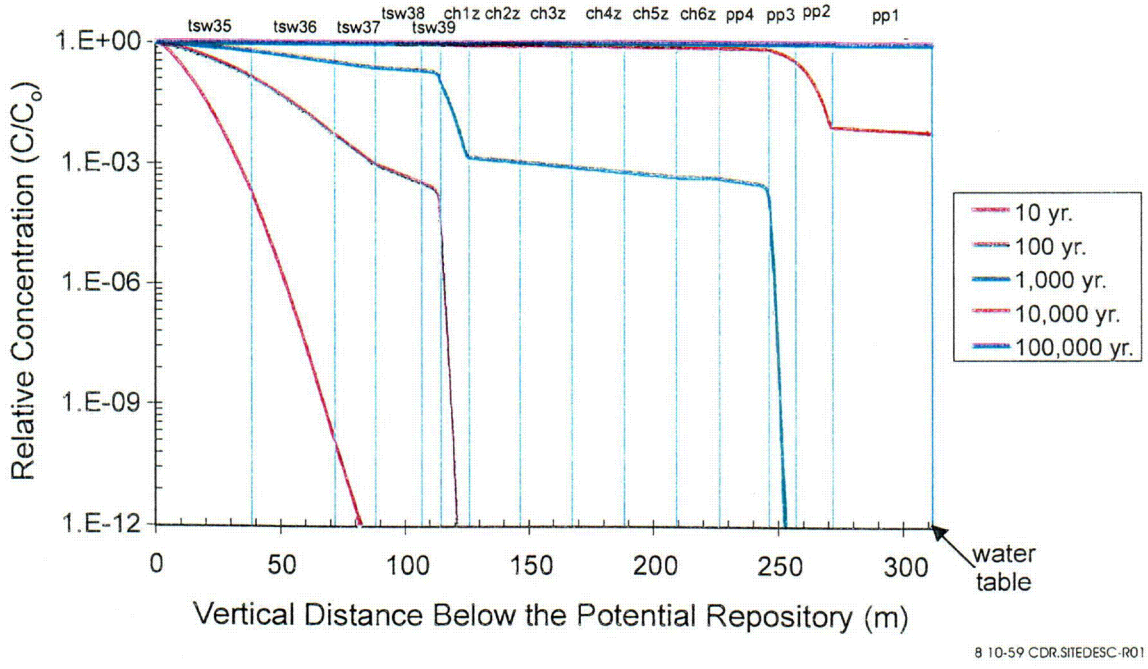

Source: CRWMS M&O (2000l, Figure V.20)

NOTE: The 100,000-yr. concentration line plots along the upper horizontal axis.

Figure 8.10-59. Simulated Time-Series Concentration Profile for Neptunium-237 under the Potential Repository in the UZ-14 Cross Section for Mean Present-Day Infiltration and a Perched-Water Regime

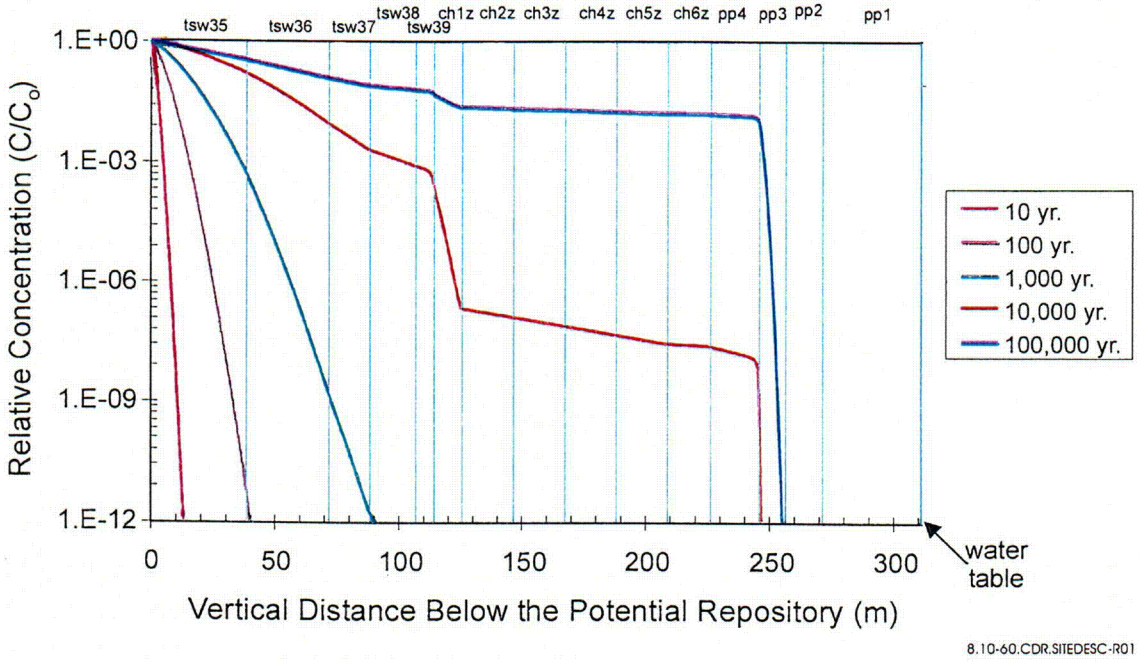

Source: CRWMS M&O (2000l, Figure V.21)

Figure 8.10-60. Simulated Time-Series Concentration Profile for Plutonium-239 under the Potential Repository in the UZ-14 Cross Section for Mean Present-Day Infiltration and a Perched-Water Regime

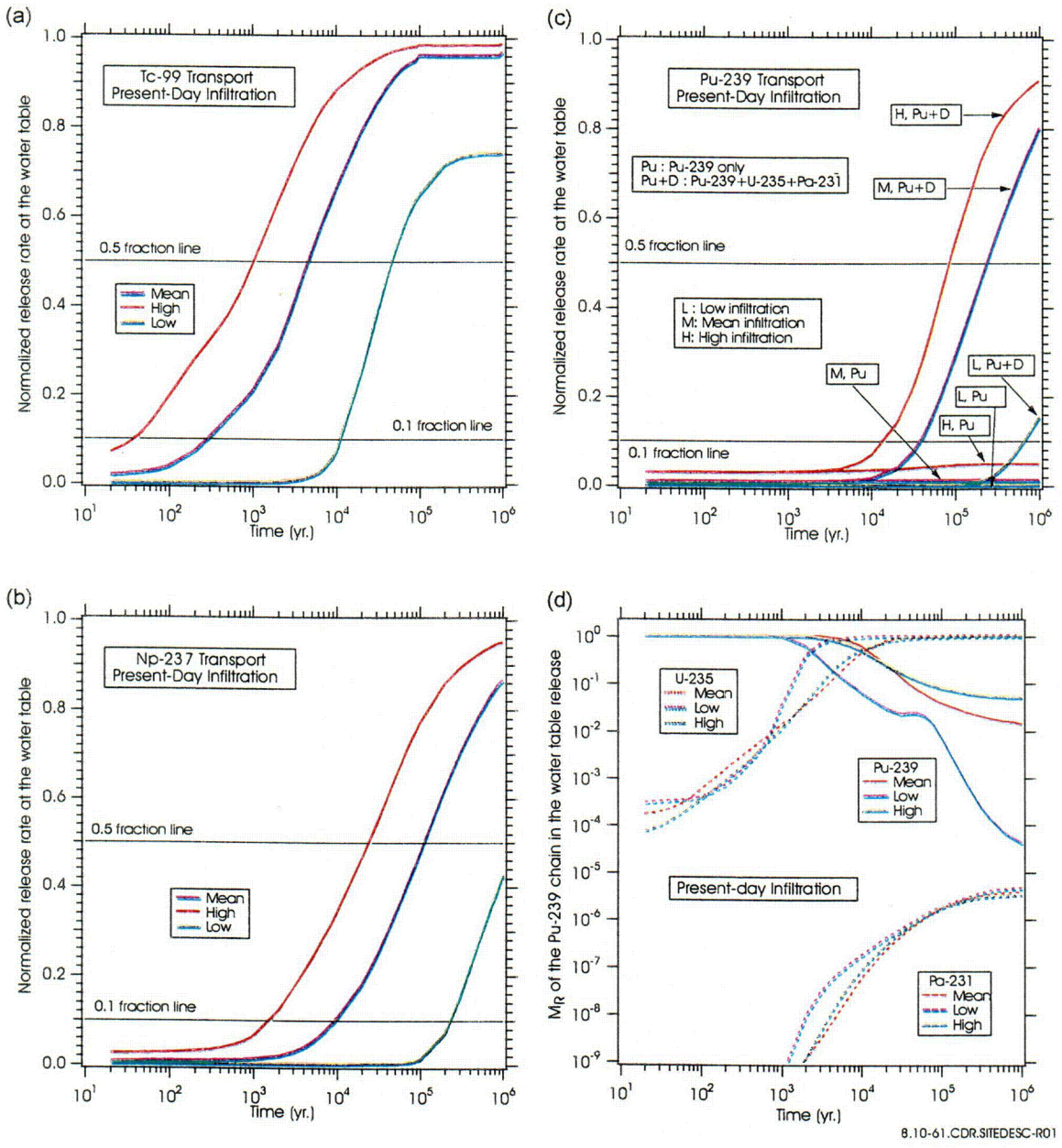

Source: CRWMS M&O (2000l, Figures 6.12.1, 6.13.1, 6.14.1, and 6.14.2)

Figure 8.10-61. Simulated Time-Series Concentration Profiles for Technetium-99, Neptunium-237, Plutonium-239, and Plutonium-239 Daughters at the Water Table for the Three Present-Day Climatic Scenarios Using the Three-Dimensional, Site-Scale Radionuclide Transport Model

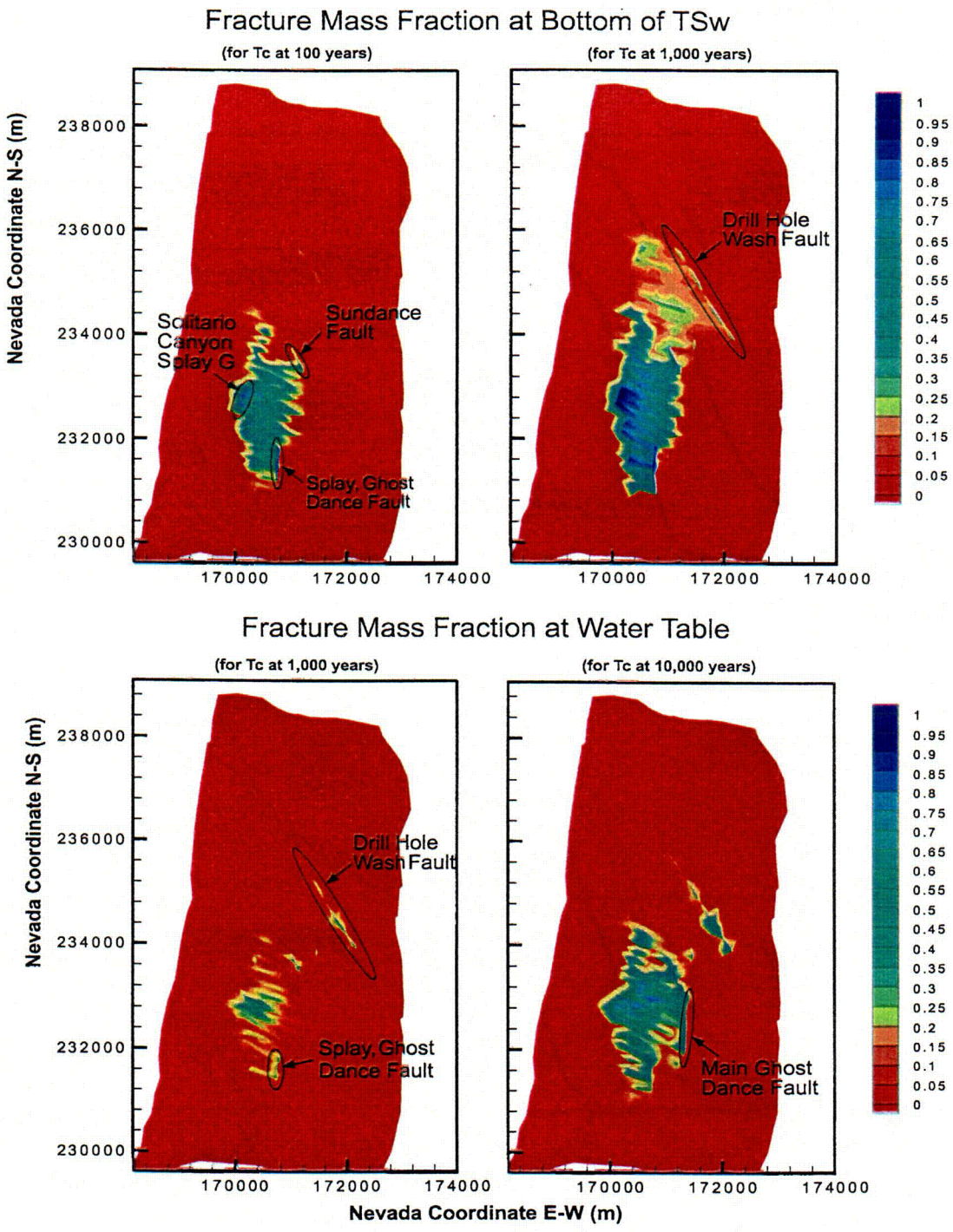

Source: CRWMS M&O (2000l, Figures 6.12.2, 6.12.4, 6.12.12, and 6.12.14)

Figure 8.10-62. Simulated Relative Mass Fraction Distribution of Technetium-99 in the Fractures at the Bottom of the Topopah Spring Welded Unit and the Water Table under Mean Present-Day Infiltration Using the Three-Dimensional, Site-Scale Radionuclide Transport Model

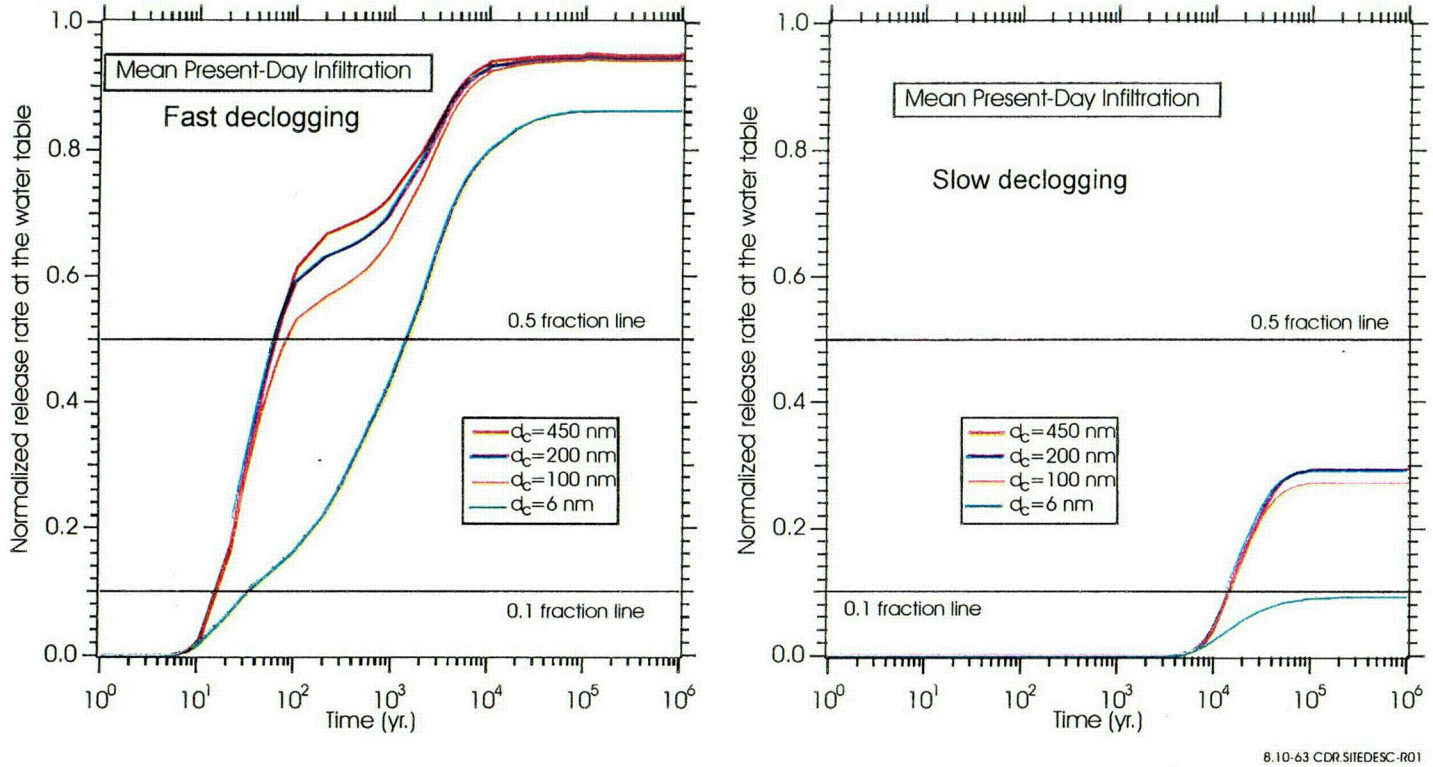

Source: CRWMS M&O (2000l, Figures 6.16.1 and 6.16.2)

Figure 8.10-63. Simulated Influence of Colloid Size and Declogging Parameter on Colloidal Transport under Mean Present-Day Infiltration Using the Three-Dimensional, Site-Scale Radionuclide Transport Model

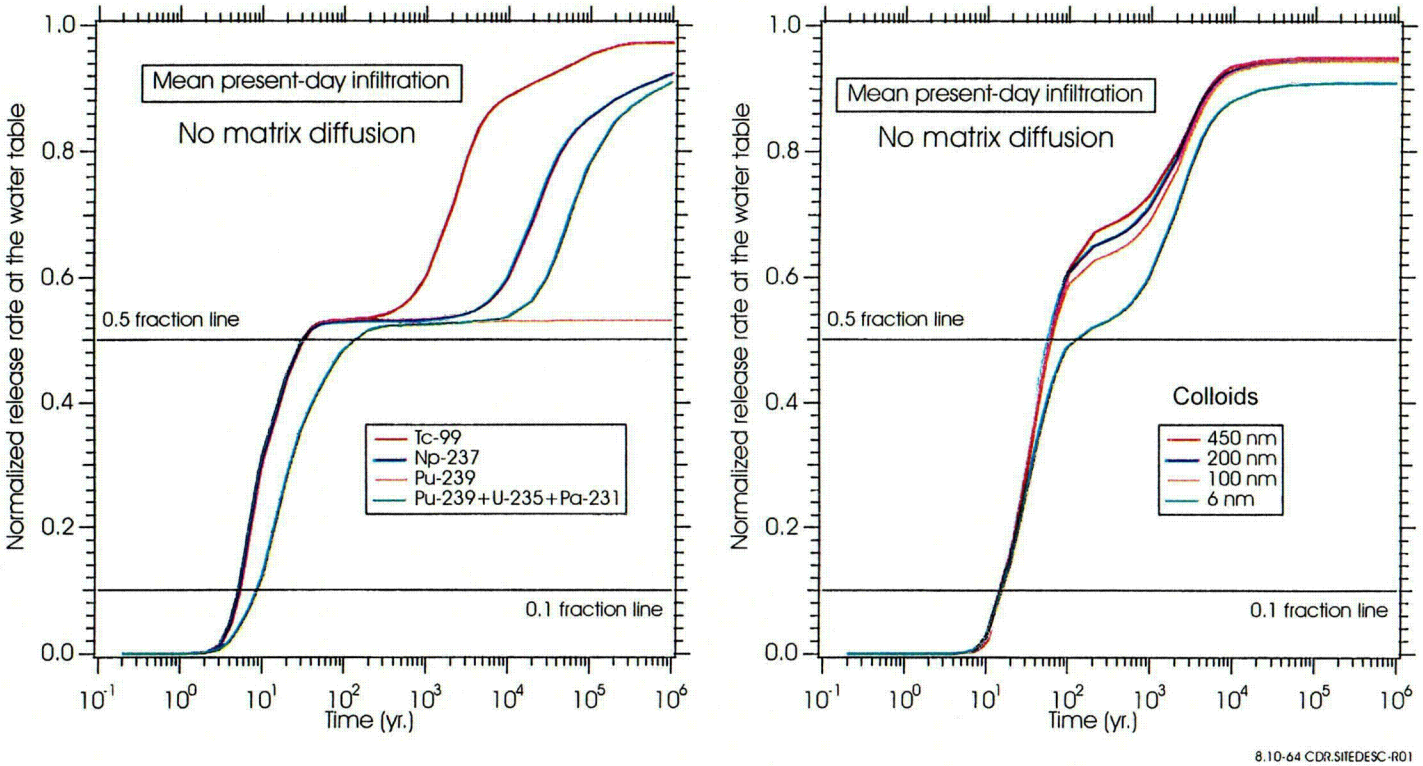

Source: CRWMS M&O (2000l, Figures 6.17.1 and 6.17.2)

Figure 8.10-64. Simulated Time-Series Concentration of Radionuclides and Colloids at the Water Table for the No-Diffusion Alternative Model under Mean Present-Day Infiltration Using the Three-Dimensional, Site-Scale Radionuclide Transport Model

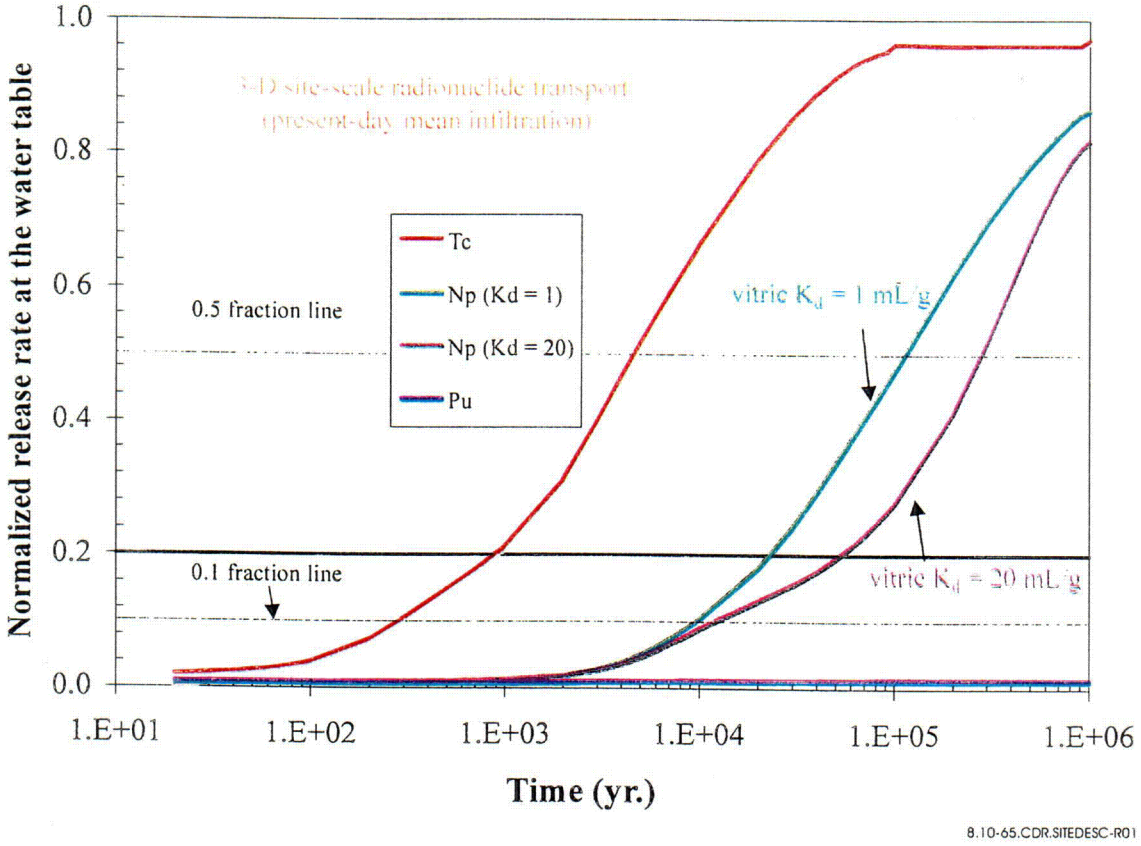

Source: CRWMS M&O (2000l, Figures 6.12.1, 6.13.1, and 6.14.1)

Figure 8.10-65. Simulated Effect of Radionuclide-Sorption (K_d) on Concentrations of Neptunium-237 at the Water Table under Mean Present-Day Infiltration Using the Three-Dimensional, Site-Scale Radionuclide Transport Model

INTENTIONALLY LEFT BLANK

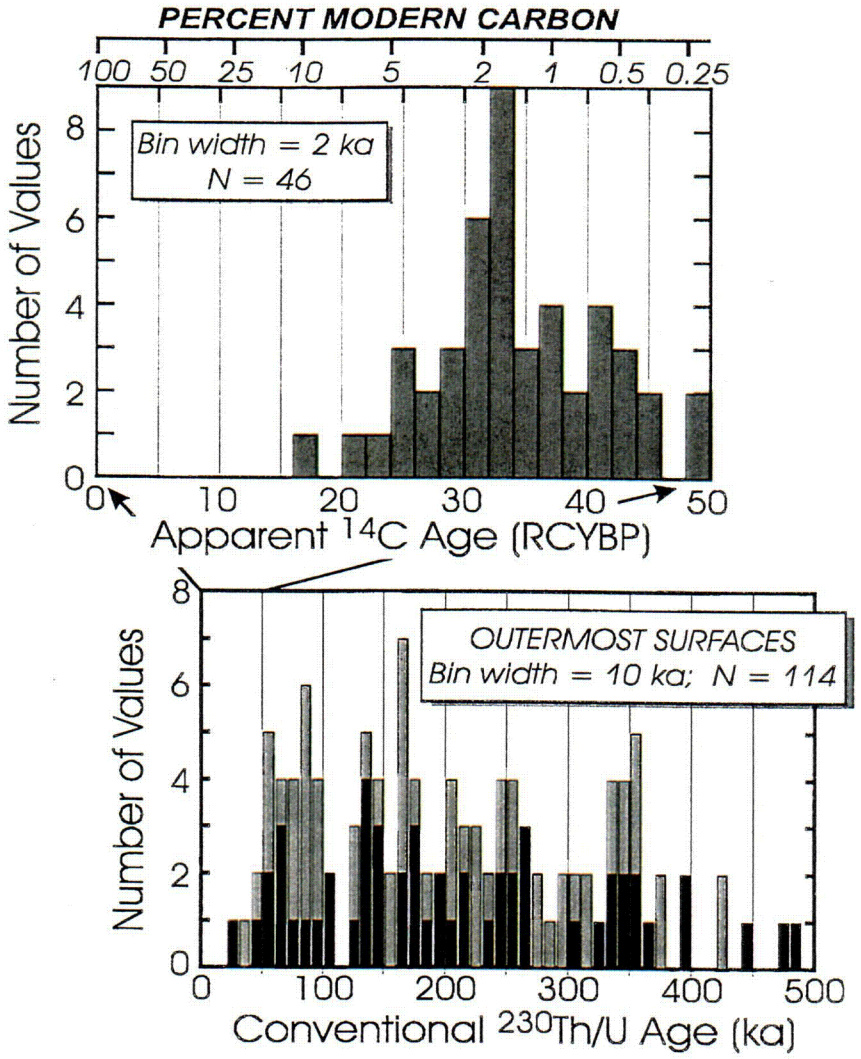

Source: Paces, Marshall et al. (1997, Figures B1 and D1)

NOTE: The histograms show radiocarbon (from calcite) and U-series (from calcite and opal) ages obtained for outermost mineral surfaces. U-series ages are shown for both lithophysal cavity (light bars) and fracture (dark bars) occurrences. RCYBP stands for radiocarbon years before present (units are thousands of years).

Figure 8.11-1. Fracture Mineral Ages

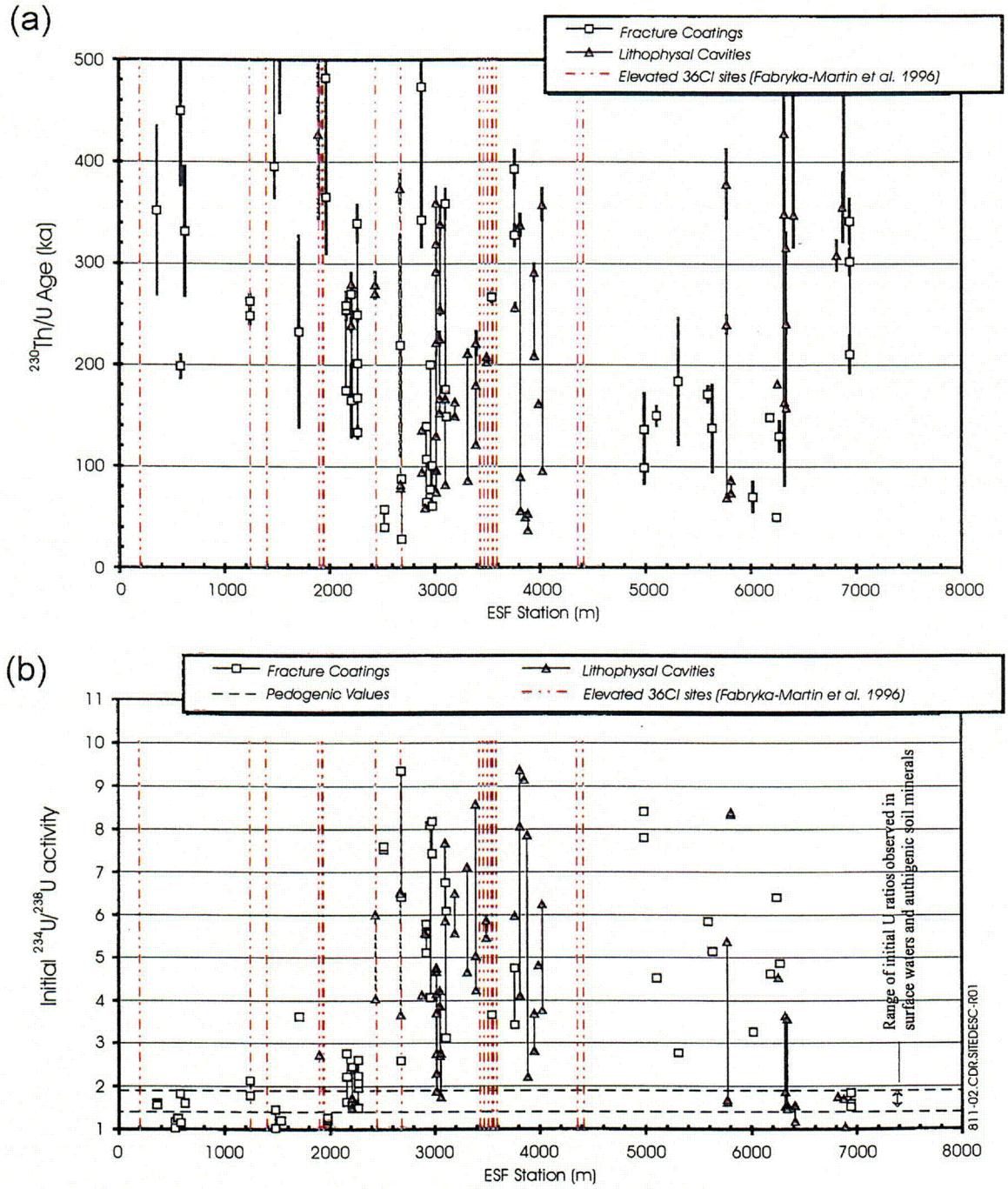

Source: Paces, Marshall et al. (1997, Figures D2 and D3)

NOTE: Plot (a) shows the distribution of $^{230}Th/U$ ages of calcite and opal from the outermost surfaces of secondary mineral coatings as a function of location in the Exploratory Studies Facility. Plot (b) shows the distribution of calculated initial $^{234}U/^{238}U$ activity ratios for the same samples. Vertical lines connect subsamples from the same occurrence.

Figure 8.11-2. Fracture Mineral Ages and Uranium Activity Ratios in the Exploratory Studies Facility

C140

Table 8.2-1. Selected Statistics for the Developed Record of Daily Precipitation (1980 to 1995) Adjusted to an Elevation of 1,400 Meters for the Area of the Potential Yucca Mountain Repository

Calender Year	Total Annual Precip. (mm)	Max. Daily Precip. (mm)	Number of Days Precip. Measured	Number of Days Precip. > 1 mm	Number of Days Precip. > 10 mm	Number of Days Precip. > 20 mm	Number of Days Precip. > 50 mm
1980	163	13	37	26	4	0	0
1981	104	16	30	20	2	0	0
1982	169	30	48	32	1	1	0
1983	294	58	53	39	7	2	1
1984	220	38	40	24	7	2	0
1985	85	16	26	14	1	0	0
1986	147	21	35	27	2	1	0
1987	207	32	46	35	4	1	0
1988	142	26	40	24	2	1	0
1989	27	3	16	7	0	0	0
1990	79	11	20	13	1	0	0
1991	194	19	34	25	8	0	0
1992	324	41	48	36	9	4	0
1993	255	30	41	31	8	1	0
1994	123	15	30	18	3	0	0
1995[a]	347	36	39	33	9	4	0
Averages	180	25	36.4	25.3	4.3	1.1	0.1

DTN: GS960908312211.003

NOTE: [a] Record for 1995 is through September 30, 1995, but little or no precipitation occurred between then and the end of the calendar year.

Table 8.2-2. Comparison of Results for a Scaled 1-Year Numerical Simulation of Net Infiltration and a 100-Year-Stochastic Numerical Simulation of Net Infiltration for Yucca Mountain

Model Area Descriptions	Modeled Areas		
	Area 1	Area 5	Area 3
Number of cells	253,597	12,900	5,040
Total area (km^2)	228.24	11.61	4.54
Average elevation (m)	1,237	1,346	1,294
Maximum elevation (m)	1,969	1,506	1,471
Minimum elevation (m)	918	1,195	1,162
Scaled 1-Yr. Simulation (Flint, A.L. et al. 1996)			
Average annual precipitation (mm/yr)	169	NA	NA
Mean net infiltration rate (mm/yr)	3.0	5.2	4.1
Maximum net infiltration rate (mm/yr)	81.9	29.2	23.4
Minimum net infiltration rate (mm/yr)	0.0	0.0	0.0
Coefficient of variation	2.2	1.1	1.2
100-Yr. Stochastic Simulation			
Average annual precipitation (mm/yr)	150	163	157
Mean net infiltration rate (mm/yr)	3.2	6.0	5.1
Maximum net infiltration rate (mm/yr)	63.2	29.7	29.7
Minimum net infiltration rate (mm/yr)	0.0	0.0	0.0
Coefficient of variation	1.7	0.9	1.1

DTN: GS960908312211.003

NOTE: NA = not available

Table 8.2-3. Numerical-Infiltration Model Results for 5-Year Periods of the 100-Year Stochastic Simulation for Yucca Mountain Under Current Climatic Conditions

Simulation Year	5-Yr. Average Precipitation (mm)	15-Yr. Sliding Average Precipitation (mm)	5-Yr. Average Runoff (mm)	15-Yr. Sliding Average Runoff (mm)	5-Yr. Average Net Infiltration (mm)	15-Yr. Sliding Average Net Infiltration (mm)
5	143.11		0.07		2.67	
10	146.22		0.00		0.45	
15	154.71	148.01	0.07	0.05	2.11	1.74
20	133.63	144.85	0.01	0.03	1.38	1.31
25	161.30	149.88	0.03	0.03	2.22	1.90
30	135.63	143.52	0.59	0.21	3.96	2.52
35	130.18	142.37	0.02	0.21	1.35	2.51
40	159.96	141.92	1.19	0.60	5.30	3.54
45	168.00	152.71	0.03	0.41	1.35	2.67
50	184.95	170.97	1.18	0.80	6.45	4.37
55	120.32	157.76	0.01	0.40	1.39	3.06
60	108.22	137.83	0.00	0.39	0.17	2.67
65	179.01	135.85	3.07	1.03	7.95	3.17
70	138.34	141.86	0.00	1.02	0.45	2.86
75	126.00	147.79	0.00	1.03	0.54	2.98
80	195.29	153.21	3.09	1.03	10.95	3.98
85	134.68	151.99	0.00	1.03	0.69	4.06
90	174.29	168.08	1.22	1.44	7.82	6.49
95	151.67	153.55	0.02	0.41	1.61	3.37
100	158.23	161.40	0.96	0.73	6.13	5.19
Average	150.19	150.20	0.58	0.60	3.25	3.24
Maximum	195.29	170.97	3.09	1.44	10.95	6.49
Minimum	108.22	135.85	0.00	0.03	0.17	1.31
Standard Deviation	22.77	9.72	0.97	0.43	3.11	1.25
Coefficient of Variation	0.15	0.06	1.68	0.71	0.96	0.39

DTN: GS960908312211.003

Table 8.2-4. Summary of Annual Results for Simulated Net Infiltration and Runoff Obtained Using the 1980 to 1995 Developed Daily Precipitation Record for Yucca Mountain

Calendar Year	Average Precipitation (mm)	Maximum Precipitation (mm)	Minimum Precipitation (mm)	Average Net Infiltration (mm)	Maximum Net Infiltration (mm)	Minimum Net Infiltration (mm)	Average Runoff (mm)	Maximum Runoff (mm)	Minimum Runoff (mm)
1980	144.0	229.2	106.9	1.70	51.20	0.00	0.00	0.00	0.00
1981	91.9	146.3	68.2	0.00	0.00	0.00	0.00	0.00	0.00
1982	149.3	237.7	110.8	0.00	9.93	0.00	0.00	0.00	0.00
1983	259.7	413.5	192.8	7.11	169.93	0.00	0.12	56.45	0.00
1984	193.5	308.0	143.6	2.59	104.87	0.00	0.01	31.80	0.00
1985	75.1	119.5	55.7	2.07	61.60	0.00	0.01	9.78	0.00
1986	129.9	206.7	96.4	0.03	30.05	0.00	0.00	0.00	0.00
1987	182.9	291.1	135.7	0.05	52.29	0.00	0.00	0.00	0.00
1988	125.4	199.7	93.1	0.53	54.81	0.00	0.00	5.10	0.00
1989	32.7	52.0	24.3	0.00	0.00	0.00	0.00	0.00	0.00
1990	69.8	111.1	51.8	0.00	0.00	0.00	0.00	0.00	0.00
1991	171.4	272.8	127.2	0.51	38.11	0.00	0.00	0.00	0.00
1992	287.1	457.1	213.1	25.96	252.54	0.00	9.25	150.07	0.00
1993	225.3	358.6	167.2	38.20	211.75	0.00	18.00	183.90	0.00
1994	108.7	173.0	80.7	0.00	29.12	0.00	0.00	0.00	0.00
1995	273.0	434.6	202.6	43.58	247.55	0.00	23.77	181.77	0.00
Average	157.5	250.7	116.9	7.64	82.11	0.00	3.20	38.68	0.00
Maximum	287.1	457.1	213.1	43.58	252.54	0.00	23.77	183.90	0.00
Minimum	32.7	52.0	24.3	0.00	0.00	0.00	0.00	0.00	0.00
Standard Deviation	75.8	120.6	56.2	14.52	88.45	0.00	7.35	68.20	0.00
Coefficient of Variation	0.5	0.5	0.5	1.90	1.08	–	2.30	1.76	–

DTN: GS960908312211.003

Table 8.2-5. Infiltration Fluxes Estimated by the Chloride Mass-Balance Method Compared to Spatially Averaged Estimates of Net Infiltration Derived from the Numerical Infiltration Model

Borehole (Infiltration Zone)	Hydrostratigraphic Unit	Sample Depth (m)	Apparent Infiltration Rate (mm/yr.)[a]	Net Infiltration for 90x90-m Area Centered on Borehole (mm/yr.)[b]	3,600-m^2 Areal Average of Net Infiltration, Numerical Model (mm/yr.)[c]
USW UZ-N37 (moderately-active channel)	Soil	5.4-10.9	0.4 to 0.8	–	0.0
USW UZ-N54 (alluvium-filled channel)	Soil	5.2-8.2	0.01	–	0.0
UZ-N55	PTn	–	0.7 to 1.3	–	0.3
UE-25 UZ #16 (terrace)	Soil PTn	5.2-7.4 49.9	0.01 to 0.03 1.6 to 3.1	0.0 0.0	0.0 0.0
USW UZ-14 (terrace)	Soil PTn	5.5-9.4 13.78	0.1 to 0.2 0.2 to 0.4	3.0 3.0	3.1 3.1
NRG-6 (terrace)	PTn	48.28	0.3 to 0.6	1.0	–
NRG-7a (terrace)	PTn	50.57	1.3 to 2.6	0.0	–
SD-7 (sideslope)	PTn	103.63	0.7 to 1.3	6.0	–
SD-9 (channel)	PTn	28.74	0.4 to 0.6	5.0	–
SD-12 (terrace)	PTn	81.08	1.0 to 2.1	1.3	–

NOTES: [a] Data are from Table 5.3-25.
[b] Data are from Table 8.7-4
[c] Flint, A.L. et al. (1996, Table 7)

Table 8.2-6. Comparison Between Measured and Model-Simulated Daily Mean Discharge at Stream Gauging Sites for Storms During January and March 1995

Calibration Watershed		Occurrences of Streamflow During 1995: Daily Mean Discharge (ft^3/s)			
		1/25/1995	1/26/1995	3/10/1995	3/11/1995
Lower Pagany Wash	Measured	0.00	0.01	0.00	8.60
	Simulated	0.00	0.00	0.00	7.23
Upper Pagany Wash	Measured	0.00	1.70	0.00	12.00
	Simulated	0.34	0.00	0.13	9.46
Upper Drill Hole Wash	Measured	0.00	0.00	0.00	5.00
	Simulated	1.55	0.00	0.00	9.33
Upper Split Wash	Measured	0.10	1.50	0.00	3.00
	Simulated	0.07	0.02	0.28	3.69
Wren Wash	Measured	0.66	0.96	0.00	2.60
	Simulated	0.71	0.19	0.70	3.92
Total	Measured	0.76	4.17	0.00	31.20
	Simulated	2.66	0.22	1.10	33.63

Source: USGS (2000b, Table 6-2)

Table 8.2-7. Results of Infiltration Modeling for Modern Climate Scenarios for the 123.7-Square-Kilometer Area of the Infiltration Model Domain

Modern Climate Scenario		Modeling Results for Modern Climate Scenarios for Area of Entire Infiltration Model Domain (123.7 km^2)		
		Lower Bound	Mean	Upper Bound
Annual Precipitation (mm/yr.)	Area mean	185.8	188.5	265.6
	Area maximum	282.2	281.8	397.1
	Area minimum	148.0	147.4	207.8
Annual Evapotranspiration (mm/yr.)	Area mean	184.8	184.1	255.5
	Area maximum	571.9	612.1	700.5
	Area minimum	54.7	56.5	71.5
Annual Infiltrated Surface-Water Run-On (mm/yr.)	Area mean	2.1	4.4	9.7
	Area maximum	474.2	994.1	2,669.0
	Area minimum	0.0	0.0	0.0
Average Annual Outflow as Streamflow (mm/yr.)		0.2	0.2	0.9
Annual Net Infiltration (mm/yr.)	Area mean	1.2	3.6	8.8
	Area maximum	252.0	958.9	2,656.6
	Area minimum	0.0	0.0	0.0

Source: USGS (2000b, Table 6-8)

Table 8.2-8. Results of Infiltration Modeling for Modern Climate Scenarios for the 38.7-Square-Kilometer Area of the 1999 Unsaturated Zone Flow and Transport Model Domain

Modern Climate Scenario		Modeling Results for Modern Climate Scenarios for Area of Unsaturated Zone Flow and Transport Model Domain (38.7 km^2)		
		Lower Bound	Mean	Upper Bound
Annual Precipitation (mm/yr.)	Area mean	186.8	190.6	268.6
	Area maximum	246.3	246.5	347.4
	Area minimum	162.7	167.1	235.5
Annual Evapotranspiration (mm/yr)	Area mean	186.2	185.3	257.1
	Area maximum	367.9	348.2	485.6
	Area minimum	62.2	59.7	77.2
Annual Infiltrated Surface-Water Run-On (mm/yr.)	Area mean	1.9	4.1	10.1
	Area maximum	194.9	277.0	802.9
	Area minimum	0.0	0.0	0.0
Average Annual Outflow as Streamflow (mm/yr.)		-0.7	-0.2	-0.3
Annual Net Infiltration (mm/yr.)	Area mean	1.3	4.6	11.1
	Area maximum	218.8	263.6	784.9
	Area minimum	0.0	0.0	0.0

Source: USGS (2000b, Table 6-9)

Table 8.2-9. Results of Infiltration Modeling for Modern Climate Scenarios for the 4.7-Square-Kilometer Area of the Potential Repository

Modern Climate Scenario		Modeling Results for Modern Climate Scenarios for Area of the Potential Repository (4.7 km^2)		
		Lower Bound	Mean	Upper Bound
Annual Precipitation (mm/yr.)	Area mean	191.6	196.9	277.5
	Area maximum	204.1	209.9	295.8
	Area minimum	178.2	183.4	258.5
Annual Evapotranspiration (mm/yr.)	Area mean	191.7	189.9	260.4
	Area maximum	252.9	273.3	423.0
	Area minimum	155.0	154.7	203.0
Annual Infiltrated Surface-Water Run-On (mm/yr.)	Area mean	1.0	3.4	8.1
	Area maximum	59.8	161.1	454.8
	Area minimum	0.0	0.0	0.0
Average Annual Outflow as Streamflow (mm/yr.)		-0.3	1.4	4.9
Annual Net Infiltration (mm/yr.)	Area mean	0.4	4.7	11.6
	Area maximum	26.6	120.1	387.4
	Area minimum	0.0	0.0	0.0

Source: USGS (2000b, Table 6-10)

Table 8.2-10. Results of Infiltration Modeling for Monsoon Climate Scenarios for the 123.7-Square-Kilometer Area of the Infiltration Model Domain

Monsoon Climate Scenario		Modeling Results for Monsoon Climate Scenarios for Area of Entire Infiltration Model Domain (123.7 km^2)		
		Lower Bound	Mean	Upper Bound
Mean Annual Air Temperature (degrees Celsius)		17.3	17.2	17.0
Annual Precipitation (mm/yr.)	Area mean	188.5	300.5	412.5
	Area maximum	281.8	397.7	513.6
	Area minimum	147.4	257.7	368.0
Annual Snowfall (mm/yr.)	Area mean	N/A	N/A	6.8
	Area maximum	N/A	N/A	39.3
	Area minimum	N/A	N/A	1.2
Annual Evapotranspiration (mm/yr.)	Area mean	184.1	285.2	386.3
	Area maximum	612.1	714.4	816.7
	Area minimum	56.5	77.9	99.3
Annual Infiltrated Surface-Water Run-On (mm/yr.)	Area mean	4.4	11.2	18.1
	Area maximum	994.1	1,794.9	2,595.7
	Area minimum	0.0	0.0	0.0
Average Annual Outflow as Streamflow (mm/yr.)		0.2	5.1	10.0
Annual Net Infiltration (mm/yr.)	Area mean	3.6	8.6	13.6
	Area maximum	958.9	1,787.1	2,615.3
	Area minimum	0.0	0.0	0.0

Source: USGS (2000b, Table 6-12)

NOTE: N/A = not applicable

Table 8.2-11. Results of Infiltration Modeling for Monsoon Climate Scenarios for the 38.7-Square-Kilometer Area of the 1999 Unsaturated Zone Flow and Transport Model Domain

Monsoon Climate Scenario		Modeling Results for Monsoon Climate Scenarios for Area of Unsaturated Zone Flow and Transport Model (38.7 km^2)		
		Lower Bound	Mean	Upper Bound
Annual Precipitation (mm/yr.)	Area mean	190.6	302.7	414.8
	Area maximum	246.5	360.9	475.4
	Area minimum	167.1	278.2	389.3
Annual Snowfall (mm/yr.)	Area mean	N/A	N/A	6.8
	Area maximum	N/A	N/A	18.8
	Area minimum	N/A	N/A	3.0
Annual Evapotranspiration (mm/yr.)	Area mean	185.3	284.0	382.8
	Area maximum	348.2	509.9	684.7
	Area minimum	59.7	81.7	103.7
Annual Infiltrated Surface-Water Run-On (mm/yr.)	Area mean	4.1	12.2	20.4
	Area maximum	277.0	642.7	1,018.2
	Area minimum	0.0	0.0	0.0
Average Annual Outflow as Streamflow (mm/yr.)		-0.2	4.6	9.5
Annual Net Infiltration (mm/yr.)	Area mean	4.6	12.2	19.8
	Area maximum	263.6	629.0	1,016.2
	Area minimum	0.0	0.0	0.0

Source: USGS (2000b, Table 6-13)

NOTE: N/A = not applicable

Table 8.2-12. Results of Infiltration Modeling for Monsoon Climate Scenarios for the 4.7-Square-Kilometer Area of the Potential Repository

Monsoon Climate Scenario		Modeling Results for Monsoon Climate Scenarios for Area of the Potential Repository (4.7 km^2)		
		Lower Bound	Mean	Upper Bound
Annual Precipitation (mm/yr.)	Area mean	196.9	309.3	421.6
	Area maximum	209.9	322.8	435.7
	Area minimum	183.4	295.2	407.0
Annual Snowfall (mm/yr.)	Area mean	N/A	N/A	7.7
	Area maximum	N/A	N/A	10.9
	Area minimum	N/A	N/A	5.3
Annual Evapotranspiration (mm/yr.)	Area mean	189.9	281.7	373.5
	Area maximum	273.3	466.4	666.0
	Area minimum	154.7	217.8	277.1
Annual Infiltrated Surface-Water Run-On (mm/yr.)	Area mean	3.4	9.1	14.8
	Area maximum	161.1	348.6	536.1
	Area minimum	0.0	0.0	0.0
Average Annual Outflow as Streamflow (mm/yr.)		1.4	13.2	25.1
Annual Net Infiltration (mm/yr.)	Area mean	4.7	12.5	20.3
	Area maximum	120.1	267.0	413.8
	Area minimum	0.0	0.0	0.0

Source: USGS (2000b, Table 6-14)

NOTE: N/A = not applicable

Table 8.2-13. Results of Infiltration Modeling for Glacial Transition Climate Scenarios for the 123.7-Square-Kilometer Area of the Infiltration Model Domain

Glacial Transition Climate Scenario		Modeling Results for Glacial Transition Climate Scenarios for Area of Entire Infiltration Model Domain (123.7 km^2)		
		Lower Bound	Mean	Upper Bound
Mean Annual Air Temperature (°C)		10.2	9.8	9.4
Annual Precipitation (mm/yr.)	Area mean	201.0	316.1	431.1
	Area maximum	250.3	393.5	536.8
	Area minimum	179.4	282.0	384.6
Annual Snowfall (mm/yr.)	Area mean	29.1	45.5	61.9
	Area maximum	109.4	181.9	254.5
	Area minimum	9.2	14.3	19.5
Annual Evapotranspiration (mm/yr.)	Area mean	194.6	294.8	395.0
	Area maximum	525.7	600.7	751.2
	Area minimum	73.6	94.9	116.3
Annual Infiltrated Surface-Water Run-On (mm/yr.)	Area mean	2.2	14.6	27.0
	Area maximum	524.3	3,913.2	7,482.0
	Area minimum	0.0	0.0	0.0
Average Annual Outflow as Streamflow (mm/yr.)		0.0	1.5	2.9
Annual Net Infiltration (mm/yr.)	Area mean	2.2	13.4	24.6
	Area maximum	370.3	3,902.5	7,489.3
	Area minimum	0.0	0.0	0.0

Source: USGS (2000b, Table 6-17)

Table 8.2-14. Results of Infiltration Modeling for Glacial Transition Climate Scenarios for the 38.7-Square-Kilometer Area of the Unsaturated Zone Flow and Transport Model Domain

Glacial Transition Climate Scenario		Modeling Results for Glacial Transition Climate Scenarios for Area of Unsaturated Zone Flow and Transport Model Domain (38.7 km^2)		
		Lower Bound	Mean	Upper Bound
Annual Precipitation (mm/yr.)	Area mean	202.2	317.8	433.5
	Area maximum	231.7	364.3	496.8
	Area minimum	189.8	298.3	406.9
Annual Snowfall (mm/yr.)	Area mean	29.1	45.1	61.1
	Area maximum	75.1	122.0	168.9
	Area minimum	16.3	25.3	34.2
Annual Evapotranspiration (mm/yr.)	Area mean	195.2	293.5	391.8
	Area maximum	343.3	502.3	733.9
	Area minimum	76.9	99.4	121.9
Annual Infiltrated Surface-Water Run-On (mm/yr.)	Area mean	1.7	15.6	29.6
	Area maximum	193.1	1,301.1	2,586.2
	Area minimum	0.0	0.0	0.0
Average Annual Outflow as Streamflow (mm/yr.)		-0.1	-0.2	-0.3
Annual Net Infiltration (mm/yr.)	Area mean	2.5	17.8	33.0
	Area maximum	219.2	1,282.9	2,555.0
	Area minimum	0.0	0.0	0.0

Source: USGS (2000b, Table 6-18)

Table 8.2-15. Results of Infiltration Modeling for Glacial Transition Climate Scenarios for the 4.7-Square-Kilometer Area of the Potential Repository

Glacial Transition Climate Scenario		Modeling Results for Glacial Transition Climate Scenarios for Area of the Potential Repository (4.7 km^2)		
		Lower Bound	Mean	Upper Bound
Annual Precipitation (mm/yr.)	Area mean	205.5	323.1	440.6
	Area maximum	212.4	333.8	455.3
	Area minimum	198.4	311.8	425.3
Annual Snowfall (mm/yr.)	Area mean	32.5	50.3	68.1
	Area maximum	42.0	65.2	88.3
	Area minimum	24.9	37.8	50.7
Annual Evapotranspiration (mm/yr.)	Area mean	197.5	287.8	378.1
	Area maximum	279.4	477.8	688.6
	Area minimum	171.0	219.3	265.3
Annual Infiltrated Surface-Water Run-On (mm/yr.)	Area mean	1.4	12.0	22.5
	Area maximum	100.5	676.6	1,334.8
	Area minimum	0.0	0.0	0.0
Average Annual Outflow as Streamflow (mm/yr.)		0.3	8.0	15.6
Annual Net Infiltration (mm/yr.)	Area mean	2.2	19.8	37.3
	Area maximum	116.3	591.0	1,181.4
	Area minimum	0.0	0.0	0.0

Source: USGS (2000b, Table 6-19)

Table 8.2-16. Summary of Infiltration Model Results Within the 4.7-Square-Kilometer Repository Area for Modern, Monsoon, and Glacial Transition Climatic Conditions

		Modern Climate	Monsoon Climate	Glacial Transition Climate
Lower Bound	Precipitation	191.6 mm/yr.	196.9 mm/yr.	205.5 mm/yr.
	Evapotranspiration	191.7 mm/yr.	189.9 mm/yr.	197.5 mm/yr.
	Surface-water outflow	-0.3 mm/yr.	1.4 mm/yr.	0.3 mm/yr.
	Infiltration	0.4 m/yr.	4.7 mm/yr.	2.2 mm/yr.
Mean Modern	Precipitation	196.9 mm/yr.	309.3 mm/yr.	323.1 mm/yr.
	Evapotranspiration	189.9 mm/yr.	281.7 mm/yr.	287.8 mm/yr.
	Surface-water outflow	1.4 mm/yr.	13.2 mm/yr.	8.0 mm/yr.
	Infiltration	4.7 mm/yr.	12.5 mm/yr.	19.8 mm/yr.
Upper Bound	Precipitation	277.5 mm/yr.	421.6 mm/yr.	440.6 mm/yr.
	Evapotranspiration	260.4 mm/yr.	373.5 mm/yr.	378.1 mm/yr.
	Surface-water outflow	4.9 mm/yr.	25.1 mm/yr.	15.6 mm/yr.
	Infiltration	11.6 mm/yr.	20.3 mm/yr.	37.3 mm/yr.

Source: USGS (2000b, Tables 6-10, 6-14, 6-19)

INTENTIONALLY LEFT BLANK

Table 8.3-1. Generalized Lithostratigraphy (after Buesch, Spengler et al. 1996; Moyer and Geslin 1995); Previously Used Informal Stratigraphic Nomenclature (after Scott and Bonk 1984), Corresponding Detailed Hydrogeologic Units (Flint, L.E. 1998), and Major Hydrogeologic Units (Montazer and Wilson 1984) at Yucca Mountain

Currently Used Formal and Informal Nomenclature	Previously Used Informal Nomenclature	Hydrogeologic Units	
		Detailed	Major
PAINTBRUSH GROUP **Tiva Canyon Tuff (Tpc)** crystal-rich member (Tpcr) vitric zone (rv) nonlithophysal zone (rn) subvitrophyre transition subzone (rn4)	vitrophyre (ccr)	**CCR** (< 10%)	Tiva Canyon welded (TCw)
pumice-poor subzone (rn3) mixed pumice subzone (rn2) crystal transition subzone (rn1) lithophysal zone (rl) crystal-poor member (Tpcp)	upper cliff (cuc)	**CUC** (> 9%)	
upper lithophysal zone (pul)	upper lithophysal (cul)	**CUL** (< 20%)	
middle nonlithophysal zone (pmn) lower lithophysal zone (pll) lower nonlithophysal zone (pln) hackly subzone (plnh) columnar subzone (plnc)	clinkstone(cks), rounded step(crs) lower lithophysal (cll) hackly (ch) columnar (cc)	CW	
argillic pumice interval (plnc2) vitric zone (pv) densely welded subzone (pv3v)	vitrophyre	**CMW** (> 15%)	
moderately welded subzone (pv2)	nonwelded base (ccs)	**CNW** (> 28%)	
non- to partially welded subzone (pv1)			Paintbrush nonwelded (PTn)
Pre-Tiva Canyon Tuff bedded tuff (Tpbt4)		BT4	
Yucca Mountain Tuff (Tpy)		**TPY** (< 30%)	
Pre-Yucca Mountain Tuff bedded tuff (Tpbt3)		BT3	
Pah Canyon Tuff (Tpp)		TPP	
Pre-Pah Canyon Tuff bedded tuff (Tpbt2) **Topopah Spring Tuff (Tpt)** crystal-rich member (Tptr) vitric zone (rv) nonwelded subzone (rv3) moderately welded subzone (rv2)		BT2	
densely welded subzone (rv1) nonlithophysal zone (rn) dense subzone (rn3)	vitrophyre (tc) rounded (tr)	TC (< 9%)	Topopah Spring welded (TSw)
vapor-phase corroded subzone (rn2)		TR	
lithophysal zone (rl) crystal-poor member (Tptp) upper lithophysal zone (pul)	upper lithophysal (tul)	TUL	
middle nonlithophysal zone (pmn)	middle nonlithophysal (tmn)	TMN	
lower lithophysal zone (pll)	lower lithophysal (tll)	TLL	
lower nonlithophysal zone (pln)	mottled (tm)	**TM2** (upper 2/3)	
		TM1 (lower 1/3)	

Table 8.3-1. Generalized Lithostratigraphy (after Buesch, Spengler et al. 1996; Moyer and Geslin 1995); Previously Used Informal Stratigraphic Nomenclature (after Scott and Bonk 1984), Corresponding Detailed Hydrogeologic Units (Flint, L.E. 1998), and Major Hydrogeologic Units (Montazer and Wilson 1984) at Yucca Mountain (Continued)

Currently Used Formal and Informal Nomenclature	Previously Used Informal Nomenclature	Hydrogeologic Units	
		Detailed	Major
vitric zone (pv)			
densely welded subzone (pv3)	basal vitrophyre (tv)	PV3	
moderately welded subzone (pv2)	nonwelded base	PV2	Calico Hills nonwelded (CHn)
nonwelded subzone (pv1)			
Pre-Topopah Spring Tuff bedded tuff (Tpbt1)		**BT1a** (altered) **BT1** (unaltered)	
CALICO HILLS FORMATION (Tac)			
Unit 4 Pumiceous pyroclastic flow	Calico Hills vitric (CHv)	**CHV** (vitric)	
Unit 3 Lithic-rich pyroclastic flow	Calico Hills zeolitized (CHz)	**CHZ** (zeolitic)	
Unit 2 Pumiceous pyroclastic flow			
Unit 1 Lithic-rich pyroclastic flow			
Bedded tuff (Tacbt)		**BT** (zeolitic)	
Basal sandstone (Tacbs)			
CRATER FLAT GROUP			
Prow Pass Tuff (Tcp)			
Unit 4 Pyroxene rich		**PP4** (zeolitic)	
Unit 3 Welded pyroclastic flow		**PP3** (welded, altered)	
		PP2 (welded)	
Unit 2 Lithic-rich pyroclastic flow		**PP1** (zeolitic)	
Unit 1 Pumiceous pyroclastic flow			
Pre-Prow Pass bedded tuff (Tcpbt)			
Bullfrog Tuff (Tcb)		**BF3** (welded)	Crater Flat (Cfu)
Unit 4			
Unit 3			
Unit 2		**BF2** (zeolitic)	
Unit 1			
Pre-Bullfrog Tuff basal sandstone (Tcbbs)			
Tram Tuff (Tct)			

Source: Flint, L.E. (1998, Table 1)

NOTE: % = percentage of matrix porosity

Table 8.3-2. Mean Values and Standard Deviations for Measured Core Properties and Estimated Saturated Hydraulic Conductivity for Each Hydrogeologic Unit

Hydrogeologic Unit	Relative Humidity Porosity (v/v)		N	Bulk Density (g/cm³)		Porosity (v/v)		Particle Density (g/cm³)		N	Volumetric Water Content (v/v)		Saturation		N	Water Potential (-bars)		N	Saturated Hydraulic Conductivity (m/s)		Saturated Hydraulic Conductivity (m/s)		N	Estimated Saturated Hydraulic Conductivity (m/s)		N
	Mean	SD		Mean	SD	Mean	SD	Mean	SD		Mean	SD	Mean	SD		Geom. Mean	SD		Geom. Mean	SD	PL Mean	SD		Geom. Mean	SD	
CCR	–	–	0	2.39	0.07	0.062	0.020	2.55	0.04	9	0.046	0.015	0.75	0.13	9	–	–	0	–	–	–	–	0	1.5E-12	2.1E-12	9
CUC	0.235	0.025	17	1.91	0.13	0.253	0.060	2.56	0.09	101	0.098	0.048	0.40	0.17	101	–	–	0	3.8E-08	2.2E-08	3.3E-08	5.9E-08	3	3.9E-08	1.4E-07	101
CUL	0.126	0.038	31	2.10	0.14	0.164	0.062	2.52	0.03	98	0.094	0.021	0.61	0.15	98	–	–	0	1.2E-08	–	1.2E-08	–	1	5.7E-10	1.2E-07	98
CW	0.066	0.026	405	2.30	0.06	0.082	0.030	2.51	0.05	599	0.064	0.026	0.80	0.14	599	8.8	8.9	183	5.4E-11	5.2E-12	4.6E-11	1.0E-10	6	3.8E-12	4.1E-09	599
CMW	0.140	0.044	61	1.97	0.14	0.203	0.054	2.47	0.06	90	0.165	0.062	0.90	0.13	90	0.9	16.0	13	5.0E-10	5.6E-08	1.6E-10	4.7E-08	4	8.8E-12	1.0E-11	90
CNW	0.300	0.088	59	1.46	0.17	0.387	0.070	2.38	0.10	101	0.259	0.081	0.69	0.24	101	0.2	0.5	25	3.1E-08	4.1E-06	7.6E-10	4.8E-07	8	2.6E-07	2.2E-06	101
BT4	0.369	0.120	24	1.31	0.29	0.439	0.123	2.34	0.14	33	0.220	0.097	0.51	0.19	33	0.1	0.0	5	1.6E-07	2.4E-04	2.6E-09	6.5E-06	3	4.1E-07	1.8E-05	33
TPY	0.234	0.082	37	1.79	0.23	0.254	0.082	2.40	0.11	43	0.163	0.046	0.68	0.20	43	0.1	0.0	9	3.3E-08	2.0E-07	1.2E-08	2.5E-07	2	1.7E-08	7.4E-07	43
BT3	0.353	0.079	60	1.39	0.18	0.411	0.079	2.37	0.10	85	0.216	0.065	0.54	0.16	85	0.1	0.1	34	5.4E-07	1.2E-06	1.7E-07	2.3E-06	17	7.8E-07	1.1E-06	85
TPP	0.469	0.038	132	1.13	0.09	0.499	0.041	2.26	0.09	164	0.178	0.064	0.36	0.13	156	0.1	0.1	64	8.8E-07	4.2E-07	7.3E-07	6.7E-07	10	3.6E-06	1.2E-06	164
BT2	0.464	0.093	118	1.20	0.26	0.489	0.105	2.37	0.23	171	0.185	0.069	0.39	0.15	171	0.3	0.7	41	3.2E-06	5.6E-06	8.8E-07	9.6E-06	19	1.7E-06	2.9E-06	171
TC	0.042	0.036	50	2.38	0.10	0.054	0.036	2.51	0.04	66	0.034	0.024	0.62	0.17	66	9.4	186.7	21	7.6E-10	7.5E-09	1.5E-10	1.3E-08	3	6.2E-13	7.1E-10	66
TR	0.146	0.034	435	2.15	0.08	0.157	0.030	2.55	0.03	439	0.078	0.019	0.51	0.13	439	1.2	4.5	159	1.7E-09	1.6E-07	8.6E-10	1.4E-06	45	3.9E-10	1.0E-09	439
TUL	0.135	0.032	455	2.13	0.08	0.154	0.031	2.51	0.02	455	0.108	0.022	0.72	0.15	455	1.4	4.7	246	2.0E-10	3.0E-08	9.7E-11	2.5E-07	33	2.3E-10	5.2E-10	455
TMN	0.089	0.021	266	2.25	0.05	0.110	0.020	2.53	0.03	266	0.093	0.019	0.85	0.12	266	8.6	10.1	176	4.0E-11	4.3E-11	2.2E-11	4.4E-10	11	1.5E-11	2.3E-11	266
TLL	0.115	0.032	453	2.21	0.17	0.130	0.031	2.54	0.17	453	0.101	0.024	0.78	0.14	453	1.3	3.6	253	2.3E-10	2.2E-09	8.7E-11	9.3E-09	43	7.0E-11	4.5E-10	453
TM2	0.092	0.033	225	2.27	0.08	0.112	0.031	2.56	0.03	225	0.095	0.026	0.85	0.10	225	3.0	9.2	157	9.6E-10	8.8E-07	1.9E-10	2.4E-06	15	1.8E-11	2.1E-09	225
TM1	0.071	0.019	102	2.30	0.05	0.094	0.019	2.54	0.03	102	0.081	0.016	0.87	0.09	102	12.8	12.8	70	7.5E-11	4.5E-12	6.5E-11	8.2E-11	2	4.8E-12	5.8E-12	102
PV3	0.020	0.018	89	2.27	0.26	0.036	0.039	2.36	0.25	89	0.034	0.039	0.88	0.14	87	4.9	66.2	70	5.0E-11	2.7E-10	2.6E-11	8.5E-10	7	1.5E-13	2.1E-12	89
PV2	0.123	0.079	39	1.96	0.25	0.173	0.106	2.37	0.03	39	0.148	0.107	0.84	0.16	39	3.3	15.9	30	7.3E-10	3.5E-08	1.5E-10	2.4E-08	4	7.4E-11	2.0E-07	39
BT1a	0.193	0.077	36	1.66	0.16	0.288	0.072	2.34	0.05	36	0.267	0.076	0.93	0.16	36	0.3	1.6	29	5.4E-09	1.6E-08	1.4E-09	4.3E-08	4	6.0E-11	8.0E-10	36
BT1	0.265	0.065	43	1.66	0.14	0.273	0.067	2.28	0.07	43	0.083	0.020	0.32	0.10	43	0.1	0.4	43	1.6E-05	–	1.6E-05	–	1	6.1E-08	3.2E-07	43
CHV	0.321	0.037	69	1.47	0.06	0.345	0.034	2.24	0.10	69	0.168	0.078	0.50	0.24	69	0.2	0.2	62	5.5E-07	2.9E-06	1.0E-07	3.2E-06	6	2.1E-07	5.5E-07	69
CHZ	0.240	0.049	293	1.57	0.10	0.331	0.039	2.35	0.05	293	0.320	0.041	0.97	0.07	293	0.5	1.8	206	4.5E-11	6.5E-10	3.2E-11	9.9E-08	69	1.1E-10	1.3E-10	293
BT	0.169	0.050	69	1.79	0.13	0.266	0.041	2.44	0.08	69	0.265	0.040	1.00	0.03	69	0.2	2.3	59	8.4E-11	8.5E-12	7.4E-11	1.0E-07	3	1.4E-11	2.1E-11	69
PP4	0.236	0.055	47	1.62	0.09	0.325	0.045	2.41	0.04	47	0.308	0.051	0.94	0.08	47	0.3	10.9	43	7.5E-11	3.4E-11	5.9E-11	1.0E-07	5	9.6E-11	1.4E-10	47
PP3	0.274	0.053	166	1.79	0.12	0.303	0.043	2.58	0.05	166	0.165	0.092	0.55	0.29	166	0.6	0.8	141	1.9E-08	2.9E-08	3.2E-09	7.0E-08	29	2.9E-10	4.0E-10	166
PP2	0.217	0.060	140	1.85	0.21	0.263	0.072	2.51	0.06	140	0.248	0.081	0.93	0.10	140	0.4	1.7	124	2.8E-10	1.2E-09	1.4E-10	9.9E-08	25	5.6E-11	1.1E-10	140
PP1	0.197	0.055	245	1.74	0.15	0.280	0.053	2.42	0.07	245	0.269	0.051	0.96	0.08	245	0.6	5.5	226	9.4E-11	1.6E-10	5.5E-11	1.0E-07	21	3.1E-11	5.6E-11	245
BF3	0.102	0.038	86	2.28	0.09	0.115	0.040	2.57	0.03	86	0.112	0.039	0.98	0.07	86	0.6	4.5	86	8.7E-11	–	8.7E-11	–	1	2.1E-12	2.4E-12	86
BF2	0.213	0.083	65	1.79	0.21	0.259	0.084	2.41	0.05	65	0.261	0.089	1.00	0.08	65	0.1	3.4	61	8.8E-10	5.4E-10	5.3E-10	9.8E-08	2	5.0E-11	7.0E-10	65

Source: Flint, L.E. (1998, Table 7)

NOTE: N = number of samples; v/v = dimensionless volume; SD = standard deviation; Geom. = geometric; PL = power-law; – = no samples

Table 8.3-3. Moisture Retention van Genuchten Curve-Fit Parameters (Alpha and n) for Each Hydrogeologic Unit

Hydrogeologic Unit	N	Laboratory Desorption Curves van Genuchten Parameters								Composite Curves van Genuchten Parameters									
		Alpha (1/bars)	SE	95 Percent Confidence Limits		n	SE	95 Percent Confidence Limits		m	Alpha (1/bars)	SE	95 Percent Confidence Limits		n	SE	95 Percent Confidence Limits		Residual Saturation (v/v)
				Upper	Lower			Upper	Lower				Upper	Lower			Upper	Lower	m	
CCR	–	0.335	0.140	–	–	1.254	0.037	–	–	0.203	–	–	–	–	–	–	–	–	–	0.20
CUC	3	0.827	0.227	1.290	0.364	1.840	0.221	2.291	1.388	0.457	–	–	–	–	–	–	–	–	–	0.04
CUL	3	1.404	0.462	2.344	0.463	1.529	0.110	1.752	1.306	0.346	–	–	–	–	–	–	–	–	–	0.06
CW	7	0.115	0.029	0.173	0.056	1.300	0.041	1.383	1.219	0.231	0.124	0.024	0.176	0.072	1.690	0.171	2.068	1.321	0.408	0.13
CMW	2	0.023	0.008	0.039	0.007	1.776	0.309	2.417	1.135	0.437	0.028	0.011	0.054	0.002	1.890	0.337	2.692	1.098	0.471	0.33
CNW	4	7.522	6.465	20.610	undef.	1.203	0.047	1.299	1.107	0.169	2.420	1.647	6.197	undef.	1.380	0.124	1.666	1.095	0.275	0.10
BT4	5	3.652	1.930	7.516	undef.	1.285	0.052	1.389	1.181	0.222	17.889	11.110	43.509	undef.	1.233	0.049	1.346	1.120	0.189	0.10
TPY	2	0.756	0.296	1.380	0.131	1.953	0.377	2.747	1.158	0.488	2.638	1.812	7.296	undef.	1.507	0.171	1.947	1.067	0.336	0.14
BT3	3	2.590	1.500	5.659	undef.	1.310	0.067	1.443	1.168	0.237	41.540	19.147	85.691	undef.	1.234	0.044	1.336	1.133	0.190	0.17
TPP	1	3.412	2.145	8.265	undef.	1.427	0.129	1.719	1.136	0.299	40.016	15.204	77.217	2.815	1.494	0.140	1.837	1.151	0.331	0.10
BT2	2	9.800	8.695	27.939	undef.	1.294	0.072	1.445	1.144	0.227	52.638	41.468	148.261	undef.	1.278	0.076	1.454	1.103	0.218	0.10
TC	2	0.335	0.140	0.632	0.039	1.254	0.037	1.332	1.175	0.203	0.885	0.418	1.907	undef.	1.249	0.043	1.354	1.145	0.199	0.11
TR	3	2.037	0.754	3.576	0.499	1.335	0.051	1.439	1.231	0.251	3.776	2.399	9.151	undef.	1.317	0.106	1.553	1.081	0.241	0.04
TUL	4	0.657	0.150	0.958	0.355	1.331	0.032	1.396	1.267	0.249	–	–	–	–	–	–	–	–	–	0.06
TMN	3	0.064	0.013	0.091	0.038	1.470	0.076	1.624	1.316	0.320	–	–	–	–	–	–	–	–	–	0.18
TLL	3	0.273	0.105	0.485	0.060	1.294	0.051	1.398	1.189	0.227	–	–	–	–	–	–	–	–	–	0.08
TM2	1	0.047	0.005	0.060	0.034	1.713	0.078	1.897	1.530	0.416	–	–	–	–	–	–	–	–	–	0.18
TM1	1	0.022	0.002	0.026	0.017	2.141	0.267	2.727	1.554	0.533	–	–	–	–	–	–	–	–	–	0.32
PV3	3	0.010	0.003	0.016	0.004	1.582	0.127	1.845	1.319	0.368	–	–	–	–	–	–	–	–	–	0.50
PV2	1	1.255	0.652	2.797	undef.	1.310	0.075	1.488	1.133	0.237	–	–	–	–	–	–	–	–	–	0.12
BT1a	3	0.019	0.008	0.035	0.003	1.561	0.180	1.931	1.191	0.359	–	–	–	–	–	–	–	–	–	0.36
BT1	–	9.800	8.695	27.939	undef.	1.294	0.072	1.445	1.144	0.227	–	–	–	–	–	–	–	–	–	0.04
CHV	–	9.800	8.695	27.939	undef.	1.294	0.072	1.445	1.144	0.227	–	–	–	–	–	–	–	–	–	0.06
CHZ	4	0.394	0.125	0.647	0.142	1.290	0.037	1.365	1.215	0.225	–	–	–	–	–	–	–	–	–	0.20
BT	1	0.015	0.001	0.018	0.012	1.909	0.111	2.151	1.667	0.476	–	–	–	–	–	–	–	–	–	0.33
PP4	1	0.010	0.001	0.009	0.007	3.035	0.404	3.967	2.104	0.671	–	–	–	–	–	–	–	–	–	0.25
PP3	3	1.817	0.599	3.032	0.601	1.455	0.071	1.599	1.311	0.313	–	–	–	–	–	–	–	–	–	0.07
PP2	3	0.072	0.012	0.097	0.046	1.603	0.081	1.768	1.439	0.376	–	–	–	–	–	–	–	–	–	0.10
PP1	2	0.179	0.060	0.305	0.054	1.454	0.078	1.616	1.292	0.312	–	–	–	–	–	–	–	–	–	0.18
BF3	1	0.036	0.010	0.063	0.009	1.680	0.202	2.240	1.119	0.405	–	–	–	–	–	–	–	–	–	0.09
BF2	1	0.012	0.001	0.014	0.010	2.477	0.275	3.353	1.602	0.596	–	–	–	–	–	–	–	–	–	0.19

Source: Flint, L.E. (1998, Table 8)

NOTE: SE = standard error; v/v = dimensionless volume; undef. = undefined values of less than or equal to zero on a log scale; N = number of data sets; m = 1-(1 n)

Parameters for unit CCR are from unit TC; parameters for units BT1 and CHV are from unit BT2.

Table 8.3-4. Properties and Hydraulic Parameters for 2-Meter Boreholes that Penetrate the Paintbrush Nonwelded Hydrogeologic Unit in the Exploratory Studies Facility North Ramp

Sample ID	Lithostratigraphic Unit	ESF Station (m)	Distance Below Top of Unit (m)	Fracture Density (per 10 m)	Average Relative Humidity Porosity	VWC of Relative Humidity Porosity	Approximate Depth of Drying Front (m)	Average Saturation beyond Drying Front	Water Potential (-bars)	Van Genuchten		Saturated Hydraulic Conductivity (m/s)
										Alpha (bars)	n	
NR-#1a	Tpcplnc	7+27	ND	32	0.27	0.02	0.7	0.96	1.2	0.3	1.30	2.4E-09
NR-#2	Tpcplnc/mw	7+50	3.2	16	0.36	0.02	0.4	0.88	0.8	1.0	1.30	1.0E-06
NR-#3	Tpcplnc/mw	7+70	2.8	18	0.36	0.03	0.6	0.97	1.3	0.6	1.40	5.0E-08
NR-#4	Tpcpv2	7+72	0.3	9	0.45	0.15	0.2	0.99	2.0	0.2	1.23	1.0E-09
NR-#5	Tpcpv2	7+83	1.5	17	0.38	0.06	0.7	0.82	0.6	2.5	1.30	1.9E-07
NR-#6	Tpcpv1	8+21	5.3	5	0.42	0.03	0.2	0.64	0.4	5.0	1.50	7.7E-06
NR-#7	Tpbt4	8+67	6.4	8	0.56	0.10	0.3	0.75	0.5	8.0	1.20	2.8E-06
NR-#8	Tpy	8+70	0.3	8	0.35	0.03	0.7	0.46	0.4	8.0	1.55	9.3E-06
NR-#8a	Tpy	8+69	0.1	ND	0.47	0.04	0.5	0.48	0.5	8.0	1.55	9.3E-06
NR-#9	Tpbt3	8+73	0.4	ND	0.46	0.03	ND	0.65	0.6	9.0	1.25	1.0E-06
NR-#10	Tpbt3	8+80	1.0	3	0.47	0.08	0.5	0.68	0.5	9.0	1.25	1.0E-06
NR-#11	Tpp	8+92	1.7	ND	0.49	0.04	ND	0.69	0.7	2.0	1.60	5.0E-06
NR-#12	Tpp	9+57	9.0	ND	0.49	0.02	ND	0.46	1.7	2.0	1.60	5.0E-06
NR-#13	Tpp	10+08	7.1	13	0.45	0.10	0.7	0.82	0.5	5.0	1.18	7.1E-08
LPCA1	Tpbt2	LPCA-lower	1.1	ND	0.54	0.10	0.3	0.80	1.0	2.0	1.22	2.9E-07
LPCA2	Tpbt2/argillic	LPCA-middle	0.1	6	0.37	0.12	ND	0.99	0.4	0.3	1.12	6.1E-09
LPCA3	Tpbt2	LPCA-upper	1.3	6	0.40	0.09	0.3	0.94	0.4	1.2	1.20	1.0E-08
NR-#14	Tptrv3	10+48	2.8	ND	0.52	0.08	0.7	0.76	1.0	1.9	1.30	1.0E-06
NR-#15	Tptrv3/rv2	10+54	0.8	10	0.44	0.08	0.7	0.42	1.8	7.0	1.35	1.0E-06
NR-#16	Tptrv2	10+69	2.1	19	0.39	0.10	0.7	0.61	0.7	8.0	1.28	1.0E-08
NR-#17	Tptrv1	10+70	0.1	ND	0.04	0.03	0.3	0.99	2.0	0.2	1.30	1.0E-10

DTNs: GS970908312242.006, GS980308312242.004, GS980308312242.005, GS980308312242.006, GS980408312242.008, GS980908312242.032, GS980908312242.033, GS980908312242.037, GS980908312242.040

NOTE: mw = moderately welded; VWC = volumetric water content; ND = no data; LPCA = Lower Paintbrush Canyon Alcove

Table 8.3-5. Mean Porosity and Saturated Hydraulic Conductivity for Samples from Busted Butte and Surface-Based Boreholes

Lithostratigraphic Unit[a] and Property		Busted Butte (N)[b]	Borehole SD-7 (N)[c]	Borehole SD-12 (N)[d]	All Surface-Based Boreholes (N)[b, e]
Tptpv2	Porosity[f]	0.37 (18)	0.09 (7)	0.15 (10)	0.173 (39)
	K_s (m/s)[g]	3.0E-6 (17)	ND (0)	4.1E-9 (1)	7.3E-10 (4)
Tptpv1/Tpbt1	Porosity[f]	0.42 (26)	0.22 (22)	0.33 (21)	0.273 (43)
	K_s (m/s)[g]	3.0E-6 (20)	1.6E-5 (1)	ND (0)	1.6E-5 (1)
Tac (vitric)	Porosity[f]	0.36 (35)	0.34 (31)	0.35 (30)	0.345 (69)
	K_s (m/s)[g]	1.5E-5 (22)	4.0E-7 (3)	ND (0)	5.5E-7 (6)

NOTES: [a] See Table 8.3-1.
[b] Data from DTNs: GS990308312242.007 and GS990708312242.008
[c] Data from DTNs: GS951108312231.009 and GS960808312231.005
[d] Data from DTNs: GS950308312231.002, GS960808312231.004, GS960808312231.005
[e] Data from Flint, L.E. (1998, Table 7)
[f] Total porosity determined by oven drying at 105° C
[g] Geometric mean
N = number of samples; porosity = cm^3/cm^3; K_s = saturated hydraulic conductivity; ND = no data

Table 8.3-6. Statistical Summary of Tiva Canyon Tuff Air-Injection Permeability Values by Lithostratigraphic Unit and Borehole

Lithostratigraphic Unit	Borehole UZ-16 Mean (#) st. dev.	Borehole SD-12 Mean (#) st. dev.	Borehole NRG-6 Mean (#) st. dev.	Borehole NRG-7a Mean (#) st. dev.
Lower Lithophysal (Tpcpll)	5.5 (1) NA	19.6 (2) 18.7	14.0 (1) NA	–
Lower Nonlithophysal Hackly (Tpcplnh)	–	1.7 (1) NA	28.0 (1) NA	–
Lower Nonlithophysal Columnar (Tpcplnc)	15.0 (1) NA	2.9 (3) 2.2	1.3 (2) 1.0	25.7 (2) 14.9
Crystal-Poor Vitric (Tpcpv)	–	–	–	0.2 (2) 0.1

Source: LeCain, G.D. (1997, Table 2)

NOTE: Permeability values are given in 10^{-12} m^2; Mean = arithmetic mean; # = number of test intervals; st.dev. = standard deviation; NA = not applicable; – = no data

Table 8.3-7. Statistical Summary of Tiva Canyon Tuff Air-Injection Permeability Values by Borehole

Borehole	Number of Test Intervals	Arithmetic Mean	Geometric Mean	Maximum Value	Minimum Value
UZ-16	4	12.3	7.6	27.0	1.5
SD-12	11	7.0	3.4	38.0	0.8
NRG-6	4	11.2	4.1	28.0	0.3
NRG-7a	4	26.6	8.4	54.0	0.24

Source: LeCain, G.D. (1997, Table 1)

NOTE: Permeability values are given in 10^{-12} m^2.

Table 8.3-8. Statistical Summary of the Air-Injection Permeability Values for Individual Lithostratigraphic Units Within the Paintbrush Nonwelded Hydrogeologic Unit

Lithostratigraphic Unit	Borehole NRG-7a Arithmetic Mean (Number of Intervals) Standard Deviation
Tiva Canyon crystal-poor vitric (Tpcpv1)	0.2 (2) 0.12
Pre-Tiva Canyon Tuff bedded tuff (Tpbt4)	0.2 (1) NA
Yucca Mountain Tuff (Tpy)	0.3 (4) 0.2
Pre-Yucca Mountain Tuff bedded tuff (Tpbt3)	3.0 (1) NA
Pah Canyon Tuff (Tpp)	0.2 (7) 0.04
Pre-Pah Canyon Tuff bedded tuff (Tpbt2)	0.7 (1) NA

Source: Modified from LeCain, G.D. (1997, Table 4)

NOTE: Permeability values are given in 10^{-12} m^2.
NA = not applicable

Table 8.3-9. Statistical Summary of the Air-Injection Permeability Values of the Paintbrush Tuff Nonwelded Hydrogeologic Unit

Borehole	Number of Test intervals	Arithmetic Mean	Geometric Mean	Maximum Value	Minimum Value
NRG-7a	18[a]	0.54	0.30	3.0	0.12

Source: LeCain, G.D. (1997, Table 3)

NOTE: [a] Includes two test intervals from the crystal-poor vitric nonwelded subzone of the Tiva Canyon Tuff, which is considered part of the PTn

Permeability values are given in 10^{-12} m^2.

Table 8.3-10. Statistical Summary of Topopah Spring Tuff Air-Injection Permeability Values by Lithostratigraphic Unit and Borehole

Lithostratigraphic Unit	Borehole UZ-16 Mean (#) st. dev.	Borehole SD-12 Mean (#) st. dev.	Borehole NRG-6 Mean (#) st. dev.	Borehole NRG-7a Mean (#) st. dev.
Crystal-rich vitric (Tptrv)	–	–	–	–
Crystal-rich nonlithophysal (Tptrn)	0.65 (1) NA	5.8 (7) 10.0	2.2 (20) 5.0	0.23 (3) 0.13
Crystal-rich lithophysal (Tptrl)	–	–	0.25 (1) NA	0.15 (3) 0.08
Crystal-poor Upper lithophysal (Tptpul)	1.8 (4) 0.34	5.4 (5) 6.6	4.1 (5) 4.4	0.32 (9) 0.10
Crystal-poor Middle nonlithophysal (Tptpmn)	0.37 (17) 0.35	2.7 (7) 2.9	1.1 (7) 0.89	0.57 (6) 0.82
Crystal-poor Lower lithophysal (Tptpll)	3.2 (16) 2.5	–	–	0.40 (15) 0.27
Crystal-poor Lower nonlithophysal (Tptpln)	1.9 (13) 1.5	1.3 (6) 0.40	–	–
Crystal-poor vitric (Tptpv)	–	–	–	–

Source: LeCain, G.D. (1997, Table 6)

NOTE: Permeability values are given in 10^{-12} m^2; Mean = arithmetic mean; # = number of test intervals; st.dev. = standard deviation; NA = not applicable; – = no data

Table 8.3-11. Statistical Summary of Topopah Spring Tuff Air-Injection Permeability Values by Borehole

Borehole	Number of Test Intervals	Arithmetic Mean	Geometric Mean	Maximum Value	Minimum Value
UZ-16	54	1.8	0.9	9.5	0.02
SD-12	27	4.7	1.7	33.0	0.12
NRG-6	34	2.1	0.8	24.0	0.08
NRG-7a	38	0.4	0.3	2.4	0.04

Source: LeCain, G.D. (1997, Table 5)

NOTE: Permeability values are given in 10^{-12} m^2.

Table 8.3-12. Average Number of Natural Fractures per Test Interval by Lithostratigraphic Unit and Borehole

Lithostratigraphic Unit	Borehole UZ-16 # Fractures (# Intervals)	Borehole SD-12 # Fractures (# Intervals)	Borehole NRG-6 # Fractures (# Intervals)	Borehole NRG-7a # Fractures (# Intervals)
Tiva Canyon Tuff	16 (4)	11 (11)	23 (4)	19 (4)
PTn	–	–	–	2 (18)
Topopah Spring Tuff	14 (54)	16 (27)	6 (34)	4 (38)

Source: LeCain, G.D. (1997, Table 7)

NOTE: Permeability values are given in 10^{-12} m^2; Mean = arithmetic mean; # = number of test intervals; st.dev. = standard deviation; NA = not applicable; – = no data

Table 8.3-13. Statistical Summary of Air-Injection Permeability Values for the Tiva Canyon Crystal-Poor Upper Lithophysal Unit in the Upper Tiva Canyon Alcove

Borehole Number	Arithmetic Mean (Standard Deviation)	Geometric Mean
RBT#1	11.0 (10.4)	7.2
RBT#2	38.5 (24.0)	27.1
RBT#3	27.8 (26.9)	13.3

Source: LeCain, G.D. (1997, Table 4)

NOTE: Units are given in 10^{-12} m^2.

Table 8.3-14. Statistical Summary of the Air-Injection Permeability Values for the Tiva Canyon Tuff Crystal-Poor Middle Nonlithophysal and Lower Lithophysal Zones in the Bow Ridge Fault Alcove

	Tiva Canyon Tuff Crystal-Poor Middle Nonlithophysal (Tpcpmn)	Tiva Canyon Tuff Crystal-Poor Lower Lithophysal (Tpcpll)
Number of Test Intervals	8	5
Arithmetic Mean	13.9	1.3
Arithmetic Standard Deviation	8.1	0.6
Geometric Mean	12.2	1.2

Source: Modified from LeCain, G.D. (1998, Table 6)

NOTE: Permeability values are given in 10^{-12} m^2.

Table 8.3-15. Air Permeability and Porosity Values from Cross-Hole Pneumatic Tests Conducted in the Bow Ridge Fault Alcove

Test Number	Injection Interval	Monitor Interval	Type Curve Analysis
4	Bow Ridge fault zone	Bow Ridge fault zone	k = 27.8 ϕ = 0.13
5	Bow Ridge fault zone	Bow Ridge fault zone	k = 25.9 ϕ = 0.20
6	pre-Rainier Mesa bedded tuff #1 (Tmbt1)	pre-Rainier Mesa bedded tuff #1 (Tmbt1)	k = 23.2 ϕ = 0.27

Source: LeCain, G.D. (1998, Table 7)

NOTE: k = permeability given in 10^{-12} m^2; ϕ = porosity

Table 8.3-16. Results from Cross-Hole Gaseous Tracer Tests Conducted in the Bow Ridge Fault Alcove

Test Number	Pumped Interval HPF #1	Release Interval HPF #2	First Arrival (min.)	Peak Arrival (min.)	Tracer Velocity (10^{-4} m/s)	Darcy Velocity (10^{-4} m/s)	ϕ_{eff}
2	Fault	Fault	16	80	6.5	3.1-3.4	0.48 to 0.52
3	Fault	Fault	16	36	14.4	3.1-3.4	0.22 to 0.24

Source: LeCain, G.D. (1998, Table 8)

NOTE: ϕ_{eff} = effective porosity

Table 8.3-17. Statistical Summary of the Air-Injection Permeability Values from the Upper Paintbrush Contact Alcove

	Tiva Canyon Crystal-Poor Lower Nonlithophysal Hackly Subzone (Tpcplnh)	Tiva Canyon Crystal-Poor Lower Nonlithophysal Columnar Subzone (Tpcplnc)	Tiva Canyon Crystal-Poor Vitric Subzones 2 and 1 (Tpcpv2 and Tpcv1)
Number of Test Intervals	11	6	12
Arithmetic Mean	3.7	0.7	16.5
Geometric Mean	2.1	0.3	7.0

Source: Based on LeCain, G.D. (1998, Table 11)

NOTE: Permeability values are given in 10^{-12} m^2.

Table 8.3-18. Arithmetic Mean Air Permeability Values for Lithostratigraphic and Hydrogeologic Units from Exploratory Studies Facility Air-Injection Tests, Surface-Based Air-Injection Tests, and Pneumatic Monitoring

Unit [a]	UTCA (ESF)	BRFA (ESF)	UPCA (ESF)	UZ-16 (SB)	SD-12 (SB)	NRG-6 (SB)	NRG-7 (SB)	NRG-6 (PM)	NRG-7a (PM)	SD-12 (PM)
Tpcpul	28.6 (27)	–	–	–	–	–	–	–	–	–
Tpcpmn	–	13.9 (8)	–	–	–	–	–	–	–	100
Tpcpll	–	1.3 (5)	–	5.5 (1)	19.5 (2)	14.0 (1)	–	3.1	–	100
Tpcpln	–	–	2.6 (17)	15.0 (1)	2.6 (4)	10.2 (3)	25.7 (2)	3.1	1.3	100
Tpcpv	–	–	16.5 (12)	–	–	–	0.20 (2)	0.5-2.1	0.65-1.3	–
PTn[a]	–	–	–	–	–	–	0.54 (18)	0.5-2.1	0.65-1.3	1.0
Tptrv	–	–	–	–	–	–	–	0.5-2.1	0.65-1.3	10.0
Tptrn	–	–	–	0.65 (1)	5.8 (7)	2.2 (20)	0.23 (3)	14.7-50.0	10.0	10.0
Tptrl	–	–	–	–	–	0.25 (1)	0.15 (3)	10.0	10.0	–
Tptpul	–	–	–	1.8 (4)	5.3 (5)	4.6 (5)	0.32 (9)	10.0	10.0	10.0
Tptpmn	–	–	–	0.37 (17)	2.7 (7)	1.1 (7)	0.57 (6)	–	–	10.0
Tptpll	–	–	–	3.2 (16)	–	–	0.40 (15)	–	–	10.0
Tptpln	–	–	–	1.9 (13)	1.3 (6)	–	–	–	–	10.0

Sources: LeCain, G.D. (1998, Tables 1 through 7, 9, and 10); LeCain, G.D. (1997, Tables 2, 3, and 6); Rousseau et al. (1999, Tables 9 and 10); Rousseau et al. (1997, Table 5.1-1)

NOTE: [a] PTn is a composite hydrogeologic unit; all others are lithostratigraphic units (see Table 8.3-1).
Air permeability values are given in 10^{-12} m^2; the number of test intervals is in parentheses.
UTCA = Upper Tiva Canyon Alcove; BRFA = Bow Ridge Fault Alcove; UPCA = Upper Paintbrush Contact Alcove; ESF = Exploratory Studies Facility; SB = surface based; PM = pneumatic monitoring

Table 8.4-1. Comparison of Mean Air Permeability and Mean Air-Filled Porosity Values Derived from Pneumatic Diffusivities Determined by Three Methods Using Pneumatic-Pressure Data from Instrumented Boreholes

Analysis Method (Boreholes)	Rousseau et al. (1999, Tables 9, 10, 11, and 12) (NRG-6, NRG-7a, UZ#4, UZ#5)		Patterson et al. (1996, Table 4) (NRG#5, NRG-6, NRG-7a, SD-7, and SD-9)		Rousseau, Loskot et al. (1997, Table 5.1-1) (SD-7, SD-12, and UZ-7a)	
Hydrogeologic Unit	Mean Air Permeability, in 10^{-12} m^2 (number of intervals)	Mean Air-Filled Porosity	Mean Air Permeability, in 10^{-12} m^2 (number of intervals)	Mean Air-Filled Porosity	Mean Air Permeability, in 10^{-12} m^2 (number of intervals)	Mean Air-Filled Porosity
Tiva Canyon Welded	3.7 (4)	0.13	801.0 (4)	0.09	303.0 (3)	0.14
Paintbrush Nonwelded	2.2 (14)	0.25	1.2 (13)	0.33	50.7 (3)	0.25
Topopah Spring Welded	14.5 (8)	0.06	146.0 (5)	0.05	16.0 (14)	0.07

Table 8.4-2. Summary of Pneumatic-Interference Events at Instrumented Boreholes Caused by Exploratory Studies Facility Excavation

Borehole	Event Producing First Interference (Date)	Position of the TBM Referenced to Exploratory Studies Facility Stations (Distance from North Portal)	Horizontal Distance From TBM Advance Point to Borehole, in feet (meters)	Lithostratigraphic Unit Exposed at the Face of Exploratory Studies Facility Tunnel
NRG#4	Penetration of PTn (06/16/95)	10 + 68.3 (1,068.3 m)	82 (25)	pre-Pah Canyon tuff (Tpbt2)
UZ#4	Crossing of fault zone (08/12/95)	12 + 61.8	1,361 (415)	Topopah Spring Crystal-Rich Nonlithophysal (Tptrn)
UZ#5	Crossing of fault zone (08/12/95)	12 + 61.8	1,237 (377)	Topopah Spring Crystal-Rich Nonlithophysal (Tptrn)
NRG#5	Close approach of TBM (09/14/95)	16 + 56.3	305 (93)	Topopah Spring Crystal-Rich Nonlithophysal (Tptrn)
NRG-6	Crossing of Drill Hole Wash Fault (10/01/95)	20 + 02.1	1,807 (551)	Topopah Spring Upper Lithophysal (Tptrl, Tptpul)
NRG-7a	Crossing of Drill Hole Wash Fault (10/21/95)	23 + 46.8	85 (26)	Topopah Spring Upper Lithophysal (Tptrl, Tptpul)
SD-9	Close approach of TBM (11/07/95)	26 + 54.7	603 (184)	Topopah Spring Middle Nonlithophysal (Tptpmn)
SD-12	Close approach of TBM (03/23/96)	46 + 23.0	161 (49)	Topopah Spring Middle Nonlithophysal (Tptpmn)
SD-7	Passage of TBM (06/05/96)	55 + 98.0	348 (106)	Topopah Spring Middle Nonlithophysal (Tptpmn)

Sources: Rousseau et al. (1999, Table 13); Rousseau et al. (1997, Table 4.1-3)

Table 8.4-3. Summary of Numerical Simulations Used to Estimate Permeabilities Near Boreholes NRG#5, NRG-6, and NRG-7a Using the MODFLOWP Gas-Flow Model

Borehole	Topopah Spring Welded Unit (TSw)		Paintbrush Nonwelded Unit (PTn)
	Horizontal Air Permeability (10^{-12} m^2)	Vertical Air Permeability (10^{-12} m^2)	Isotropic Air Permeability (10^{-12} m^2)
NRG-6	30	NA	0.90
NRG#5/NRG-6	49	94	0.54
NRG#5/NRG-6	42	80	0.7 (fixed)
NRG-6/NRG-7a	34	68	0.67
NRG#5/NRG-6/NRG-7a	56	83	0.50
NRG#5/NRG-6/NRG-7a	45	72	0.7 (fixed)

Source: Patterson et al. (1996, Table 6)

Table 8.4-4. Summary of Numerical Simulations to Estimate Permeabilities Near Boreholes UZ#4 and UZ#5 Using the MODFLOWP Gas-Flow Model

Borehole	Permeability (10^{-12} m^2)	
	Topopah Spring Welded Unit (TSw)	Paintbrush Nonwelded Unit (PTn)
UZ#4	800	0.22
UZ#5	2,200	0.23
UZ#4 and UZ#5	1,100	0.23

Source: Patterson et al. (1996, Table 8)

INTENTIONALLY LEFT BLANK

Table 8.7-1. Estimated Percolation Flux from Borehole Temperature Data

Borehole	Percolation Flux (mm/yr.)
UE-25 a#7	7
USW G-1	5
USW G-2	11
USW G-3	4
USW G-4	5
USW H-1	9
USW H-3	3
USW H-4	0
USW H-5	5
USW H-6	4
USW SD-12	15
USW UZ-1	8
UE-25 UZ#4	18[a]
UE-25 UZ#5	5[a]
USW WT-1	7
USW WT-2	0.5
UE-25 WT-4	7
USW WT-7	3
UE-25 WT-17	0
USW SD-12	15

Source: Data from Rousseau et al. (1999, p. 200); other data from Bodvarsson et al. (1997, Chapter 11, Table 11.4)

Table 8.7-2. Average Pore Water Chloride Concentration within Various Hydrostratigraphic or Lithostratigraphic Units and Perched or Saturated Zone Water

Unit	Borehole							Borehole Average
	UZ #16	UZ-14	NRG-6	NRG-7a	SD-7	SD-9	SD-12	
PTn	35.5 (2)	86.6 (17)	97.0 (7)	46.2 (2)	77.2 (1)	131.5 (2)	49.61 (1)	74.8
Tptpv 1, 2	NA	101.7 (3)	NA	NA	NA	15.8 (1)	NA	58.8
Perched	NA	8.6 (8)	NA	7.0 (1)	4.2 (5)	5.6 (1)	NA	6.4
Tac	32.2 (20)	23.8 (18)	NA	40.7 (3)	28.0 (3)	32.9 (6)	33.6 (4)	31.9
Tcp	55.3 (4)	24.1 (9)	NA	NA	NA	NA	29.0 (2)	36.1
SZ	10.8 (4)	NA	NA	NA	NA	NA	NA	10.8

Sources: Yang et al. (1996, Tables 2, 3, 4, 5, and 6); Yang et al. (1998, Tables 2, 3, and 4)

NOTES: Number of samples used to compute average values are in parentheses. Concentrations are in milligrams per liter.
NA = no measurements available; SZ = saturated zone

Table 8.7-3. Apparent Vertical Percolation Rate Based on Average Pore Water Chloride Concentration within Hydrostratigraphic or Lithostratigraphic Units and Perched or Saturated Zone Water

Unit	Borehole							Borehole Average
	UZ #16	UZ-14	NRG-6	NRG-7a	SD-7	SD-9	SD-12	
PTn	3.0	1.2	1.1	2.3	1.4	0.8	2.1	1.7
Tptpv 1, 2	NA	1.0	NA	NA	NA	6.7	NA	3.9
Perched	NA	12.3	NA	15.1	25.1	18.8	NA	17.8
Tac	3.3	4.4	NA	2.6	3.8	3.2	3.1	3.4
Tcp	1.9	4.4	NA	NA	NA	NA	3.6	3.3
SZ	9.8	NA	NA	NA	NA	NA	NA	9.8
All								6.7

NOTE: Percolation flux rates are in millimeters per year.
NA = no measurements available; SZ = saturated zone

Table 8.7-4. Comparison of Values of Net Infiltration at Selected Boreholes with Percolation Flux Estimated by Various Methods

Borehole ID (prefix omitted)	Nevada State Plane Coordinates		Net Infiltration (mm/yr.)	Percolation Flux (mm/yr.)					
					Hydraulic Conductivity/ Potential Gradient (Section 8.7.4)		Chloride Mass Balance (Section 8.7.3)		
	Location, Easting (m)	Location, Northing (m)	Infiltration Model for 90- by 90-m Area Centered on Borehole (Section 8.2; Flint, A.L. et al. 1996)	Borehole Temperature (Section 8.7.2)	Bodvarsson and Bandurraga (1996, Ch. 3)	Ahlers, Bandurraga et al. (1995b)	PTn	Tac	PW
H-1	171416	234774	2.1	9[a]	–	0.02	–	–	–
H-3	170216	230594	7.8	3[a]	–	–	–	–	–
H-4	171880	232149	1.9	0[a]	–	–	–	–	–
H-5	170356	233671	11.4	5[a]	–	–	–	–	–
H-6	168882	232654	2.4	4[a]	–	–	–	–	–
G-1	170993	234849	3.0	5[a]	–	0.02	–	–	–
G-2	170842	237386	3.0	11[a]	–	–	–	–	–
G-3	170225	229448	8.1	4[a]	–	–	–	–	–
G-4	171628	233418	0.1	5[a]	–	–	–	–	–
UZ-1	170756	235085	3.2	8[a]	–	–	–	–	–
WT-1	171828	229802	0.0	7[a]	–	–	–	–	–
WT-2	171275	231850	1.9	0.5[a]	–	–	–	–	–
WT#4	173139	234243	0.9	7[a]	–	–	–	–	–
WT-7	168860	230276	0.0	3[a]	–	–	–	–	–
WT#12	172825	225469	2.2	–	–	–	–	–	–
WT#17	172581	228119	1.9	0[a]	–	–	–	–	–
WT#18	172168	235052	2.3	12[a]	–	–	–	–	–
A#1	172624	233142	0.0	–	–	0.02	–	–	–
A#7	172355	233533	1.7	7[a]	–	–	–	–	–
SD-12	171178	232245	1.3	15[a]	0.1	0.02	2.1	3.1	–
NRG-6	171965	233699	1.0	–	–	0.02	1.1	–	–
NRG-7a	171598	234355	0.0	–	–	–	2.3	2.6	15.1
UZ#4	172560	234305	3	18[b]	–	0.02	1.1	–	–
UZ#5	172558	234267	3	5[b]	–	0.02	2	–	–

Table 8.7-4. Comparison of Values of Net Infiltration at Selected Boreholes with Percolation Flux Estimated by Various Methods (Continued)

Borehole ID (prefix omitted)	Nevada State Plane Coordinates		Net Infiltration (mm/yr.)	Percolation Flux (mm/yr.)					
					Hydraulic Conductivity/ Potential Gradient (Section 8.7.4)		Chloride Mass Balance (Section 8.7.3)		
	Location, Easting (m)	Location, Northing (m)	Infiltration Model for 90- by 90-m Area Centered on Borehole (Section 8.2; Flint, A.L. et al. 1996)	Borehole Temperature (Section 8.7.2)	Bodvarsson and Bandurraga (1996, Ch. 3)	Ahlers, Bandurraga et al. (1995b)	PTn	Tac	PW
SD-7	171066	231328	6	–	0.1	0.02	1.4	3.8	25.1
SD-9	171242	234086	5	–	0.1	0.02	0.8	3.2	18.8
UZ-14	170731	235096	3	–	0.1	0.02	1.2	4.4	12.3
UZ#16	172169	231812	0	–	0.1	0.02	3	3.3	–
UZ-6	170178	231566	14	–	–	–	–	–	–
UZ-13	170227	229195	9	–	–	0.02	–	–	–
UZ-6S	170086	231609	–	–	–	0.02	–	–	–
UZ-7	171575	231903	–	–	–	0.02	–	–	–

NOTES: [a] Bodvarsson et al. (1997, Chapter 11, Table 11.4)

[b] Rousseau et al. (1999, p. 200)

PTn = Paintbrush nonwelded unit; Tac = Calico Hills Formation; PW = perched water; – = no estimate available using this method

Table 8.8-1. Statistical Summary of Permeability Values from the Type-Curve Analytical Solutions of Cross-Hole Air-Injection Testing of the Northern Ghost Dance Fault Drill Room Boreholes

Structural Unit	Permeability Values, Arithmetic Mean	Permeability Values, Range	Permeability Values, Geometric Mean
Hanging wall	5.0	0.7 to 12.8	4.1
Fault zone	18.1	7.0 to 37.9	14.6
Footwall	8.7	1.1 to 34.1	7.8

Source: LeCain, G.D. et al. (2000, Table 13)

NOTE: Permeability values are given in 10^{-12} m^2.

Table 8.8-2. Statistical Summary of Porosity Values from the Type-Curve Analytical Solutions of Cross-Hole Air-Injection Testing of the Northern Ghost Dance Fault Drill Room Boreholes

Structural Unit	Arithmetic Mean (m^3/m^3)	Arithmetic Range (m^3/m^3)	Geometric Mean (m^3/m^3)
Hanging wall	0.04	0.01 to 0.09	0.03
Fault zone	0.13	0.05 to 0.27	0.10
Footwall	0.04	0.01 to 0.12	0.03

Source: LeCain, G.D. et al. (2000, Table 14)

Table 8.8-3. Transmissivity Distributions and Equivalent Permeability Values for the Discrete-Feature Model

Structural Unit	Distribution Type	Transmissivity, Mean (m^2/s)	Transmissivity, Standard Deviation (m^2/s)	Permeability, Mean (m^2)
Footwall	Log-normal	9.06×10^{-4}	2.30×10^{-4}	45.3×10^{-12}
Fault zone	Log-normal	9.06×10^{-4}	2.30×10^{-4}	45.3×10^{-12}
Hanging wall	Log-normal	2.31×10^{-4}	8.30×10^{-4}	11.6×10^{-12}

Source: LeCain, G.D. et al. (2000, Table 17)

Table 8.8-4. Statistical Summary of Northern Ghost Dance Fault Transport-Porosity and Longitudinal-Dispersivity Values by Geologic Structure

Geologic Structure	Transport-Porosity Range (Arithmetic Mean) (m^3/m^3)	Longitudinal-Dispersivity Range (Arithmetic Mean) (m)
Footwall	0.003 to 0.032 (0.013)	0.42 to 1.54 (1.03)
Fault zone	0.004 to 0.034 (0.014)	0.37 to 1.38 (0.62)
Hanging wall	0.001 to 0.070 (0.013)	0.06 to 2.63 (0.76)

Source: LeCain, G.D. et al. (2000, Table 19)

Table 8.8-5. Comparison of Geometric Means and Standard Deviations of Air Permeability for Niches in the Exploratory Studies Facility Main Drift

Borehole Cluster	Type of Site	log(k) (m^2)	
		Mean	Standard Deviation
Niche 3566 Pre-excavation	Intersects brecciated zone	-13.0	0.92
Niche 3566 Radial	Predominantly within brecciated zone	-11.8	0.66
Niche 3650 Pre-excavation	Moderately fractured welded tuff	-13.4	0.81
Niche 3650 Post-excavation	Post-excavation welded tuff	-11.8	0.88
Niche 3107 Pre-excavation	Moderately fractured welded tuff	-13.4	0.70
Niche 3107 Post-excavation	Post-excavation welded tuff	-12.4	0.82
Niche 3107 Radial	Moderately fractured welded tuff	-13.8	0.92
Niche 4788 Pre-excavation	Highly fractured welded tuff	-13.0	0.85
Niche 4788 Post-excavation	Post-excavation welded tuff	-11.9	0.78

Source: CRWMS M&O (2000a, Table 6)

NOTE: k = air permeability

Table 8.8-6. Capillary Height Values for the Fractures Obtained From Seepage Tests at Niche 3650

Borehole and Test Interval (m)	Seepage Threshold Flux, K_o^* (m/s)	Saturated Hydraulic Conductivity, K_1 (m/s)	Capillary Height, α^{-1} (m)
Fracture Networks			
UR 4.88 to 5.18	9.92E-07	9.87E-05	0.0205
UL 7.01 to 7.32	3.55E-06	8.98E-05	0.0855
UR 4.27 to 4.57	1.03E-06	4.08E-05	0.0532
UM 4.27 to 4.57	2.89E-07	2.62E-05	0.0225
UM 5.49 to 5.79	3.50E-07	2.16E-05	0.0334
UR 5.49 to 5.79	4.31E-06	1.71E-05	0.714
Geometric Mean			0.0607
Individual or Small Groups of High-Angle Fractures			
UM 4.88 to 5.18	1.03E-06	2.52E-03	0.000816
UR 6.71 to 7.01	1.63E-07	2.28E-04	0.00143
UL 7.62 to 7.92	9.80E-08	1.51E-04	0.00130
UR 6.10 to 6.40	6.35E-09	3.01E-05	0.000421
Geometric Mean			0.000893

Source: CRWMS M&O (2000a, Table 8)

Table 8.8-7. Initial Parameter Set for Inverse Calibration of the Seepage Calibration Model

Parameter	Value	Units
Fracture permeability, *kf*	2.18E-12	m^2
Fracture permeability, *kf*	1.70E-11	m^2
Porosity, ϕ	0.01	–
van Genuchten α_v	5.16E-4	Pa^{-1}
van Genuchten *m*	0.608	–
van Genuchten *n*	2.551	–
Residual saturation, *Slrf*	0.01	–
Satiated saturation, *Slsf*	1.0	–

Source: CRWMS M&O (2000s, Table 8)

Table 8.8-8. Parameter Estimates, Estimation Uncertainties, and Correlation Coefficients for the Inverse Calibration of the Seepage Calibration Model

Model	$\log(1/\alpha_v[Pa])$[a]		Log Porosity (ϕ)		Correlation Coefficient
	Estimate	Standard Deviation	Estimate	Standard Deviation	
Two-Dimensional, Homogeneous	2.25	0.09	-2.46	0.06	-0.75
Two-Dimensional, Heterogeneous	2.95	0.06	-2.49	0.05	-0.63
Three-Dimensional, Homogeneous	1.50	0.03	-2.87	0.02	-0.74
Three-Dimensional, Heterogeneous	1.82	0.01	-2.89	0.01	-0.77

Source: CRWMS M&O (2000s, Table 10)

NOTE: [a] In the heterogeneous models, $1/\alpha_v$ is the reference capillary strength, which is related to the reference permeability $k = 10^{-12}$ m^2 through Leverett's scaling rule.

Table 8.10-1. Correlation among Major Hydrogeologic Units, Geologic Framework Model Version 3.1 Lithostratigraphic Units, Unsaturated Zone Model Layers, and Detailed Hydrogeologic Units

Major Hydrogeologic Unit (Modified from Montazer and Wilson 1984)	GFM3.1 Lithostratigraphic Nomenclature[a]	Fiscal Year 1999 Unsaturated Zone Model Layer	Detailed Hydrogeologic Unit (Flint, L.E. 1998, Table 1)
Tiva Canyon welded (TCw)	Tiva_Rainier	tcw11	CCR, CUC
	Tpcp	tcw12	CUL, CW
	TpcLD		
	Tpcpv3	tcw13	CMW
	Tpcpv2		
Paintbrush nonwelded (PTn)	Tpcpv1	ptn21	CNW
	Tpbt4	ptn22	BT4
	Tpy (Yucca)		
		ptn23	TPY
	Tpbt3	ptn24	BT3
	Tpp (Pah)	ptn25	TPP
	Tpbt2	ptn26	BT2
	Tptrv3		
	Tptrv2		
Topopah Spring welded (TSw)	Tptrv1	tsw31	TC
	Tptrn	tsw32	TR
	Tptrl, Tptf	tsw33	TUL
	Tptpul		
	Tptpmn	tsw34	TMN
	Tptpll	tsw35	TLL
	Tptpln	tsw36	TM2 (upper 2/3 of Tptpln)
		tsw37	TM1 (lower 1/3 of Tpln)
	Tptpv3	tsw38	PV3
	Tptpv2	tsw39	PV2
Calico Hills nonwelded (CHn)	Tptpv1	ch1 (vit, zeo)	BT1 or BT1a (altered)
	Tpbt1		
	Tac (Calico)	ch2 (vit, zeo)	CHV (vitric) or CHZ (zeolitic)
		ch3 (vit, zeo)	
		ch4 (vit, zeo)	
		ch5 (vit, zeo)	
	Tacbt (Calicobt)	ch6	BT
	Tcpuv (Prowuv)	pp4	PP4 (zeolitic)
	Tcpuc (Prowuc)	pp3	PP3 (devitrified)
	Tcpm (Prowmd)	pp2	PP2 (devitrified)
	Tcplc (Prowlc)		
	Tcplv (Prowlv)	pp1	PP1 (zeolitic
	Tcpbt (Prowbt)		
	Tcbuv (Bullfroguv)		

Table 8.10-1. Correlation among Major Hydrogeologic Units, Geologic Framework Model Version 3.1 Lithostratigraphic Units, Unsaturated Zone Model Layers, and Detailed Hydrogeologic Units (Continued)

Major Hydrogeologic Unit (Modified from Montazer and Wilson 1984)	GFM3.1 Lithostratigraphic Nomenclature[a]	Fiscal Year 1999 Unsaturated Zone Model Layer	Detailed Hydrogeologic Unit (Flint, L.E. 1998, Table 1)
Crater Flat undifferentiated (CFu)	Tcbuc (Bullfroguc)	bf3	BF3 (welded)
	Tcbm (Bullfrogmd)		
	Tcblc (Bullfroglc)		
	Tcblv (Bullfroglv)	bf2	BF2 (nonwelded)
	Tcbbt (Bullfrogbt)		
	Tctuv (Tramuv)		
	Tctuc (Tramuc)	tr3	Not Available
	Tctm (Trammd)		
	Tctlc (Tramlc)		
	Tctlv (Tramlv)	tr2	Not Available
	Tctlb (Trambt)		

Source: CRWMS M&O (2000e, Table 10)

NOTE: [a] Gelogic framework model, version 3.1, nomenclature uses the symbols that are included parenthetically below layer Tpbt1.

Table 8.10-2. Calibrated Parameters for Nonfaulted Rock from One-Dimensional Mountain-Scale Inversions of Saturation, Water Potential, and Pneumatic Data for Base-Case Infiltration

Model Layer	Matrix Permeability (m^2)	Matrix van Genuchten Alpha (1/Pa)	Matrix van Genuchten m (-)	Fracture Permeability (m^2)	Fracture van Genuchten Alpha (1/Pa)	Fracture van Genuchten m (-)	Fracture-Activity Parameter (-)
tcw11	3.86E-15	4.00E-5	0.470	2.41E-12	3.15E-3	0.627	0.30
tcw12	2.74E-19	1.81E-5	0.241	1.00E-10	2.13E-3	0.613	0.30
tcw13	9.23E-17	3.44E-6	0.398	5.42E-12	1.26E-3	0.607	0.30
ptn21	9.90E-13	1.01E-5	0.176	1.86E-12	1.68E-3	0.580	0.09
ptn22	2.65E-12	1.60E-4	0.326	2.00E-11	7.68E-4	0.580	0.09
ptn23	1.23E-13	5.58E-6	0.397	2.60E-13	9.23E-4	0.610	0.09
ptn24	7.86E-14	1.53E-4	0.225	4.67E-13	3.37E-3	0.623	0.09
ptn25	7.00E-14	5.27E-5	0.323	7.03E-13	6.33E-4	0.644	0.09
ptn26	2.21E-13	2.49E-4	0.285	4.44E-13	2.79E-4	0.552	0.09
tsw31	6.32E-17	3.61E-5	0.303	3.21E-11	2.49E-4	0.566	0.06
tsw32	5.83E-16	3.61E-5	0.333	3.56E-11	1.27E-3	0.608	0.41
tsw33	3.08E-17	2.13E-5	0.298	3.86E-11	1.46E-3	0.608	0.41
tsw34	4.07E-18	3.86E-6	0.291	1.70E-11	5.16E-4	0.608	0.41
tsw35	3.04E-17	6.44E-6	0.236	4.51E-11	7.39E-4	0.611	0.41
tsw36	5.71E-18	3.55E-6	0.380	7.01E-11	7.84E-4	0.610	0.41
tsw37	4.49E-18	5.33E-6	0.425	7.01E-11	7.84E-4	0.610	0.41
tsw38	4.53E-18	6.94E-6	0.324	5.92E-13	4.87E-4	0.612	0.41
tsw39	5.46E-17	2.29E-5	0.380	4.57E-13	9.63E-4	0.634	0.41
ch1z	1.96E-19	2.68E-7	0.316	3.40E-13	1.43E-3	0.631	0.10
ch1v	9.90E-13	1.43E-5	0.350	1.84E-12	1.09E-3	0.624	0.13
ch2v	9.27E-14	5.13E-5	0.299	2.89E-13	5.18E-4	0.628	0.13
ch3v	9.27E-14	5.13E-5	0.299	2.89E-13	5.18E-4	0.628	0.13
ch4v	9.27E-14	5.13E-5	0.299	2.89E-13	5.18E-4	0.628	0.13
ch5v	9.27E-14	5.13E-5	0.299	2.89E-13	5.18E-4	0.628	0.13
ch2z	6.07E-18	3.47E-6	0.244	3.12E-14	4.88E-4	0.598	0.10
ch3z	6.07E-18	3.47E-6	0.244	3.12E-14	4.88E-4	0.598	0.10
ch4z	6.07E-18	3.47E-6	0.244	3.12E-14	4.88E-4	0.598	0.10
ch5z	6.07E-18	3.47E-6	0.244	3.12E-14	4.88E-4	0.598	0.10
ch6	4.23E-19	3.38E-7	0.510	1.67E-14	7.49E-4	0.604	0.10
pp4	4.28E-18	1.51E-7	0.676	3.84E-14	5.72E-4	0.627	0.10
pp3	2.56E-14	2.60E-5	0.363	7.60E-12	8.73E-4	0.655	0.46
pp2	1.57E-16	2.67E-6	0.369	1.38E-13	1.21E-3	0.606	0.46
pp1	6.40E-17	1.14E-6	0.409	1.12E-13	5.33E-4	0.622	0.10
bf3	2.34E-14	4.48E-6	0.481	4.08E-13	9.95E-4	0.624	0.46
bf2	2.51E-17	1.54E-7	0.569	1.30E-14	5.42E-4	0.608	0.10

Source: CRWMS M&O (2000f, Table 13)

Table 8.10-3. Calibrated Drift-Scale Fracture Permeabilities for the Model Layers in the Topopah Spring Welded Unit

Model Layer	Base-Case Infiltration	Upper-Bound Infiltration	Lower-Bound Infiltration
Tsw32	1.26E-12	7.08E-12	8.91E-13
Tsw33	5.50E-13	1.50E-12	6.07E-13
Tsw34	2.76E-13	4.63E-13	4.99E-13
Tsw35	1.29E-12	5.09E-12	1.82E-12
Tsw36	9.91E-13	1.48E-12	1.43E-12
Tsw37	9.91E-13	1.48E-12	1.43E-12

Source: CRWMS M&O (2000f, Table 17)

NOTE: Fracture permeability is given in square meters.

Table 8.10-4. Calibrated Fault Parameters from Two-Dimensional Inversions of Saturation, Water Potential, and Pneumatic Data

Model Layer[a]	Matrix Permeability (m^2)	Matrix van Genuchten Alpha (1/Pa)	Matrix van Genuchten m (-)	Fracture Permeability (m^2)	Fracture van Genuchten Alpha (1/Pa)	Fracture van Genuchten m (-)	Fracture-Activity Parameter (-)
Tcwf	4.97E-19	9.92E-6	0.181	8.88E-11	3.80E-3	0.633	0.30
Ptnf	1.21E-13	3.71E-5	0.254	2.37E-11	2.80E-3	0.633	0.10
Tswf	1.11E-15	6.36E-6	0.401	6.38E-11	1.27E-3	0.633	0.50
Chnf[b]	4.0E-18	9.79E-7	0.386	3.6E-13	2.3E-3	0.633	0.30

Source: CRWMS M&O (2000f, Table 20)

NOTES: [a] Layers in the faulted-rock inversion model correspond to the major hydrogeologic units (TCw, PTn, TSw, and CHn) rather than the detailed hydrogeologic units listed in Table 8.10-3.

[b] Parameters for layer Chnf were not calibrated but were taken directly from CRWMS M&O (2000g, Tables 9 and 10).

Table 8.10-5. Average Net Infiltration Over the Domain of the Unsaturated Zone Model for the Nine Infiltration Scenarios

Climate Scenario	Lower-Bound Infiltration	Mean Infiltration	Upper-Bound Infiltration
Present-day	1.20	4.56	11.24
Monsoon	4.60	12.36	20.12
Glacial transition	2.40	17.96	33.52

Source: CRWMS M&O (2000d, Table 6-3)

NOTE: Net infiltration is given in millimeters per year.

Table 8.10-6. Comparison of Water-Balance-Model Infiltration with Chloride-Based Infiltration for Regions within the Domain of the Unsaturated Zone Model

Region (see Figure 8.10-18)	Area		Infiltration Volume				Infiltration Rate	
			Water-Balance Model		Chloride-Based Model		Water Balance	Chloride-Based
	km^2	Percent	$m^3/yr.$	Percent	$m^3/yr.$	Percent	mm/yr.	mm/yr.
I	9.9	25.5	104,732	59	104,732	58	10.60	10.60
II	5.3	13.8	12,353	7	12,353	7	2.32	2.32
III	3.7	9.6	26,341	15	25,910	14	7.12	7.00
IV	3.6	9.4	8,844	5	8,718	5	2.43	2.40
V	4.6	11.9	12,545	7	13,835	8	2.72	3.00
VI	2.2	5.6	2,486	1	2,168	1	1.15	1.00
VII	1.8	4.6	3,355	2	2,662	1	1.89	1.50
VIII	3.0	7.7	2,162	1	2,162	1	0.73	0.73
IX	4.7	12.0	5,010	3	6,993	4	1.07	1.50
Total	38.7	100.0	177,828	100	179,534	100	NA	NA
						Average	4.56	4.64

Source: CRWMS M&O (2000d, Table 6-13)

NOTE: NA = not applicable

Table 8.10-7. Fracture and Matrix Components of Percolation Flux at the Potential Repository Horizon and the Water Table for the Two Perched-Water Conceptual Models and the Mean Present-Day, Monsoon, and Glacial Transition Infiltration Scenarios

Simulation	Flux at Potential Repository Horizon (percent)		Flux at Water Table (percent)	
Mean Infiltration Scenario Conceptual Model	Fracture	Matrix	Fracture	Matrix
Present-day, flow-through	83.69	16.31	86.69	13.31
Present-day, bypassing	83.66	16.34	71.19	28.81
Monsoon, flow-through	89.53	10.47	90.21	9.79
Monsoon, bypassing	89.50	10.50	80.87	19.13
Glacial transition, flow-through	91.38	8.62	90.47	9.53
Glacial transition, bypassing	91.37	8.63	83.43	16.57

Source: CRWMS M&O (2000d, Tables 6-22 to 6-24)

Table 8.10-8. Liquid Water Travel and Tracer Transport Times at 10 Percent and 50 Percent Mass Breakthrough for Transport Simulations for the Two Perched-Water Conceptual Models and the Mean Present-Day Monsoon and Glacial Transition Infiltration Scenarios

Transport Simulation: Mean Infiltration Scenario Conceptual Model	Type of Tracer	10 Percent Breakthrough Times at Water Table (yr.)	50 Percent Breakthrough Times at Water Table (yr.)
Present-day, flow-through	Nonsorbing	75	3,700
Present-day, flow-through	Sorbing	12,000	170,000
Present-day, bypassing	Nonsorbing	100	4,300
Present-day, bypassing	Sorbing	11,000	140,000
Monsoon, flow-through	Nonsorbing	12	630
Monsoon, flow-through	Sorbing	1,500	35,000
Monsoon, bypassing	Nonsorbing	6	670
Monsoon, bypassing	Sorbing	1,200	26,000
Glacial transition, flow-through	Nonsorbing	7	310
Glacial transition, flow-through	Sorbing	740	18,000
Glacial transition, bypassing	Nonsorbing	4	330
Glacial transition, bypassing	Sorbing	620	12,000

Source: CRWMS M&O (2000d, Tables 6-29 to 6-31)

Table 8.10-9. Infiltration Rates and Corresponding Rock Properties Sets Used in Thermohydrological-Chemical Seepage Model Simulations

Infiltration Case	Infiltration Rate (mm/yr.)	Time Periods for Climate Conditions (present-day, monsoon, glacial transition[a]) (yr.)	Calibrated Rock Properties Set (Section 8.10.5.3)
Ambient, Present-Day Mean Infiltration at Borehole USW SD-9 (no thermal load)	1.05	0 to 100,000 (no climate change)	Present-day mean (base case)
Lower-Bound Infiltration (representative of potential repository area)	0.6	0 to 600	Present-day lower bound
	6	600 to 2,000	
	3	2,000 to 100,000[a]	
Mean Infiltration (representative of potential repository area)	6	0 to 600	Present-day mean (base case)
	16	600 to 2,000	
	25	2,000 to 100,000[a]	
Upper-Bound Infiltration (representative of potential repository area)	15	0 to 600	Present-day upper bound
	26	600 to 2,000	
	47	2,000 to 100,000[a]	

Source: CRWMS M&O (2000j, Table 12)

NOTE: [a]The glacial transition climate condition was defined only out to 10,000 yr. from the present (Section 8.2.10). Infiltration rates beyond 10,000 yr. are likely to be different than shown here.

Table 8.10-10. Sorption Coefficient Distributions for Rock Types within the Unsaturated Zone at Yucca Mountain

Element	Rock Type	Min K_d (mL/g)	Max K_d (mL/g)	E[x][a]	COV[b]	Distribution Type
Americium	Devitrified	100	2000			Uniform
	Vitric	100	1000	400	0.20	Beta
	Zeolitic	100	1000			Uniform
	Iron oxide	1000	5000			Uniform
Plutonium	Devitrified	5	70			Beta
	Vitric	30	200	100	0.25	Beta
	Zeolitic	30	200	100	0.25	Beta
	Iron oxide	1000	5000			Uniform
Uranium	Devitrified	0	2.0	0.5	0.3	Beta
	Vitric	0	1.0	0.5	0.3	Beta
	Zeolitic	0	10.0	4.0	1.0	Beta (exp)
	Iron oxide	100	1000			Uniform
Neptunium	Devitrified	0	1.0	0.3	0.3	Beta
	Vitric	0	1.0	0.3	1.0	Beta (exp)
	Zeolitic	0	3.0	0.5	0.25	Beta
	Iron oxide	500	1000			Uniform
Radium	Devitrified	70	300			Uniform
	Vitric	50	100			Uniform
	Zeolitic	800	2000			Uniform
	Iron oxide	0	500	30	1.0	Beta (exp)
Cesium	Devitrified	10	700			Uniform
	Vitric	10	100			Uniform
	Zeolitic	300	3000			Uniform
	Iron oxide	0	300	30	1.0	Beta (exp)
Strontium	Devitrified	5	30			Uniform
	Vitric	0	20			Uniform
	Zeolitic	200	2000			Uniform
	Iron oxide	0	20	10	0.25	Beta
Nickel	Devitrified	0	200	50	0.33	Beta
	Vitric	0	50	30	0.33	Beta
	Zeolitic	0	200	50	0.33	Beta
	Iron oxide	0	500			Uniform
Lead	Devitrified	100	500			Uniform
	Vitric	100	500			Uniform
	Zeolitic	100	500			Uniform
	Iron oxide	100	1000			Uniform
Tin	Devitrified	20	200			Uniform
	Vitric	20	200			Uniform
	Zeolitic	100	300			Uniform
	Iron oxide	0	5000			Uniform

Table 8.10-10. Sorption Coefficient Distributions for Rock Types within the Unsaturated Zone at Yucca Mountain (Continued)

Element	Rock Type	Min K_d (mL/g)	Max K_d (mL/g)	E[x][a]	COV[b]	Distribution Type
Protactinium	Devitrified	0	100			Uniform
	Vitric	0	100			Uniform
	Zeolitic	0	100			Uniform
	Iron oxide	500	1000			Uniform
Selenium	Devitrified	0	1	0.1	1.0	Beta (exp)
	Vitric	0	1	0.1	1.0	Beta (exp)
	Zeolitic	0	1	0.2	1.0	Beta (exp)
	Iron oxide	0	200	30	1.0	Beta (exp)
Carbon	Iron oxide	10	100			Uniform
Actinium, Niobium, Samarium, Thorium, Zirconium: see Americium						
Chlorine, Technetium, Iodine		0	0			

Source: CRWMS M&O (2000n, Table 1)

NOTES: [a] E[x] = expected value
[b] Coefficient of variation: COV = σ[x]/E[x]

Table 8.10-11. Summary of Diffusion-Coefficient Data

Radionuclide Type	Mean (m^2/s)	Standard Deviation (m^2/s)	Maximum (m^2/s)	Minimum (m^2/s)	Distribution Type
Anionic	3.2×10^{-11}	1.0×10^{-11}	1×10^{-9}	0	Beta
Cationic	1.6×10^{-10}	0.5×10^{-10}	1×10^{-9}	0	Beta

Source: CRWMS M&O (2000n, Section 6.6.3)

Table 8.10-12. Percolation Fluxes for Different Climatic Regimes Used in the Three-Dimensional Site-Scale Radionuclide Transport Simulations

Value	Present-Day (mm/yr.)	Monsoon (mm/yr.)	Glacial Transition (mm/yr.)
Lower Bound	1.20	4.60	2.40
Mean	4.60	12.36	17.96
Upper Bound	11.24	20.12	33.52

Source: CRWMS M&O (2000l, Table 6.11)

Table 8.10-13. Breakthrough Times of Radionuclides at the Water Table under Present-Day Infiltration

Radionuclide	Time	Present-Day Infiltration (yr.)		
		Low	Mean	High
^{99}Tc	t_{10}	10,000	300	45
	t_{50}	45,000	4,000	1,000
^{237}Np	t_{10}	220,000	10,000	1,700
	t_{50}	>1,000,000	120,000	22,000
^{239}Pu + ^{235}U + ^{231}Pa	t_{10}	600,000	40,000	12,000
	t_{50}	>1,000,000	250,000	90,000

Source: CRWMS M&O (2000l, Table 6.15)

Table 8.10-14. Summary of Radionuclide Sorption Results from Busted Butte Tests

Sample Source	Geologic Unit (Model Layer)	Approximate Average K_d (mL/g)		
		Np	Am	Pu
Phase 1A, BH 3	Tptpv1 (ch1v)	20	380	19
Phase 1A, BH 4	Tac (ch2v)	21	470	2500
Phase 1B, BH 7	Tptpv2 (tsw39)	21	450	1100

Source: CRWMS M&O (2000n, Tables 27 and 28)

INTENTIONALLY LEFT BLANK